

***Klf4* has an unexpected protective role in perivascular cells  
within the microvasculature**

Ryan Michael Haskins  
Charlottesville, Virginia

Bachelor of Science, Biology, Case Western Reserve University, 2012

A Dissertation presented to the Graduate Faculty of the  
University of Virginia in Candidacy for the  
Degree of Doctor of Philosophy

Department of Pathology

University of Virginia  
August 2018



## Abstract

Recent smooth muscle cell (SMC) lineage tracing studies have revealed that SMCs undergo remarkable changes in phenotype during the development of atherosclerosis. Of major interest, this work demonstrated that *Klf4* in SMCs is detrimental for overall lesion pathogenesis in that SMC-specific conditional knockout of *Klf4* resulted in smaller, more stable lesions that exhibited marked reductions in the numbers of SMC-derived macrophage-like and mesenchymal stem cell-like cells. However, since the clinical consequences of atherosclerosis typically occur well after our reproductive years, we sought to identify beneficial KLF4-dependent SMC functions that were likely to be evolutionarily conserved. Herein the hypothesis that *Klf4* dependent SMC transitions play an important role in tissue repair following injury was tested.

Utilizing SMC-specific lineage tracing mice +/- simultaneous SMC-specific conditional knockout of *Klf4*, we demonstrate that SMCs in the remodeling heart following ischemia-reperfusion injury (IRI) express KLF4 and transition to a *Klf4* dependent macrophage-like state and a *Klf4* independent myofibroblast-like state. Moreover, SMC-*Klf4* knockout mice had exacerbated heart failure following IRI. Surprisingly, significant cardiac dilation was observed in SMC-*Klf4* knockout mice prior to IRI. This cardiac dilation was accompanied by a reduction in peripheral resistance, as evidenced by a reduction in blood pressure, an increase in blood flow, and a larger passive diameter of mesenteric resistance arteries as measured by pressure myography. KLF4 ChIP-Seq analysis on mesenteric

vascular beds identified potential baseline SMC KLF4 target genes in numerous pathways previously shown to be important for perivascular cell investment including PDGF and FGF. Moreover, microvascular tissue beds in SMC-*Klf4* knockout mice had gaps in lineage traced SMC coverage along the resistance arteries and exhibited increased permeability. Taken together, these results provide novel evidence that *Klf4* has a critical maintenance role within microvascular SMCs, including being required for normal SMC function and coverage of resistance arteries.

## Acknowledgements

I would like to thank my mentor, Dr. Gary Owens, for his guidance and support over the entirety of this project. I appreciate him challenging me to think critically about all aspects of an experiment as well as the direction of a project as a whole.

I would also like to thank Dr. Anh Nguyen. Anh started this project and performed the majority of the preliminary studies, providing me with a great start to my thesis work. In addition, Anh taught me the majority of the scientific techniques I performed in this manuscript and provided valuable intellectual support throughout the project.

I would also like to thank the extensive network of collaborators who helped Anh and I over the course of the project. In particular, I would like to acknowledge the Isakson lab for the extensive myography studies they performed, only some of which are presented here.

I would also like to acknowledge the current and former members of the Owens' lab. They have provided countless hours of advice and support, from lab meetings to late nights in the lab. In particular I would like to thank: Dr. Olga Cherepanova for always pushing me to be the best scientist I can be; Melissa (Missy) Bevard for histology and tissue processing expertise and advice; and Gabe Alencar for bioinformatics expertise and overall support.

Last but not least, I would also like to acknowledge the members of my thesis committee, including Dr. Janet Cross (chair), Dr. Adam Goldfarb, Dr.

Adrian Halme, Dr. Ann Sutherland, and Dr. Brant Isakson. My thesis project changed significantly from what I initially proposed during my qualifying exam and I appreciate your patience and help in guiding the project through that transition to a completed thesis.

## Table of Contents

Abstract .....	III
Acknowledgements .....	V
List of Abbreviations .....	X
Chapter I: Introduction .....	1
<b>The Vascular Smooth Muscle Cell</b> .....	2
Smooth muscle cell function .....	2
SMC phenotypic switching.....	3
<b><i>Klf4</i> mediates SMC phenotypic modulation</b> .....	7
Krüppel-like factor 4 ( <i>Klf4</i> ) .....	7
<i>Klf4</i> influences multiple axes of SMC marker gene expression .....	7
<b><i>Klf4</i>-dependent SMC transitions and functions are detrimental to overall plaque pathogenesis during atherosclerosis</b> .....	11
Lineage tracing SMCs <i>in vivo</i> reveals SMCs contribute to multiple cell types .....	11
Knockout of <i>Klf4</i> in SMC results in smaller, more stable atherosclerotic lesions .....	15
<i>Klf4</i> binds over 800 putative target genes within SMC in advanced atherosclerotic lesions .....	16
<b>Identification of a <i>Klf4</i> dependent SMC role in injury repair</b> .....	17
SMCs may contribute to the healing process post ischemia reperfusion injury (IRI) .....	17
Conclusion .....	20
Chapter II: <i>Klf4</i> has an unexpected protective role in perivascular cells within the microvasculature .....	26
<b>Abstract</b> .....	27
<b>Introduction</b> .....	28
<b>Material and Methods</b> .....	32
Generation of SMC eYFP <sup>+/+</sup> <i>Klf4</i> <sup>WT/WT</sup> and SMC eYFP <sup>+/+</sup> <i>Klf4</i> <sup>Δ/Δ</sup> animals.....	32
Ischemia-Reperfusion – Acute Myocardial infarction .....	32
Tissue harvest and processing .....	33
Immunohistochemical and immunofluorescent analysis .....	34
Image capture and analysis.....	34
Echocardiography .....	35
Blood pressure measurements.....	36
Blood flow measurements .....	36

Pressure myography .....	37
KLF4 chromatin immunoprecipitation-sequencing (ChIP-seq) analysis .....	38
Intravital confocal microscopy.....	40
Permeability measurements and quantification.....	40
Bone marrow transfer .....	41
Statistical Analysis.....	42
<b>Results</b> .....	42
KLF4 is upregulated in SMC within the infarct zone post ischemia-reperfusion (acute MI).....	42
A subset of SMC transitioned to macrophage- and myofibroblast-like cells following IRI-MI .....	43
SMC specific <i>Klf4</i> knockout induced cardiac dilation at baseline and exacerbated development of an ischemic dilated cardiomyopathy .....	46
SMC <i>Klf4</i> knockout resulted in increased resistance vessel passive diameter indicative of outward remodeling .....	54
<i>In vivo</i> KLF4 ChIP-Seq identified PDGF signaling as a key pathway regulated by <i>Klf4</i> within the mesenteric vascular bed.....	58
Resistance vessels from SMC <i>Klf4</i> knockout mice exhibit gaps in SMC coverage .....	62
<b>Discussion</b> .....	66
Chapter III: Additional Studies .....	72
<b>Knockout of <i>Klf4</i> in SMC alters metabolic pathways</b> .....	73
Experimental background.....	73
Results: .....	73
SMC specific <i>Klf4</i> knockout results in metabolic dysregulation .....	73
Discussion.....	74
<b>Aging SMC eYFP<sup>+/+</sup> <i>Klf4</i><sup>Δ/Δ</sup> and SMC eYFP<sup>+/+</sup> <i>Klf4</i><sup>WT/WT</sup> results in gaps in eYFP+ coverage within vascular beds</b> .....	78
Experimental background.....	78
Results: .....	78
Wild type and SMC specific <i>Klf4</i> knockout mice develop gaps in eYFP+ SMC coverage with age .....	78
Discussion.....	79
Chapter IV: Future Directions .....	84

<b>What are the pathways downstream of KLF4 that lead to the development of gaps in eYFP+ SMC coverage within the microvasculature following SMC specific knockout of KLF4?</b> .....	87
<b>What is the source of the eYFP- replacement cells that fill in the eYFP+ gaps within the microvasculature?</b> .....	94
<b>Is there a compensatory mechanism for loss of KLF4 in SMC?</b> .....	98
<b>How does SMC specific <i>Klf4</i> knockout result in dysregulated metabolic pathways?</b> .....	102
<b>Summary</b> .....	105
Chapter V: References .....	107

**List of Abbreviations**

ACTA2, smooth muscle alpha actin

AngII, angiotensin II

APOE, apolipoprotein E

CArG, CC(A/T)<sub>6</sub>GG DNA sequences

CD105, endoglin

CD11b, integrin alpha M (ITGAM)

CD11c, integrin alpha X (ITGAX)

CD31, Platelet endothelial cell adhesion molecule (PECAM-1)

ChIP, Chromatin ImmunoPrecipitation

DAB, 3,3'-diaminobenzidine

DAPI, 4',6-diamidino-2-phenylindole

DIO, diet induced obesity

ECM, extracellular matrix

ER<sup>T2</sup> cre, tamoxifen inducible cre recombinase-mutated estrogen receptor

ES cells, embryonic stem cells

ETS, E26 transformation-specific

eYFP, enhanced yellow fluorescent protein

F4/80, EGF-like module-containing mucin-like hormone receptor-like 1

FGF, fibroblast growth factor

GMP, guanosine monophosphate

H2A, H2B, H3, H4, histone 2A, 2B, 3 and 4

H3K4, histone 3, lysine 4

HDAC, histone deacetylase

IL-1 $\beta$ , interleukin 1 beta

IP, intraperitoneal injection

IRI, ischemia reperfusion injury

kDa, kilodalton

KLF4, Krüppel-like factor 4

LAD, left anterior descending artery

LDLR, low density lipoprotein receptor

LGALS3, lectin galactoside-binding soluble 3 (mac-2)

MI, myocardial infarction

miR, microRNA

MSC, mesenchymal stem cell

MYH11, smooth muscle myosin heavy chain 11

NADPH, nicotinamide adenine dinucleotide phosphate

NO, nitric oxide

Oct4, octamer-binding transcription factor 4 or POU5F1

PDGF-BB, platelet-derived growth factor BB

pELK-1, phosphorylated ELK-1

POVPC, 1-palmytoyl-2-(5-oxovaleroyl)-sn-glycero-3-phosphocholine

Sca1, stem cell antigen-1

SEM, standard error of the mean

Seq, sequencing

siRNA, small interfering RNA

SMC, smooth muscle cell

SNP, sodium nitroprusside

Sox2, SRY (sex determining region Y)-box 2

Sp1, specificity protein 1

SRF, serum response factor

Tagln, smooth muscle 22 alpha

TCE, TGF- $\beta$  control element

TGF- $\beta$ , transforming growth factor beta

UTR, untranslated region

# **Chapter I: Introduction**

## The Vascular Smooth Muscle Cell

### Smooth muscle cell function

Maintaining blood flow throughout the body is critical to an organism's survival. Indeed, mouse embryos that fail to develop a functioning vasculature die early in development<sup>1-3</sup>. In adult organisms, one of the principal cells responsible for control of blood flow is the vascular smooth muscle cell (SMC)<sup>4-6</sup>. SMCs are found within arteries and veins where they are circumferentially oriented around endothelial tubes. Adult SMCs within the vasculature have a low basal proliferation rate and express a unique cohort of contractile genes including *Acta2*, *Myh11* and *Tagln*<sup>6</sup>. Contraction is the main function of SMCs in healthy adult vessels; consequently SMCs regulate blood pressure and blood flow distribution through control of blood vessel diameter<sup>4-6</sup>.

The primary site of blood pressure control is the resistance arteries<sup>7</sup>. These smaller arterioles (20-300  $\mu\text{m}$ ) respond to a wide range of cytokines and physiological stimuli to regulate blood vessel diameter and peripheral resistance through contraction and dilation of the SMC layer<sup>8,9</sup>. One of the key signaling molecules for blood vessel dilation is nitric oxide (NO)<sup>10,11</sup>.

Upon endothelial cell stimulation (e.g. acetylcholine), NO is generated from L-arginine, free oxygen, and NADPH (nicotinamide adenine dinucleotide phosphate) by nitric oxide synthases within the endothelial cell<sup>12</sup>. The NO then freely diffuses into the surrounding SMCs, activating the soluble guanylate cyclase as well as directly acting on calcium dependent potassium channels<sup>13-15</sup>.

Activation of the soluble guanylate cyclase leads to increased cyclic-GMP levels, activation of protein kinase G, and a reduction in intracellular calcium<sup>13,14,16</sup>. The net effect of these changes is an overall relaxation of the SMC. Intriguingly, NO has also been shown to regulate the magnitude of the constrictive response in SMCs exposed to vasoconstrictors<sup>17,18</sup>. Vasoconstrictors, such as angiotensin II (AngII) and  $\alpha$ 1D-adrenoceptor agonists (e.g. phenylephrine), raise intracellular calcium levels initiating a contraction of the SMC<sup>19,20</sup>.

Fascinatingly, blood vessel diameter control is not the only function of SMCs in the adult. SMCs are also active participants in the angiogenic process<sup>21,22</sup> and contribute during injury repair<sup>23–25</sup>. They do this through coordinate downregulation of their contractile genes in a process known as phenotypic switching.

### **SMC phenotypic switching**

SMCs are a non-terminally differentiated cell type. Upon vascular injury<sup>23,26,27</sup> or disease progression<sup>25,28–32</sup>, SMCs phenotypically modulate in response to local environmental cues. The consequence of this phenotypic modulation is a downregulation of the SMC contractile genes (e.g. *Acta2*, *Myh11*) and an increase in SMC proliferation, migration and synthesis of extracellular matrix<sup>5</sup>. Recent work from the Owens' lab and others has demonstrated, through SMC specific lineage tracing systems, that upon phenotypic modulation SMCs can transition to a multitude of cell types *in vivo*, including macrophage-like, myofibroblast-like, and mesenchymal-stem cell-like cells<sup>25,30,31,33,34</sup>. This ability of

SMCs to phenotypically modulate in response to environmental cues was likely subject to heavy evolutionary selection pressure. Organisms with mutations that impaired their SMCs ability to phenotypically modulate would have impaired vascular repair following injury as well as impaired angiogenesis. These impairments would result in a reduction in overall fitness. Indeed, the promoter elements (discussed in detail below) that control SMC contractile protein expression are highly conserved across evolutionarily distant species including chickens and humans <sup>4</sup>. As uncontrolled and/or spontaneous phenotypic modulation of SMCs would result in a vast array of complications (e.g. drastic drops in blood pressure), this process is tightly regulated.

One of the common regulatory elements among SMC marker genes are the CC(A/T)<sub>6</sub>GG DNA sequences (CArG elements) found within 2-3 kb of the genes transcription start site (reviewed in <sup>35</sup>, diagramed in Figure 1A). These CArG elements serve as binding sites for serum response factor (SRF), a ubiquitously expressed MADS box transcription factor that binds as a homodimer to the CArG box DNA <sup>35</sup>. Interestingly, several of the SMC marker gene's CArG elements have been demonstrated to be degenerate <sup>36-38</sup>. SRF has a reduced binding affinity to the degenerate SMC CArG elements compared to the consensus CArG sequences found in other serum response genes such as *c-fos* <sup>36-38</sup>. Intriguingly, the degenerative nature of the SMC contractile gene CArG elements does not appear to be required for normal development but is critical for injury induced downregulation of marker gene expression (i.e. phenotypic switching) after carotid balloon injury <sup>38</sup>. Thus, it would appear that SMC evolved

degenerative CArG boxes to enable phenotypic switching (described in detail below).

Another key component of the SMC differentiation profile is expression of the SRF coactivator myocardin<sup>39,40</sup>. Myocardin strongly associates with SRF to induce expression of CArG-dependent SMC genes<sup>39,40</sup>. A growing body of evidence suggests that myocardin-SRF complexes activate the SMC genes with multiple CArG elements (e.g. *Acta2*, *Myh11*) more efficaciously than those with one or none by forming higher order complexes along the same DNA face<sup>41,42</sup>. Indeed, myocardin overexpression by adenovirus is sufficient to drive multiple CArG-dependent SMC marker genes, but fails to recapitulate the entire differentiation program (reviewed in<sup>43</sup>).

One final component of SMC differentiation control is epigenetic regulation of DNA accessibility at SMC gene promoters. Chromatin is organized into strings of nucleosomes, 146 bp units of genomic DNA wrapped around a core of histone proteins (2 copies each of histones H2A, H2B, H3, H4)<sup>44</sup>. Organizing the DNA into nucleosome units and larger higher order DNA structures enables the cell to store all of its DNA within the nucleus and to dynamically control physical access to gene promoters. This is done in part through post translational modifications to the histone proteins, such as acetylation and methylation of histone lysine residues<sup>45</sup>. Histone acetylation structurally opens chromatin, making it more accessible to DNA binding proteins and subsequent transcription. This opening is thought to occur in part through disruption of adjacent nucleosome interactions as well as possibly reducing the histones ability to interact with DNA<sup>46-48</sup>.

Histone methylation also results in a more transcriptionally active genomic region, albeit in a different way. Histone methylation can serve as a docking site for transcription factors <sup>49</sup>. Both histone acetylation and methylation have been shown to be important in SMC gene expression <sup>48</sup>. SMC marker gene promoters were shown to be heavily acetylated on histone H4 and have enrichment of H3K4 dimethylation <sup>48</sup>. This H3K4 dimethylation is proposed to enable tethering of myocardin to SMC gene promoters, resulting in stabilization of SRF binding to the degenerate CArG boxes found in SMC marker gene promoters <sup>48</sup>.

Stabilization of SRF and myocardin on SMC gene promoters would, in turn, lead to expression of the differentiated SMC gene program. Dimethylation of H3K4 on SMC gene promoters appears to be SMC specific and may serve as a mechanism for lineage memory to enable or facilitate phenotypically modulated SMCs ability to return to their differentiated state upon resolution/removal of the de-differentiation cue <sup>33,50</sup>.

A variety of cytokines and environmental cues (i.e. PDGF-BB, oxidized phospholipids) have been demonstrated to influence these SMC marker gene control elements to induce phenotypic modulation *in vitro* and *in vivo*. However, less is known about the downstream mechanisms <sup>51-53</sup>. One of the downstream factors that has been shown to play a key role in SMC phenotypic switching is the transcription factor KLF4 <sup>23,24,27,34</sup>.

## ***Klf4* mediates SMC phenotypic modulation**

### **Krüppel-like factor 4 (Klf4)**

*Klf4* was originally identified from a NIH 3T3 library using a zinc finger probe of the transcription factor zif/268<sup>54</sup>. Further characterization *in vivo* identified that *Klf4* is heavily enriched in gut tissues and was given the name gut-enriched Krüppel-like factor (*GKLF*)<sup>54</sup>. Like Krüppel-like factors 1-3, *Klf4* has 3 highly conserved two cysteine and two histidine zinc fingers (C<sub>2</sub>H<sub>2</sub>) that enable the transcription factor to bind to the major groove of DNA<sup>55</sup>. *Klf4* has been shown to both activate and repress gene expression<sup>27,30</sup>. Within SMCs, *Klf4* was first identified using a yeast-one hybrid screen to identify binding partners of a key TGF- $\beta$  control element (TCE) within the *Tagln* promoter<sup>56</sup>. Further characterization of the *Klf4* binding site revealed that it does not bind directly to the TCE element, but rather to a G/C repressor region of the gene promoter where it represses expression of SMC marker genes<sup>23,27</sup>. Consistent with its repressive role, *Klf4* has historically been shown to not be expressed within differentiated SMCs<sup>56</sup>. However, *Klf4* is upregulated in phenotypically modulated SMCs<sup>23,27,34,57</sup>. *Klf4* activation is driven, at least in part, by binding of Sp1 to the *Klf4* promoter<sup>23</sup>.

### ***Klf4* influences multiple axes of SMC marker gene expression**

*Klf4* regulates SMC marker gene expression through several key mechanisms. The first mechanism is deacetylation of SMC marker gene

promoters. The Owens' lab and others have demonstrated that following stimulation *in vitro* with either PDGF-BB or oxidized phospholipids (e.g. POVPC), pELK-1 binds to the overlapping ETS binding site near G/C repressor regions on SMC marker gene promoters and recruits KLF4<sup>58,59</sup>. This recruitment was also shown to occur *in vivo* following carotid ligation injury, and was dependent on an intact G/C repressor region<sup>27</sup>. The interaction between pELK-1 and Klf4, as well as pELK-1's ability to interact with SRF and interrupt myocardin SRF complexes on SMC gene promoters, is dependent on its phosphorylation<sup>27,59</sup>. Following its recruitment to SMC gene promoters, KLF4 recruits histone deacetylases (HDAC) 2, HDAC4, and HDAC5 to hypo-acetylate the promoter<sup>27,58,60</sup>.

Co-immunoprecipitation assays have shown interaction between KLF4 and HDAC5 *in vitro* following POVPC treatment<sup>58</sup>. Following carotid artery ligation *in vivo*, both HDAC2 and HDAC5 were shown to bind to the G/C repressor region of SMC promoters<sup>27</sup>. However, only HDAC2 was shown through sequential ChIP assays to form a higher order complex with pELK-1 and KLF4<sup>27</sup>. The formation of this higher order complex was dependent on the G/C repressor as mutations in the repressor resulted in loss of complex formation<sup>27</sup>. Hypo-acetylation of the SMC marker gene promoters results in physically compact and less accessible chromatin.

*Klf4* also regulates SMC marker gene expression through downregulation of the SMC master regulator myocardin (described previously). KLF4 has been shown to regulate myocardin expression in both rat<sup>57</sup> and human cells<sup>61</sup>. In both systems, viral mediated overexpression of KLF4 led to a drastic decrease in

myocardin expression<sup>57,61</sup>. Further characterization of the myocardin promoter identified three KLF4 binding sites in a region -4016 to -2226 bp upstream of the transcription start site<sup>61</sup>. Utilizing luciferase reporter constructs with mutations to one or all three KLF4 binding sites, Turner *et al.* demonstrated that the three binding sites work cooperatively to reduce myocardin expression following PDGF-BB induced phenotypic switching<sup>61</sup>. This reduction in myocardin leads to a decrease in SMC marker gene expression.

Finally, it is worth mentioning the interactions between *miR-143*, *miR-145* and *Klf4*. MicroRNAs are small, non-coding RNAs that have been implicated in a wide range of cellular events, including proliferation and differentiation of cells<sup>62–64</sup>. *miR-143* and *miR-145* are thought to be transcribed as a bicistronic unit and share common regulatory elements<sup>65</sup>. SRF and myocardin have been demonstrated to activate an enhancer region for these microRNAs in luciferase reporter assays and in *in vivo* lacZ reporter constructs in developing mouse embryos<sup>65</sup>. Activation of miR-143 and miR-145 by these transcription factors parallels the microRNAs high expression levels in differentiated SMCs. Indeed, *miR-143* binds to the *Elk-1* promoter and represses luciferase activity in promoter activation studies, while *miR-145* had binding sites within the myocardin promoter and was shown to drive activity of the promoter with a luciferase reporter assay<sup>65</sup>. Like myocardin and the SMC marker genes, *miR-143* and *miR-145* are downregulated following injury or disease progression (i.e. carotid ligation, atherosclerosis)<sup>65</sup>. Intriguingly, *miR-145* has a binding site within the *Klf4* 3' UTR and has been shown reduce KLF4 expression<sup>65,66</sup>. *miR-145* also

represses *Klf4*, as well as *Oct4* and *Sox2*, in human embryonic stem cells to allow for normal differentiation into mesoderm, ectoderm and endoderm<sup>67</sup>. Taken together, these data suggest that the expression profiles of *miR-145* and *Klf4* are reciprocal and the expression of one leads to the repression of the other through both direct and indirect mechanisms.

It is important to note that *Klf4* is not the only regulator of SMC marker gene expression. Global conditional knockout of *Klf4* resulted in only a transient delay in SMC phenotypic switching<sup>24</sup> and si*Klf4* knockdown only partially attenuates the SMC phenotypic modulation following PDGF-BB treatment<sup>27</sup>. *Klf5*, another member of the Krüppel-like factor family, has also been shown to be important in SMC responses to injury. The Nagai lab has demonstrated that global *Klf5* +/- animals had reduced neointima formation and medial thickening following vascular injury<sup>68</sup>. *miR-145* has also been shown to target KLF5 for degradation, while PDGF-BB stimulation increases KLF5 protein levels<sup>69</sup>. KLF5 was also shown to reduce myocardin expression in SMCs *in vitro*<sup>61,69</sup>. These results suggest that *Klf5* regulates SMC marker gene expression through the same pathways as *Klf4*. It is likely that *Klf2*, *Klf4*, and *Klf5* form a regulatory network in SMC to regulate SMC marker gene expression during phenotypic modulation, similar to how they form a regulatory network to enable embryonic stem cell self-renewal<sup>70</sup>.

*Klf4* has also been shown to regulate SMC proliferation. Following carotid ligation, global conditional knockout of *Klf4* resulted in enhanced neointimal formation and increased cellular proliferation within the vessel media<sup>24</sup>.

Consistent with this, KLF4 was shown to bind to the p21<sup>WAF1/Cip1</sup> promoter with p53 to induce expression of p21<sup>WAF1/Cip1</sup> and reduce SMC proliferation *in vitro*<sup>24</sup>. KLF4 was also shown to bind to the p21<sup>WAF1/Cip1</sup> promoter following vascular injury by *in vivo* ChIP assays<sup>24</sup>.

Taken together, the above results demonstrate that *Klf4* is not normally expressed within differentiated SMC, but is induced upon vascular injury or stimulation *in vitro* by PDGF-BB or oxidized phospholipids. *Klf4* regulates a robust network of cellular responses to down regulate SMC contractile genes and enable SMC phenotypic modulation both *in vitro* and *in vivo* (see Figure 1B). However, it remained unclear if *Klf4*-dependent phenotypic transitions had any functional consequences following disruption of vascular homeostasis, such as during atherosclerotic lesion formation.

## ***Klf4*-dependent SMC transitions and functions are detrimental to overall plaque pathogenesis during atherosclerosis**

### **Lineage tracing SMCs *in vivo* reveals SMCs contribute to multiple cell types**

As described in detail in the previous sections, SMCs retain a remarkable capacity to phenotypically modulate in response to environmental cues. This phenotypic modulation includes downregulation of all known SMC marker genes, including the most specific SMC marker gene *Myh11*. This makes positive

identification of phenotypically modulated SMCs by marker gene expression nearly impossible. To address this, the Owens' lab<sup>30,33,34</sup>, as well as others<sup>71,72</sup>, developed novel lineage tracing systems to conditionally label SMCs at the time of tamoxifen injection with a lineage tag. The Owens' system utilizes a tamoxifen inducible, conditional ER<sup>T2</sup> cre recombinase coupled to a Myh11 promoter construct (originally cloned by the Owens lab) made by Stefan Offermanns group<sup>73</sup> (detailed schematic in Figure 2A). Dr. Laura Shankman crossed this mouse with a ROSA26 STOP-floxed eYFP reporter mouse to generate a mouse in which all cells expressing Myh11 at the time of tamoxifen injection are permanently labeled with the lineage tag eYFP. This lineage tag is also passed to the progeny of the initially labeled cells. A series of 10 tamoxifen injections from 6-8 weeks of age resulted in greater than 95% labeling efficiency of SMC within large arteries<sup>33</sup>. There was also high efficiency labeling of SMCs within smaller arteries and veins, as well as microvascular labeling including the vessels within tissues such as the heart and lungs<sup>33</sup>. No eYFP expression was seen within the bone marrow or in circulating cells confirming there was no expression of Myh11 by bone marrow derived cells during the time of tamoxifen injection<sup>34</sup>. There was also no eYFP expression in animals not treated with tamoxifen, nor was there eYFP expression in eYFP<sup>-/-</sup> animals treated with tamoxifen<sup>33</sup>. An unfortunate drawback of the Owens' system is that the Myh11 ER<sup>T2</sup> cre promoter constructed inserted into the Y chromosome, so only male mice can be studied. Importantly (as discussed in the next sections), this SMC lineage tracing system also

enables conditional knockout of genes of interest (i.e. *Klf4*) by crossing the lineage tracing reporter mice to mice with floxed genes of interest.

Atherosclerosis is a chronic disease that results in lipid accumulation within arterial walls<sup>74,75</sup>. This lipid accumulation results in the infiltration of a variety of cell types into the newly formed lesions including SMCs and macrophages. These lesions can rupture, leading to thrombotic events and myocardial infarction (MI) or stroke. Unfortunately cardiovascular disease, including atherosclerosis and MI, remains a leading cause of death in the United States and across the globe<sup>76</sup>. Previous work in the atherosclerosis field primarily relied on expression of ACTA2 to identify putative SMCs<sup>74,77</sup>. As discussed at length in previous sections, ACTA2 positivity is insufficient to identify phenotypically modulated SMCs. Utilizing ACTA2 as a SMC identifier would also misidentify other cell types that have been shown to express ACTA2, such as macrophages, as SMCs<sup>78</sup>. Thus, utilization of a SMC lineage tracing system like the Owens' system (described above) is required to definitively identify SMCs. It is necessary to utilize an APOE<sup>-/-</sup> or a LDLR<sup>-/-</sup> mouse to study atherosclerosis in murine models as mice do not naturally develop the disease. Crossing an APOE<sup>-/-</sup> mouse to the Owens' system yields *Myh11-CreER<sup>T2</sup>* ROSA floxed STOP eYFP APOE<sup>-/-</sup> (SMC YFP<sup>+/+</sup> APOE<sup>-/-</sup>) mice. These mice were subsequently used to identify the contributions of SMCs to advanced stage atherosclerotic lesions<sup>34</sup>.

Utilizing the SMC YFP<sup>+/+</sup> APOE<sup>-/-</sup> mice, Shankman *et al.* identified that a remarkable 82% of lineage traced SMC within atherosclerotic lesions are ACTA2- and thus would not have been identified by traditional SMC markers<sup>34</sup>.

Additionally, they described a subset of SMCs that became macrophage-like within lesions<sup>34</sup>. These macrophage-like SMCs contributed 36% of all LGALS3+ (a macrophage marker) cells within the lesions as determined by single cell counting of high resolution, z-stack, confocal images<sup>34</sup>. Further characterization of the macrophage-like SMCs by flow cytometry revealed that they expressed multiple markers of macrophages including CD11b, CD11c, and F4/80<sup>34</sup>. A significant fraction of these macrophage-like SMCs co-expressed CD11b and F4/80<sup>34</sup>. Utilizing transmission electron microscopy with eYFP immunogold labeling, eYFP+ lineage traced SMCs within lesions were identified that contained multiple large lipid vacuoles suggesting SMC derived macrophage-like cells may be functionally phagocytizing lipoproteins and/or apoptotic cells within the lesion.

SMCs were also shown to undergo a transition to a mesenchymal stem cell (MSC)-like state (Sca1+CD105+) and an activated mesenchymal state (ACTA2+PDGF $\beta$ R+)<sup>34</sup>. Previous reports had suggested that pericytes (cousins of SMCs that wrap small arterioles and venules, as well as capillaries) isolated from adipose tissue had MSC-like properties after expansion *in vitro*<sup>79,80</sup>. To test whether the MSC-like SMCs within atherosclerotic vessels had these MSC-like properties, I flow sorted MSC-like SMCs (eYFP+SCA1+CD105+) and non-SMC MSCs (eYFP-SCA1+CD105+) from 18-week western diet fed atherosclerotic mice and grew them in MSC maintenance media<sup>34</sup>. I also isolated non MSC-like SMCs (eYFP+SCA1-CD105-) to determine if exposure to the MSC culture media could induce a switch to the MSC-like phenotype<sup>34</sup>. After two passages, these

non-MS-C-like SMCs became unhealthy and died<sup>34</sup>. The SMC derived MS-C-like cells grew very slowly in the MS-C culture media compared to the non-SMC MS-Cs and appeared to be senescent<sup>34</sup>. They also failed to differentiate into adipocytes or osteoblasts when exposed to the appropriate differentiation culture medium, while the non-SMC MS-Cs were able to differentiate<sup>34</sup>. These results suggest that SMC MS-C-like cells within atherosclerotic vessels are not functional MS-Cs. Shankman *et al.* next investigated whether *Klf4* is involved in these SMC phenotypic transitions.

### **Knockout of *Klf4* in SMC results in smaller, more stable atherosclerotic lesions**

To generate a SMC specific knockout of *Klf4*, the SMC eYFP<sup>+/+</sup> APOE<sup>-/-</sup> mouse was crossed to a *Klf4<sup>fl/fl</sup>* mouse with flox sites between exons 1-2 and exons 3-4 of the *Klf4* gene (diagramed in Figure 2B, with the addition of APOE<sup>-/-</sup>). Upon tamoxifen injection, all cells expressing MYH11 will be labeled with eYFP and excise exons 2 and 3 of the *Klf4* gene resulting in knockout of *Klf4* (henceforth referred to as “SMC eYFP<sup>+/+</sup> APOE<sup>-/-</sup> Klf4<sup>Δ/Δ</sup>” and “SMC eYFP<sup>+/+</sup> APOE<sup>-/-</sup> Klf4<sup>WT/WT</sup>” littermate control mice for simplicity). After 18 weeks of western diet, SMC eYFP<sup>+/+</sup> APOE<sup>-/-</sup> Klf4<sup>Δ/Δ</sup> mice had an approximately 50% reduction in overall lesion size as well as an improvement in multiple indices of plaque stability, both signs of a less pathological lesion<sup>34</sup>. These indices included more than a doubling of the protective fibrous cap, an increase in the ACTA2+ cells within the cap, and a decrease in the overall LGALS3+/ACTA2+ ratio<sup>34</sup>.

Such a decrease is indicative of a lesion with less macrophage-like cells compared to matrix producing cells. Interestingly, these profound morphological changes were also accompanied by shifts in the SMC populations within the lesion and media. SMC eYFP<sup>+/+</sup> APOE<sup>-/-</sup> Klf4<sup>Δ/Δ</sup> mice had the same number of eYFP<sup>+</sup> SMC within the lesion as SMC eYFP<sup>+/+</sup> APOE<sup>-/-</sup> Klf4<sup>WT/WT</sup> mice, but had a 53% reduction in SMC derived macrophage-like cells within lesion and a 70% reduction in SMC derived MSC-like SMCs within the media<sup>34</sup>. These results were confirmed both by single cell counting and flow cytometric analysis (although flow cytometry does not provide spatial information). To identify the downstream KLF4 target genes within SMCs that are resulting in destabilization of lesions and an increase in macrophage-like SMCs, comparative *in vivo* KLF4 ChIP-Seq analyses was performed on advanced atherosclerotic lesions from wild type and SMC *Klf4* knockout mice.

### ***Klf4* binds over 800 putative target genes within SMC in advanced atherosclerotic lesions**

KLF4 ChIP-Seq analysis was performed on tissue samples pooled (16 mice per genotype) from both wild type and knockout animals fed 18 weeks of western diet<sup>34</sup>. The samples were isolated from an atherosclerosis prone region of the vasculature that included part of the aortic arch, the brachiocephalic artery, and the left and right carotids up to the internal/external carotid bifurcation<sup>34</sup>. This region is made up of a mixed pool of cells, thus Shankman *et al.* utilized the power of the cell specific knockout system to isolate only *Klf4* targets within

SMCs (or *Klf4* targets that had a reduction in enrichment as a result of *Klf4* knockout in SMC) by comparing sequencing reads from SMC eYFP<sup>+/+</sup> APOE<sup>-/-</sup> *Klf4*<sup>WT/WT</sup> mice to reads from SMC eYFP<sup>+/+</sup> APOE<sup>-/-</sup> *Klf4*<sup>Δ/Δ</sup> mice<sup>34</sup>. This analysis identified over 800 genes that were selectively enriched in SMC eYFP<sup>+/+</sup> APOE<sup>-/-</sup> *Klf4*<sup>WT/WT</sup> mice compared to SMC eYFP<sup>+/+</sup> APOE<sup>-/-</sup> *Klf4*<sup>Δ/Δ</sup> mice<sup>34</sup>. The identified genes included *Acta2* and *Tagln*, two SMC marker genes that have known *Klf4* binding sites and have been shown to be bound by KLF4 during phenotypic switching<sup>34</sup>. Pathway analysis of the 800+ differentially enriched genes identified an assortment of impacted pathways, including markers of macrophage activation, antigen processing, and immune responses<sup>34</sup>.

Taken together the previous results demonstrate that *Klf4* is critical for the transition of SMCs to a macrophage-like state, and that activation of *Klf4* within SMCs in atherosclerotic lesions has detrimental consequences on overall lesion pathogenesis.

## **Identification of a *Klf4* dependent SMC role in injury repair**

### **SMCs may contribute to the healing process post ischemia reperfusion injury (IRI)**

*Klf4* activation within SMCs did not evolve to enable SMCs to transition to macrophage-like cells in the setting of atherosclerosis. Atherosclerosis related mortality occurs after our reproductive years, therefore *Klf4* expression within

SMCs in atherosclerosis is likely maladaptive and *Klf4* expression in SMCs likely evolved for another purpose. To investigate another role for *Klf4* activation in SMCs, we focused on injury repair processes. During injury repair, SMCs need to undergo phenotypic modulation to contribute to the angiogenic process<sup>81</sup>. Macrophages and other inflammatory cells, potentially including phenotypically modulated SMCs, are also recruited to the site of injury<sup>82</sup>. One example of such an injury repair process is the healing of the myocardium post ischemia-reperfusion injury induced myocardial infarction (IRI-MI).

Following IRI-MI, healing of the injured myocardium occurs through a series of events involving multiple cell types<sup>83</sup>. Initially, inflammatory cells infiltrate the infarct zone and release cytokines such as IL-1 $\beta$  and TNF $\alpha$ <sup>83,84</sup>. They also release matrix metalloproteinases for degradation of the collagen scaffold<sup>83,84</sup>. Next, phagocytes clear the wound of dead cells and extracellular matrix debris, while stimulating myofibroblasts to synthesize and deposit new collagen for formation of fibrotic scar tissue<sup>83</sup>. During this early proliferative stage, neovascularization occurs to restore oxygen and nutrient flow to the cells within the infarct zone. Finally, collagen fibrils are formed through matrix cross-linking, neovessels mature, and at least some myofibroblasts undergo apoptosis<sup>83,85</sup>. However, the persistence of myofibroblasts in the scar tissue leads to progressive fibrosis<sup>85</sup>. Additionally, myofibroblasts can contribute to interstitial fibrosis in remote sites within the non-infarcted myocardium, causing adverse ventricular remodeling. Over time, accumulating fibrotic tissue results in

cardiac stiffness which, combined with the loss of cardiomyocytes, leads to left ventricular dilation and dysfunction, culminating in heart failure<sup>85,86</sup>.

SMCs may contribute to the macrophage/phagocytic cell and/or myofibroblast populations following myocardial infarction, as we have previously seen these transitions occur in the setting of atherosclerosis (described in detail previously)<sup>30,34</sup>. Recent work from Kanisicak *et al.* has provided compelling evidence based on rigorous lineage tracing models that SMCs contributed only a small fraction of the total myofibroblast population<sup>25</sup>. Interstitial cardiac fibroblasts, and not SMCs or cells of myeloid origin, are the primary source of myofibroblasts within the infarct zone<sup>25</sup>. However, the origin of the macrophage population following MI remains unclear. Heidt *et al.* demonstrated that a population of CD11b+, F4/80<sup>high</sup>, and Ly-6C<sup>low</sup> resident macrophages within the heart rapidly disappear within 24 hours after myocardial infarction and are replaced by circulating monocytes, suggesting a minimal role of resident macrophages in the healing myocardium<sup>87</sup>. However, this population of macrophages only comprises approximately two percent of total cardiac macrophages and is only one of the four groups of resident macrophages found within the myocardium<sup>88</sup>. Two of these groups of resident macrophages (CD11b+, F4/80+, Ly-6C-, and MHC-II<sup>Hi</sup> or MHC-II<sup>Low</sup>) are Ly-6C- and thus would have not been included in their analysis<sup>88</sup>. Indeed, following AngII induced inflammation or myocardial infarction, these two groups of resident macrophage populations expand, through local proliferation and monocyte infiltration, and remain the primary contributors to the cardiac macrophage population that has

been shown to be important in cardiac remodeling post-myocardial infarction<sup>88</sup>. SMCs may contribute to the expansion of these groups of macrophages by transitioning to a macrophage-like state through a *Klf4* dependent mechanism, similar to what we have previously seen in atherosclerosis<sup>30,34</sup>. Moreover, additional *Klf4* dependent changes in SMC function may also play a key role in the healing myocardium including being involved in neovascularization of the infarct zone and/or secreting various growth factors and cytokines.

## Conclusion

Overall, IRI is an excellent model to study *Klf4* dependent SMC functions in the setting of injury repair. The heart is a self-contained functional system, allowing us to assay functional output following injury with or without knockout of *Klf4* in SMCs. An additional benefit of working within the heart is the ability to use non-invasive imaging modalities, such as echocardiography, to follow a variety of functional parameters over time in the same animals. Thus, in combination with our lineage tracing and knockout mouse models we can investigate SMC contributions to the cell populations discussed above, as well as assay whether knockout of *Klf4* in SMCs leads to any changes in heart function post IRI.

**We hypothesize that the summation of *Klf4* dependent transitions in SMC phenotype and function play a critical, beneficial role in maintenance of vascular integrity and/or neovascularization during tissue repair.** Our previous work in the setting of atherosclerosis suggests that *Klf4* is important to SMC phenotypic modulation to a macrophage-like state. It remains to be seen

whether this state is detrimental post IRI, like it is in atherosclerotic lesions, or if it has beneficial effects within the healing myocardium.

**Figure 1: Schematic of factors that control SMC marker gene expression in differentiated and de-differentiated states**

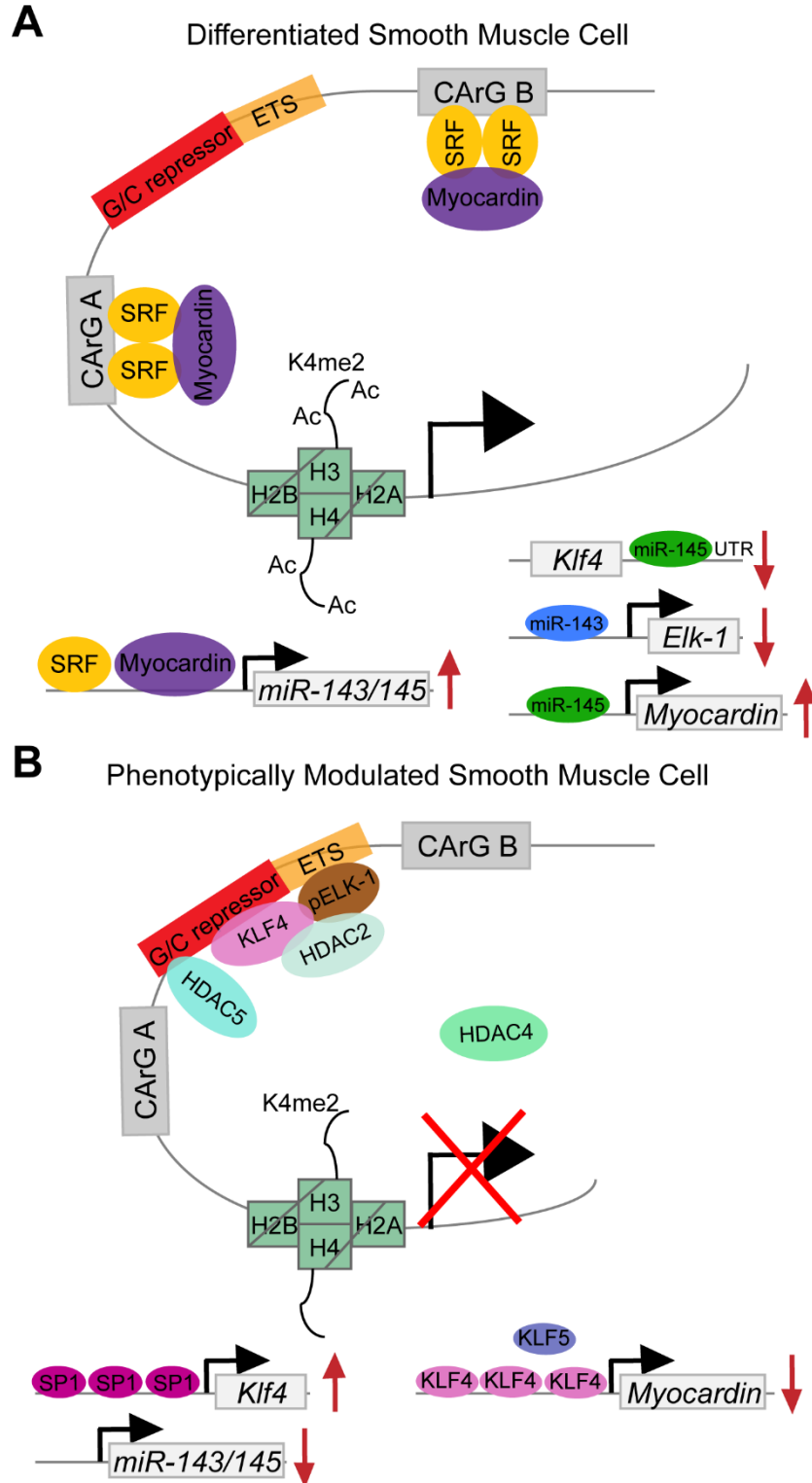


**Figure 1: Schematic of factors that control SMC marker gene expression in differentiated and de-differentiated states**

(A) Representative schematic of control of the differentiated SMC state. SRF and myocardin complexes are bound to the CArG boxes driving transcription of SMC marker genes. They are also bound to the miR-143/145 promoter driving expression of miR143 and miR145 which in turn downregulate KLF4 and ELK-1 and upregulate myocardin. The chromatin is in an open state with histones H3 and H4 acetylated (one nucleosome and one of each of the pairs of histones shown for simplicity). H3K4 is methylated, perhaps tethering myocardin to SMC gene promoters.

(B) Representative schematic of de-differentiation of a SMC. pELK-1 binds to the ETS site overlapping the G/C repressor, both disrupting myocardin's interaction with SRF and recruiting KLF4 to the G/C repressor. KLF4 then recruits HDAC2, HDAC4, and HDAC5 to the promoter, which results in deacetylation of histones H3 and H4 and a closed chromatin state. HDAC2 and HDAC5 directly bind to the G/C repressor region, however only HDAC2 forms a higher order complex with KLF4 and pELK-1. KLF4 is upregulated by binding of SP1 to its promoter, while it in turn binds to the myocardin promoter and downregulates its expression. KLF5 also binds to the myocardin promoter and downregulates its expression.

**Figure 2: SMC lineage tracing mouse schematic with and without knockout**

of *Klf4*

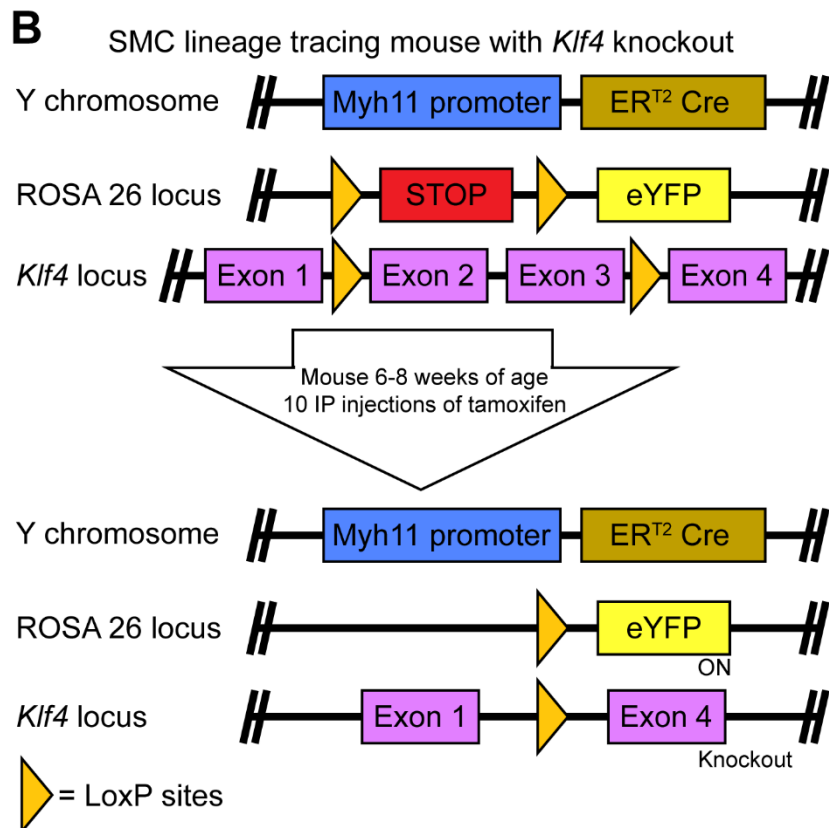
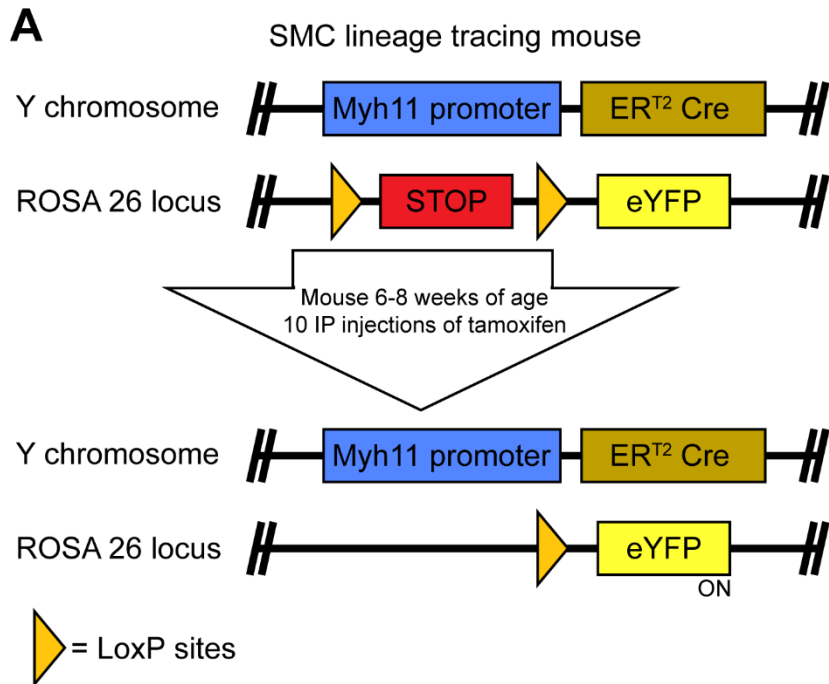


**Figure 2: SMC lineage tracing mouse schematic with and without knockout of *Klf4***

(A) SMC lineage tracing mouse schematic. Cre recombinase expression is driven by a *Myh11* promoter construct. Upon tamoxifen injection (6-8 weeks of age, 10 IP injections), the cre recombinase traffics to the nucleus where it recombines the DNA between the loxp sites, in this case the STOP codon in the ROSA 26 locus. This results in expression of the eYFP gene in cells expressing *Myh11* at the time of tamoxifen injection.

(B) Schematic representation of the SMC lineage tracing mouse with *Klf4* knockout. Upon tamoxifen injection, cells expressing *Myh11* have their cre recombinase trafficked to the nucleus where it recombines the DNA between the loxp sites in the ROSA26 locus and the *Klf4* locus. This results in permanent labeling of these cells with eYFP, as well as knockout of *Klf4*.

**Chapter II: *Klf4* has an unexpected protective role  
in perivascular cells within the microvasculature**

Authors: Ryan M Haskins, Anh T Nguyen, Gabriel F Alencar, Marie Billaud, Molly R Kelly-Goss, Miranda E Good, Katharina Bottermann, Alexander L Klibanov, Brent A French, Thurl E Harris, Shayn M Peirce, Brant E Isakson, Gary K Owens

Adapted from *American Journal of Physiology – Heart and Circulatory Physiology* article

## **Abstract**

Recent smooth muscle cell (SMC) lineage tracing studies have revealed SMCs undergo remarkable changes in phenotype during development of atherosclerosis. Of major interest, we demonstrated that KLF4 in SMC is detrimental for overall lesion pathogenesis in that SMC-specific conditional knockout of *Klf4* resulted in smaller, more stable lesions that exhibited marked reductions in the numbers of SMC-derived macrophage-like and mesenchymal stem cell-like cells. However, since the clinical consequences of atherosclerosis typically occur well after our reproductive years, we sought to identify beneficial KLF4-dependent SMC functions that were likely to be evolutionarily conserved. Herein we tested the hypothesis that *Klf4*-dependent SMC transitions play an important role in tissue injury-repair.

Utilizing SMC-specific lineage tracing mice +/- simultaneous SMC-specific conditional knockout of *Klf4*, we demonstrate that SMCs in the remodeling heart following ischemia-reperfusion injury (IRI) express KLF4 and transition to a *Klf4*-dependent macrophage-like state and a *Klf4*-independent myofibroblast-like state. Moreover, SMC-*Klf4* knockout mice had exacerbated heart failure following IRI. Surprisingly, we observed significant cardiac dilation in SMC-*Klf4* knockout mice prior to IRI, as well as a reduction in peripheral resistance. KLF4 ChIP-Seq analysis on mesenteric vascular beds identified potential baseline SMC KLF4 target genes in numerous pathways including PDGF and FGF. Moreover, microvascular tissue beds in SMC-*Klf4* knockout mice had gaps in lineage traced SMC coverage along the resistance arteries and exhibited increased

permeability. Taken together, these results provide novel evidence that *Klf4* has a critical maintenance role within microvascular SMCs, including being required for normal SMC function and coverage of resistance arteries.

## **Introduction**

Smooth muscle cells (SMC) are non-terminally differentiated, highly plastic cells that can undergo reversible phenotypic switching from a differentiated, contractile state to a proliferative, migratory state that also exhibits increased ECM synthesis<sup>4</sup>. This plasticity is essential for the development of new blood vessels and the repair of damaged ones. Upon vascular injury or stimulation with a variety of cytokines, including PDGFBB or IL-1 $\beta$ , SMC upregulate the stem cell pluripotency factor KLF4 resulting in the subsequent down regulation of SMC contractile/marker genes such as *Myh11*, *Acta2* and *Tagln*<sup>24</sup>. Indeed, recent SMC lineage tracing studies by our lab and others have shown that attempts to identify SMC-derived cells following injury or during development of atherosclerosis using typical SMC marker panels not only fails to identify the majority of SMC-derived cells but also misidentifies them as being other cell types<sup>30,33,34</sup>. For example, we showed that >80% of SMC-derived cells are negative for SMC markers like ACTA2, and of these, >50% have activated multiple markers of macrophages including LGALS3, CD11b, F4/80, and CD11c, myofibroblasts (ACTA2+ MYH11-), and/or mesenchymal stem cells (Sca1+ CD105+) <sup>34</sup>. Similar SMC lineage tracing model systems have been used by other labs to show that SMC also transition to a variety of other cell types,

including beige adipocytes in response to cold stress<sup>89</sup>, and to myofibroblasts following myocardial infarction (MI) induced by permanent ligation of the left anterior descending artery<sup>25</sup>.

One of the key proteins that controls SMC phenotypic switching is the zinc finger transcription factor KLF4. KLF4 is not normally expressed within SMC in large conduit arteries, but is rapidly induced upon vascular injury<sup>57</sup>. Upon induction, KLF4 contributes to the down regulation of SMC marker genes through several known mechanisms including KLF4 recruitment by pELK-1 to the G/C repressor regions of SMC marker gene promoters and the subsequent recruitment of HDAC2, HDAC4, and HDAC5, resulting in epigenetic silencing of the locus through deacetylation<sup>27,58</sup>. KLF4 induction also reduces expression of the SMC master differentiation control gene myocardin and destabilizes serum response factor (SRF) binding to SMC marker gene promoters<sup>57</sup>. KLF4 can also repress SMC growth at least in part through binding to the p21<sup>WAF1/Cip1</sup> promoter along with p53<sup>24</sup>. Taken together the preceding results indicate that *Klf4* is activated upon vascular injury and plays a critical role in regulating phenotypic transitions of arterial SMC but is not normally expressed in healthy conduit arteries.

Little is known about the factors and mechanisms that control SMC phenotypic transitions *in vivo*. However, recent studies in our lab have shown that *Klf4*-dependent transitions in SMC phenotype and function play a critical role in the pathogenesis of atherosclerosis. SMC specific conditional knockout of *Klf4* within Western diet fed ApoE<sup>-/-</sup> mice resulted in marked reductions in lesion size

and increased multiple indices of plaque stability including a doubling of the fibrous cap thickness<sup>34</sup>. Notably, loss of *Klf4* in SMC did not result in a change in the overall number of SMC within lesions but significantly reduced the number of SMC-derived macrophage- and MSC-like cells while increasing the ACTA2+ cells that invested in the fibrous cap<sup>34</sup>. Comparative *in vivo* ChIP-Seq analyses of advanced atherosclerotic lesions from wild type and SMC *Klf4* knockout mice identified over 800 putative KLF4 regulated genes, including >70 encoding markers of macrophage activation, antigen processing, and immune responses<sup>34</sup>. These results suggest that *Klf4* is critical for the transition of SMC to a macrophage-like state, and that activation of *Klf4* within SMC in atherosclerotic lesions has detrimental consequences on overall lesion pathogenesis. This suggests that *Klf4* activation in atherosclerosis is maladaptive, and that *Klf4*'s activation and function in SMC evolved for another purpose.

One possible setting where *Klf4* activation in SMC may be beneficial, and thus evolutionarily conserved, is in the setting of injury-repair. During injury-repair, SMC need to phenotypically modulate to contribute to the angiogenic process<sup>81</sup>. Macrophages and other inflammatory cells, potentially including phenotypically modulated SMC, are also recruited to the site of injury<sup>82</sup>. One example of such an injury-repair process is the healing myocardium post ischemia-reperfusion injury MI (IRI-MI). Following acute IRI-MI, healing of the injured myocardium begins with an influx of inflammatory cells including large numbers of phagocytic cells positive for macrophage markers that infiltrate the infarct zone and release cytokines as well as matrix metalloproteinases<sup>83,84</sup>.

These phagocytic cells also play a critical role in clearing the infarct zone of dead cells and ECM debris, while stimulating myofibroblasts to produce new collagen for formation of fibrotic scar tissue<sup>85</sup> as well as stimulating angiogenesis and revascularization of the infarct zone<sup>90</sup>. SMC may contribute to the expansion of these groups of phagocytic cells by transitioning to a macrophage-like state through a *Klf4* dependent mechanism, similar to what we have previously seen in atherosclerosis<sup>30,34</sup>. Moreover, additional *Klf4* dependent changes in SMC function may influence neovascularization of the infarct zone, including through the secretion of various growth factors and cytokines by SMC.

*Studies herein utilize our novel SMC lineage tracing and conditional Klf4 knockout mice to test the hypothesis that the summation of Klf4 dependent transitions in SMC phenotype and function play a critical, beneficial role in maintenance of vascular integrity and/or neovascularization during tissue repair.*

Using an IRI model, we found that SMC are a relatively minor source of myofibroblasts and macrophages post IRI-MI, with the macrophage-like transitions being *Klf4* dependent. However, contrary to expectations, we discovered that *Klf4* plays a critical protective role within resistance vessels at baseline, in that conditional SMC-specific *Klf4* knockout resulted in acute reductions in peripheral resistance, a dilated heart, and evidence for increased vascular leakage. These changes appear to be due, at least in part, to a reduced coverage of resistance vessels with SMC and SMC derivatives, as well as dysregulation of key SMC signaling pathways including PDGF and FGF signaling.

## **Material and Methods**

### **Generation of SMC eYFP<sup>+/+</sup> Klf4<sup>WT/WT</sup> and SMC eYFP<sup>+/+</sup> Klf4<sup>Δ/Δ</sup> animals**

All animal protocols and procedures were performed in accordance with a University of Virginia Institutional Animal Care and Use Committee approved protocol. *Myh11*-CreER<sup>T2</sup> ROSA floxed STOP eYFP, *Myh11*-CreER<sup>T2</sup> ROSA floxed STOP eYFP *Klf4*<sup>wt/wt</sup>, and *Myh11*-CreER<sup>T2</sup> ROSA floxed STOP eYFP *Klf4*<sup>fl/fl</sup> male littermate control mice were used for this study. Mice were genotyped as previously described<sup>33,34</sup>. The *Myh11*-CreER<sup>T2</sup> transgene is located on the Y chromosome, thus experimental mice were exclusively male in the study. Cre recombinase was activated in male mice with a series of ten 1-mg tamoxifen (Sigma, T-5648) intraperitoneal injections from 6 to 8 weeks of age, for a total of 10 mg of tamoxifen per mouse. Mice were then given at least a 2 week period to recover before experiments/tissue isolation were performed to allow residual tamoxifen to leave the system.

### **Ischemia-Reperfusion – Acute Myocardial infarction**

SMC eYFP<sup>+/+</sup> Klf4<sup>WT/WT</sup> (n=10) and SMC eYFP<sup>+/+</sup> Klf4<sup>Δ/Δ</sup> (n=12) mice were anesthetized with pentobarbital sodium (100 mg/kg; intraperitoneal) or ketamine/xylazine (80/8 mg/kg body weight; intraperitoneal) and orally intubated. Mice were ventilated with a small animal respirator (150 strokes/min and 150-200 μl stroke volume). The heart was exposed by left thoracotomy, and the coronary artery is occluded by passing a suture beneath the left anterior descending artery (LAD) and tightening over a piece of polyethylene-60 tubing for a period of 60 minutes. Reperfusion was induced by removing the tubing. Ketoprofen or

buprenorphin (0.1 mg/kg body weight; subcutaneous) were administered as post-operative analgesics.

### **Tissue harvest and processing**

Mice were euthanized via carbon dioxide asphyxiation. Following euthanasia, mice whose tissues were to be used for whole mount preparations or paraffin embedding were perfused through the left ventricle of the heart near the apex with 5 mL phosphate buffered saline (PBS), followed by 10 mL 4% paraformaldehyde and another 5 mL PBS. Hearts, mesentery, retinas, and spinotrapezius muscle were dissected, post-fixed in 4% paraformaldehyde for 30 mins (whole mounts) or 2 hours (paraffin embedding) and either paraffin embedded or processed for whole mount imaging. Paraffin embedded sections were subsequently sectioned serially at 10  $\mu$ m thickness for further analysis. Heart tissues that were used for frozen sections were processed as above except used periodate-lysine-paraformaldehyde (PLP) in the place of 4% paraformaldehyde. After post fixation, frozen sections were equilibrated in increasing sucrose gradients at 4°C (7.5% sucrose overnight, 15% sucrose for 4 hours, 30% sucrose for 2 hours). After the final sucrose equilibration, tissues were embedded in optimum cutting temperature formulation (OCT), cooled in liquid nitrogen and stored at -80°C until sectioned. Frozen tissues were sectioned serially at 5  $\mu$ m thickness for further analysis.

### **Immunohistochemical and immunofluorescent analysis**

Hematoxylin and eosin staining was done on 7 day post ischemia-reperfusion injury hearts. Masson's trichrome staining was done on 7 day ischemia-reperfusion injury hearts. Immunohistochemical staining was done on baseline and 7 day post ischemia-reperfusion injury hearts using an antibody specific for KLF4 (Santa Cruz sc20691) and visualized by 3,3'-diaminobenzidine (DAB, Acros Organic). Immunofluorescent staining of paraffin embedded, frozen and whole mount tissues (heart, retina, spinotrapezius muscle) of SMC eYFP<sup>+/+</sup> Klf4<sup>WT/WT</sup> and SMC eYFP<sup>+/+</sup> Klf4<sup>Δ/Δ</sup> mice was done utilizing primary antibodies specific for GFP (Abcam ab6673, 4 μg/ml), KLF4 (R&D Systems AF3158, 1 μg/ml), LGALS3 (Cedarlane CL8942AP, 2 μg/mL), MYH11 (Kamiya Biomedical Company MC-352, 1 μg/ml), GFP biotinylated (Abcam ab6658, 4 μg/ml), and CD31 (DIA-310, 0.8 μg/ml). A primarily conjugated ACTA2-FITC (Sigma-Aldrich F3777; 1:500) antibody was also used. Secondary antibodies used for immunofluorescence include donkey anti-goat 555 (Life Technologies A21432, 1:250), donkey anti-goat 647 (Life Technologies A21447, 1:250) streptavidin, Alexa Fluor 555 (Life Technologies S32355, 1:250), and donkey anti-rat Dylight 650 (Abcam ab102263; 1:200). Animal numbers are listed in the appropriate figure legends. DAPI (Thermo Fisher Scientific D3571, 0.05 mg/mL) was also used to label DNA.

### **Image capture and analysis**

Hematoxylin and eosin, Masson's trichrome and KLF4 DAB staining were captured using a Zeiss Axioskop2 microscope fitted with an AxioCamMR3

camera. Image acquisition was performed with AxioVision40 V4.6.3.0 software (Carl Zeiss Imaging Solution). Digitized images of Masson's trichrome staining were analyzed using Image Pro Plus Software 7.0 (Media Cybernetics Inc.). Areas of interest were drawn within the software to demarcate the infarct zone and the left ventricle and then the areas of these regions were calculated.

Immunofluorescent images were captured using a Zeiss LSM700 confocal microscope. Zen 2009 Light Edition Software (Zeiss) was used to acquire a z-stack image at 1  $\mu\text{m}$  intervals at 2048 x 2048 or 1024 x 1024 resolution. Analysis of z-stack images was performed in Zen 2009 Light Edition Software (Zeiss). Quantification of cell markers was done manually in the Zen 2009 software on z-stack images to assess co-localization of markers within a single cell (DAPI+ nucleus). Quantification of gaps in eYFP+ cell coverage was done utilizing the line segment distance tool in the Zen 2009 software. Images in figures are maximum intensity projections of the confocal z-stacks. CD31 immunofluorescence pixilation was done in Image Pro Plus Software 7.0 (Media Cybernetics Inc.). Positive staining color in the left ventricle was chosen at the pixel level and defined using a color cube-based method. Area of the left ventricle was calculated as described for Masson's trichrome analysis.

### **Echocardiography**

Echocardiography was performed on a FUJIFILM VisualSonics VEVO 2100 system. In brief, mice were anesthetized via inhaled isoflurane induction at 2.5% + 500 mL/min oxygen flow and maintained at 1% + 500 mL/min oxygen flow. Mouse temperature, heart rate, and respiration rate were monitored

throughout the procedure. Warmed Aquasonic (Parker labs 01-08) ultrasound gel is applied over the thorax and a 30 MHz probe is positioned over the chest in a parasternal position to acquire images. Long and short axis B-mode and M-mode images were captured at heart rates between 400-600 beats per min and respiration rates between 100-120 respirations per minute. Analysis of heart parameters and function was done on the VEVO 2100 machine software using Simpson's method. Animal numbers are listed in appropriate figure legends.

### **Blood pressure measurements**

SMC eYFP<sup>+/+</sup> Klf4<sup>WT/WT</sup> (n=7) and SMC eYFP<sup>+/+</sup> Klf4<sup>Δ/Δ</sup> (n=5) mice were anesthetized with inhaled isoflurane + oxygen and placed on a heated surgery table. The right carotid artery was exposed and cannulated with a Millar catheter. Blood pressure measurements were taken and then animals were euthanized.

### **Blood flow measurements**

Perfluorobutane microbubbles stabilized with the lipid monolayer shell were prepared as described previously<sup>91</sup>. Microbubbles were subjected to flotation to remove large size particles to assure lack of microbubble retention in the capillaries. Microbubbles (~900 million particles per ml concentration, mean size ~2 μm, as determined by Coulter counter) were injected as intravenous bolus to isoflurane-anesthetized SMC eYFP<sup>+/+</sup> Klf4<sup>WT/WT</sup> (n = 7) and SMC eYFP<sup>+/+</sup> Klf4<sup>Δ/Δ</sup> (n = 5) animals on a warming pad. Contrast ultrasound imaging of hind limb vasculature was performed with a clinical-grade Sequoia c512 instrument equipped with 15L8 probe, in CPS mode, at 7 MHz. Lateral spatial resolution of contrast ultrasound imaging at the frequency utilized (7MHz) is ~0.2 mm; beam

elevation at focal zone is <1mm. Coupling between the tissue and the probe was achieved with ultrasound gel. Microbubbles in the target vasculature were destroyed by a high-intensity pulse (MI, 1.9), and inflow of microbubbles into the muscle was observed as replenishment of contrast, in real time (10 Hz), at MI = 0.2, which is not destructive to the microbubbles present in the field of view. Contrast replenishment video was processed using Siemens Syngo software, to compute the time constant of the replenishment curve according to a single exponential equation  $y = A(1 - e^{-\beta t})$ , where A is the plateau video intensity or microvascular cross-sectional area and  $\beta$  is the rate of rise of the video intensity or microbubble velocity. Relative volumetric flow,  $f$ , was calculated using the equation  $f = A\beta$ <sup>92</sup>. Flow was measured within a region of interest in the microvasculature of the quadriceps femoris (adjacent to the femoral artery).

### **Pressure myography**

Pressure myography was done on SMC eYFP<sup>+/+</sup> Klf4<sup>WT/WT</sup> (n = 3) and SMC eYFP<sup>+/+</sup> Klf4 <sup>$\Delta/\Delta$</sup>  (n = 3) animals as previously described<sup>93</sup>. In brief, mice were euthanized by CO<sub>2</sub> asphyxia and first order mesenteric arteries were isolated and placed in Krebs-HEPES containing (in mM) NaCl 118.4, KCl 4.7, MgSO<sub>4</sub> 1.2, NaHCO<sub>3</sub> 4, KH<sub>2</sub>PO<sub>4</sub> 1.2, CaCl<sub>2</sub> 2, HEPES 10, and glucose 6. Isolated vessels were then transferred to a pressure arteriograph (Danish MyoTechnology), cannulated at both ends with glass micropipettes, and secured with 10–0 nylon monofilament suture. Arteries were perfused with Krebs-HEPES supplemented with 1% BSA and superfused with Krebs-HEPES. Arteries were pressurized to 80 mmHg and heated to 37°C for a 30 minute equilibration step.

Following equilibration, vessels were stimulated with cumulative concentrations of phenylephrine (2 vessels per animal, PE,  $10^{-9}$  to  $10^{-4}$  M; Sigma), acetylcholine (4 wild type vessels, 3 knockout vessels, ACh,  $10^{-9}$  to  $10^{-3}$  M) or sodium nitroprussiate (7 wild type vessels, 8 knockout vessels, SNP,  $10^{-10}$  to  $10^{-3}$  M) and luminal diameter was assessed in  $\mu\text{m}$  using the DMT vessel acquisition suite. Results are expressed in mean  $\pm$  SEM or percent maximal lumen diameter. The maximal lumen diameter was determined at the end of the PE dose response by incubating arteries in calcium-free Krebs-HEPES containing ethylenbis-(oxyethyleninitrolo) tetra-acetic acid (EGTA, 2 mmol/L) and sodium nitroprussiate (SNP, 10  $\mu\text{mol/L}$ ).

Passive diameter (2 vessels per animal) was measured by increasing the intraluminal pressure from 0 mmHg to 140 mmHg by steps of 20 mmHg in a calcium free Krebs-HEPES supplemented with EGTA and SNP as described above. The lumen diameter was measured as described above and expressed in mean  $\pm$  SEM or % increase from 0 mmHg.

#### **KLF4 chromatin immunoprecipitation-sequencing (ChIP-seq) analysis**

Mesenteric arcades were isolated from SMC eYFP<sup>+/+</sup> Klf4<sup>WT/WT</sup> (n=7) and SMC eYFP<sup>+/+</sup> Klf4 <sup>$\Delta/\Delta$</sup>  mice (n=7) and snap-frozen in liquid nitrogen. Frozen tissues were ground in a mortar and pestle, resuspended in PBS with sodium butyrate (Sigma-Aldrich B5887, 20mM), and subsequently spun at 500g in a centrifuge to remove lipids. Remaining cells were then pooled by mouse genotype and processed for ChIP-seq as previously described<sup>34</sup>. In brief, cells were fixed with 1% paraformaldehyde for 10 minutes at room temperature.

Cross-linked chromatin was then sheared by sonication into fragments 200-600 base pairs in size. The chromatin fragments were then immunoprecipitated with anti-KLF4 (Santa Cruz sc20691, 2  $\mu$ g) antibody complexed with magnetic bead-coupled protein G (ThermoFisher 10004D, 10  $\mu$ L beads per sample). Genomic DNA was then eluted and purified off the bead complexes and library construction was performed using the TruSeq DNA Sample Guide protocol by Illumina following manufacturer's instructions. Sequencing was performed at the University of Virginia Genomics Core using an Illumina MiSeq Sequencing System.

Sequencing reads from an Illumina MiSeq Sequencing System were aligned to the mouse genome (mm9 assembly) using the BOWTIE alignment tool<sup>94</sup>. These aligned reads were then processed and converted into bam/bai format (<http://genome.ucsc.edu/goldenPath/help/bam.html>), and then loaded in the Integrative Genomics Viewer (<http://www.broadinstitute.org/igv/>) for visualization. The processing steps involved removing duplicate reads and format conversions using the SAMtools suite<sup>95</sup>. The reads were also converted to BED format (<http://genome.ucsc.edu/FAQ/FAQformat#format1>) for further data analysis processes such as peak calling. KLF4 peaks were identified using MACS14<sup>96</sup> using the SMC eYFP<sup>+/+</sup> Klf4 $\Delta/\Delta$  as input and with a *P* value for significant peak calling  $\leq 1 \times 10^{-6}$ . Once peaks were obtained, BEDtools<sup>97</sup> was used to identify the closest genes to each peak. Functional annotation was performed using DAVID<sup>98</sup> and PANTHER (<http://pantherdb.org/>)<sup>99</sup>. The GSE accession number is GSE107641.

### **Intravital confocal microscopy**

Intravital confocal microscopy of the cornea was performed as previously described<sup>100</sup>. Briefly, SMC eYFP<sup>+/+</sup> Klf4<sup>WT/WT</sup> (n=7) and SMC eYFP<sup>+/+</sup> Klf4<sup>Δ/Δ</sup> (n=7) mice were anesthetized with an intraperitoneal injection of ketamine/xylazine/atropine (60/4/0.2 mg/kg body weight) (Zoetis; Kalamazoo, MI/West-Ward; Eatontown, NJ/Lloyd Laboratories; Shenandoah, IA). Topical anesthetic to numb the eye was administered as a drop of sterile 0.5% Proparacaine Hydrochloride Ophthalmic Solution before imaging. Mice were imaged on a confocal microscope (Nikon Instruments Incorporated, Melville, NY; Model TE200-E2; 20X objective optimized for 2 channels-laser excitation wavelengths at 488 and 543). Ophthalmic lubricant Genteal gel (Alcon; Fort Worth, TX) was applied to the eye to prevent drying during imaging. Eyelashes and whiskers were gently pushed back with Genteal gel, mice were placed on a microscope stage with a warming pad, and the snout was gently restrained with a nosecone.

### **Permeability measurements and quantification**

Following anesthetization, 70 kilodalton Dextran-Rhodamine B (ThermoFisher D1841, 5 mg/ml) was administered via a retro-orbital injection immediately prior to imaging, such that movie recording started < 5 minutes post-injection. Digital images of the vascular networks were acquired using a NikonTE200-E2 confocal microscope, as described above. One field of view per cornea was imaged with full-thickness Z-stacks (25-30 slices at 3 μm between each slice) on repetition for 60 minutes. To capture the entire corneal vascular

network in the field of view, we created volume renders of z-stacks using the maximum intensity projection. Then, using ImageJ, we measured the mean pixel intensity in three equal-size regions of interest (ROIs) that were evenly distributed across three different areas in the field of view (above limbus, in vascular loops within the limbus, and below the A-V pair defining the start of the limbus), for a total of nine ROIs being analyzed per frame. These values were then plotted against time. Finally, we quantified the Area Under the Curve to capture the total leak of dextran from the vasculature over time. Researchers were blinded to the genotype of the animals until the end of analysis.

### **Bone marrow transfer**

Bone marrow transfers were performed as previously described<sup>101</sup>. Briefly, eYFP<sup>+/+</sup> Klf4<sup>Δ/Δ</sup> (n=3) recipient mice were lethally irradiated with a dose of 1200RADS (2x 600RADS, 3 hours apart). 30 minutes after radiation, unfractionated bone marrow cells taken from femurs of whole body DsRED+ mice were administered to recipient mice via retro-orbital injections, 1 x 10<sup>6</sup> cells/mouse. Bone marrow was allowed to reconstitute for 6 weeks. After 6 weeks, mice received the normal series of 10 intraperitoneal tamoxifen injections (1-mg tamoxifen, Sigma, T-5648). Following a 2 week rest period, mice received a retro-orbital injection of isolectin-Alexa fluor 647 (ThermoFisher I32450) 30 minutes prior to euthanasia. Tissues were then isolated and processed for whole mount imaging.

## Statistical Analysis

Statistics were performed using GraphPad Prism Version 6 software. The Kolmogorov-Smirnoff normality test was used to determine if data were normal. To assess genotype contributions to various echocardiography parameters across multiple time points, two-way analysis of variance (ANOVA) was performed. ANOVA was also used to compare groups in pressure myography experiments. For individual comparisons between data, unpaired two-tailed *t*-tests were performed. Welch's correction was applied when variance was not equal between groups. Mann Whitney *U* tests were performed instead of *t*-tests if the data was non-normally distributed. The statistical tests used for each set are detailed in the figure legends.

## Results

### **KLF4 is upregulated in SMC within the infarct zone post ischemia-reperfusion (acute MI)**

We began by determining if SMC express KLF4 post IRI-MI utilizing our previously described tamoxifen inducible SMC lineage tracing system (*Myh11-CreER<sup>T2</sup> ROSA floxed STOP eYFP, SMC YFP<sup>+/+</sup>*)<sup>33</sup>. In agreement with the literature, we found no evidence of eYFP+ lineage traced SMC expressing KLF4 at baseline (Figure 3A, yellow arrows). However, after a 1 hour left anterior descending artery occlusion followed by reperfusion, there was a marked increase in KLF4 expression within the heart, especially within the infarct zone (Figure 3B). A subset of these KLF4 expressing cells were eYFP+, indicating

they were of SMC origin (see SMC highlighted with white arrows in Figure 3C). Based on these observations, we proceeded to test how SMC specific conditional knockout of *Klf4* impacted cardiac function before and after IRI-MI induced by a sixty minute ligation of the left anterior descending artery. *Myh11-CreER<sup>T2</sup>* ROSA floxed STOP eYFP *Klf4<sup>fl/wt</sup>* male and ROSA floxed STOP eYFP *Klf4<sup>fl/wt</sup>* female mice were bred yielding a 1:2:1 ratio of *Myh11-CreER<sup>T2</sup>* ROSA floxed STOP eYFP *Klf4<sup>wt/wt</sup>* and *Myh11-CreER<sup>T2</sup>* ROSA floxed STOP eYFP *Klf4<sup>fl/fl</sup>* male littermate control mice for experimental use. After a series of 10 tamoxifen injections at 6-8 weeks of age, we observed high efficiency (>95%), simultaneous activation of the eYFP reporter gene and knockout of *Klf4* exclusively in SMC in the *Klf4<sup>fl/fl</sup>* mice yielding *Myh11-CreER<sup>T2</sup>* ROSA floxed STOP eYFP *Klf4<sup>Δ/Δ</sup>* mice (Figure 3C and D) [henceforth referred to as “SMC eYFP<sup>+/+</sup> *Klf4<sup>Δ/Δ</sup>*” and “SMC eYFP<sup>+/+</sup> *Klf4<sup>WT/WT</sup>*” littermate control mice for simplicity].

### **A subset of SMC transitioned to macrophage- and myofibroblast-like cells following IRI-MI**

To determine if SMC are contributing to macrophage and myofibroblast cell populations post IRI-MI, we utilized our SMC YFP<sup>+/+</sup> mice to ascertain SMC phenotypic switching. Seven days post IRI-MI a subset of SMC transitioned to a LGALS3<sup>+</sup> macrophage-like state (Figure 4A). However, these macrophage-like SMC comprised less than 2% of the overall LGALS3<sup>+</sup> macrophage population (Figure 4B). Utilizing our SMC eYFP<sup>+/+</sup> *Klf4<sup>Δ/Δ</sup>* mice, we found that *Klf4* knockout

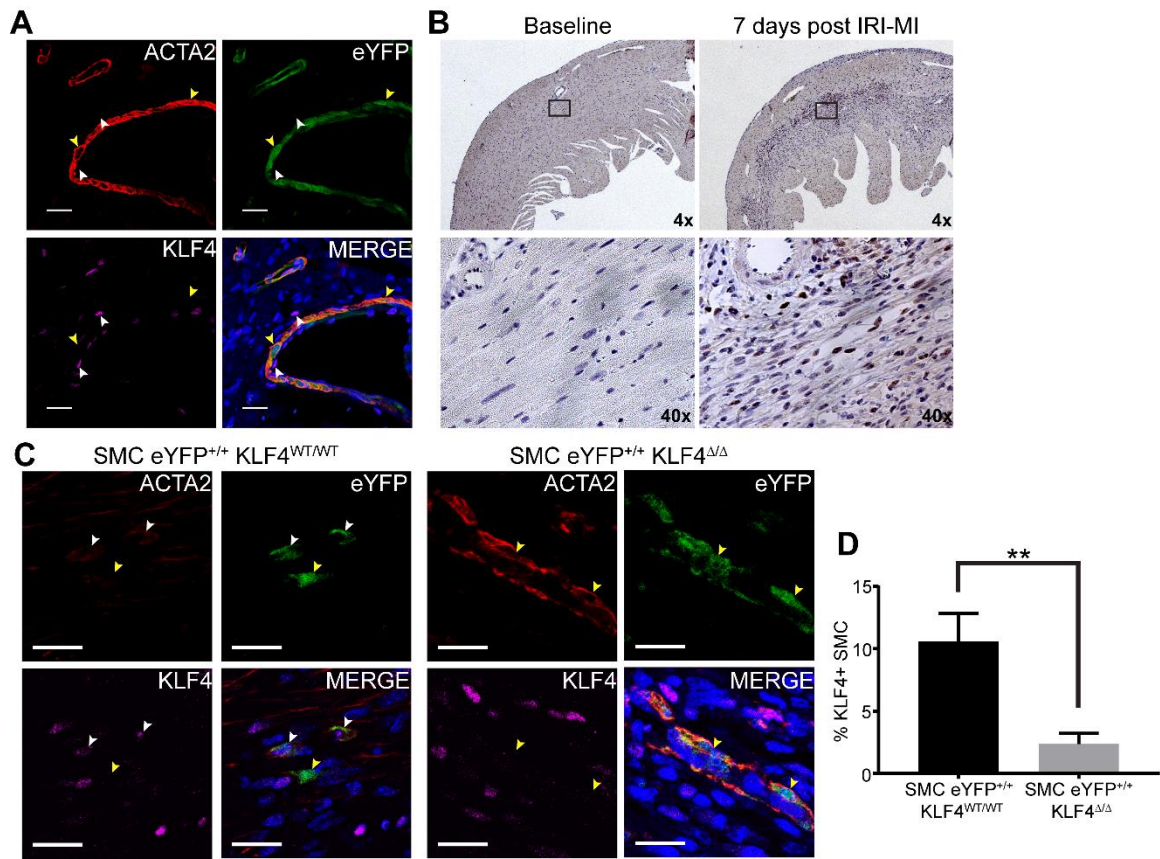


**Figure 3: KLF4 is upregulated in SMC in the infarct zone post IRI-MI**

**Figure 3: KLF4 is upregulated in SMC in the infarct zone post IRI-MI**

(A) Representative immunofluorescence images of baseline hearts from SMC eYFP<sup>+/+</sup> mice (n = 8). Yellow arrows are highlighting eYFP+KLF4<sup>-</sup> cells. White arrows are highlighting eYFP-Klf4<sup>+</sup> cells. Scale bars represent 20  $\mu$ m. (B) Representative 3,3'-Diaminobenzidine (DAB) staining for KLF4 within baseline and seven day post IRI-MI hearts. (C) Representative immunofluorescence images from SMC eYFP<sup>+/+</sup> Klf4<sup>WT/WT</sup> (n = 7) and SMC eYFP<sup>+/+</sup> Klf4 <sup>$\Delta/\Delta$</sup>  (n = 9) animals seven days post IRI-MI showing a marked decrease in eYFP+KLF4<sup>+</sup> cells in SMC eYFP<sup>+/+</sup> Klf4 <sup>$\Delta/\Delta$</sup>  animals. White arrows are highlighting eYFP+KLF4<sup>+</sup> cells. Yellow arrows are highlighting eYFP+KLF4<sup>-</sup> cells. Scale bars represent 20  $\mu$ m. (D) Quantification of eYFP+KLF4<sup>+</sup> cells in SMC eYFP<sup>+/+</sup> Klf4<sup>WT/WT</sup> (n = 7) and SMC eYFP<sup>+/+</sup> Klf4 <sup>$\Delta/\Delta$</sup>  (n = 9) animals seven days post IRI-MI. *p* value was determined by unpaired, two tailed *t*-test with Welch's correction. \*\* = *p* < 0.01.

significantly reduced the number of SMC that transitioned to a LGALS3+ macrophage-like state (Figure 4A & B). This reduction in SMC derived LGALS3+ macrophage-like cells following SMC specific *Klf4* knockout is consistent with our previous work in the setting of atherosclerosis<sup>34</sup>. We also examined whether the previously reported SMC to myofibroblast transitions<sup>25</sup> were *Klf4* dependent. Knockout of *Klf4* had no effect on SMC transitions to a myofibroblast-like state (eYFP+Acta2+Myh11-), again consistent with our published work on late stage atherosclerosis (Figure 4C & D). Taken together, these results demonstrate a role for *Klf4* in the phenotypic switching of SMC to a macrophage- but not myofibroblast-like state. However, the overall contributions of SMC to these populations was <1% for MFs<sup>25</sup> and <2% for macrophages. Nevertheless, given that *Klf4* regulates multiple SMC responses, including growth and suppression of SMC marker genes<sup>24,27,58</sup>, as well as our previous evidence of >800 KLF4 target genes in SMC, we proceeded to analyze if knockout of *Klf4* in SMC had any functional effects following IRI-MI.

### **SMC specific *Klf4* knockout induced cardiac dilation at baseline and exacerbated development of an ischemic dilated cardiomyopathy**

Hematoxylin and eosin staining of hearts seven days post IRI-MI revealed that SMC eYFP<sup>+/+</sup> *Klf4*<sup>Δ/Δ</sup> animals had dilated hearts when compared to wild type littermate controls (Figure 5A) and also exhibited an increased heart to body weight ratio at twenty one days post IRI-MI (Figure 5B). Infarct size relative to left ventricle size was not increased in knockout animals compared to wild type

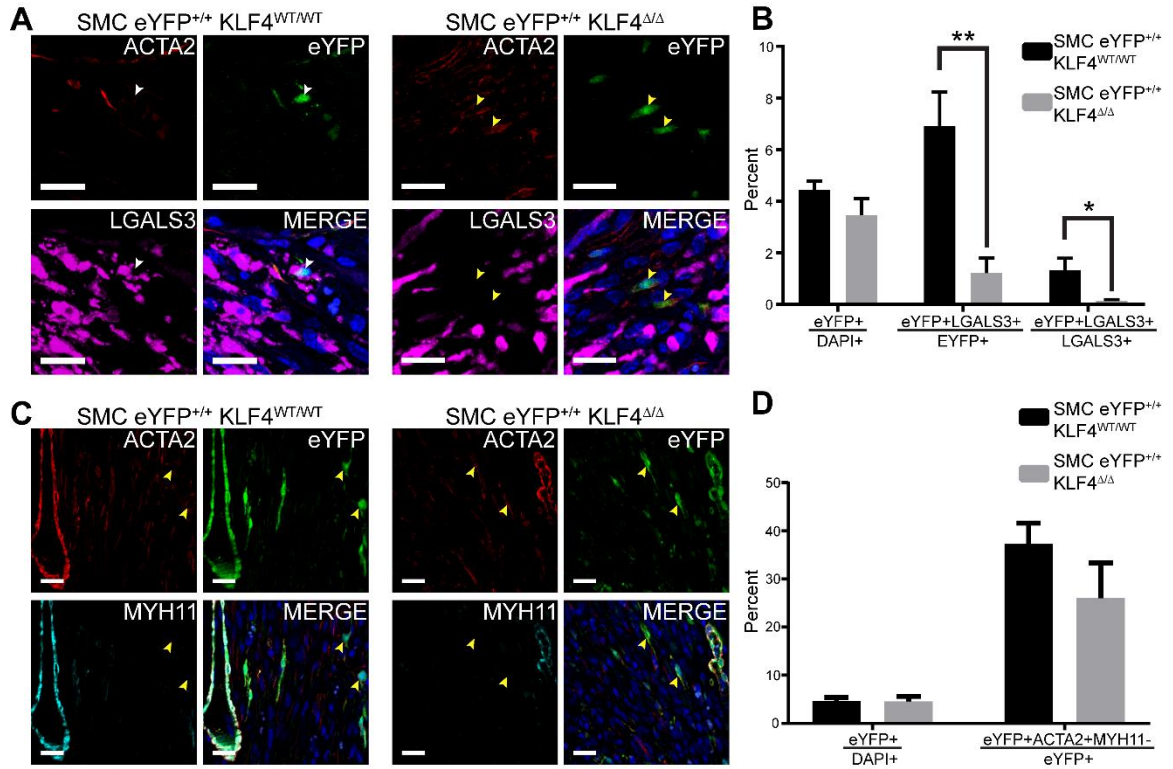


**Figure 4: SMC specific *Klf4* knockout impairs SMC phenotypic switching to macrophage-like but not myofibroblast-like cells**

**Figure 4: SMC specific *Klf4* knockout impairs SMC phenotypic switching to macrophage-like but not myofibroblast-like cells**

(A) Representative immunofluorescence images of SMC eYFP<sup>+/+</sup> Klf4<sup>WT/WT</sup> (n = 7) and SMC eYFP<sup>+/+</sup> Klf4<sup>Δ/Δ</sup> (n = 9) animals seven days post IRI-MI showing a marked decrease in eYFP+LGALS3+ cells in SMC eYFP<sup>+/+</sup> Klf4<sup>Δ/Δ</sup> animals. White arrows are highlighting eYFP+LGALS3+ cells. Yellow arrows are highlighting eYFP+LGALS3- cells. Scale bars represent 20 μm. (B) Quantification of percent eYFP+ cells within the infarct zone, percent of eYFP+ cells that are LGALS3+ within the infarct zone and percent of LGALS3+ cells that are eYFP+. Knockout of KLF4 resulted in a decrease of eYFP+LGALS3+ cells. *p* value was determined by unpaired, two tailed *t*-test for percent eYFP+ cells and unpaired, two tailed *t*-test with Welch's correction for percent eYFP+ cells that are LGALS3+ and percent LGALS3+ cells that are eYFP+. (C) Representative immunofluorescence images of SMC eYFP<sup>+/+</sup> Klf4<sup>WT/WT</sup> (n = 7) and SMC eYFP<sup>+/+</sup> Klf4<sup>Δ/Δ</sup> (n = 7) animals seven days post IRI-MI showing no difference in eYFP+ACTA2+MYH11- cells in SMC eYFP<sup>+/+</sup> Klf4<sup>Δ/Δ</sup> animals when compared to SMC eYFP<sup>+/+</sup> Klf4<sup>WT/WT</sup>. Yellow arrows are highlighting eYFP+Acta2+Myh11- cells. Scale bars represent 20 μm. (D) Quantification of percent eYFP+ cells within the infarct zone, and the percent of eYFP+ cells that are eYFP+ACTA2+MYH11- myofibroblast-like cells within the infarct zone. *p* value was determined by unpaired, two tailed *t*-test. \* = *p* < 0.05, \*\* = *p* < 0.01.

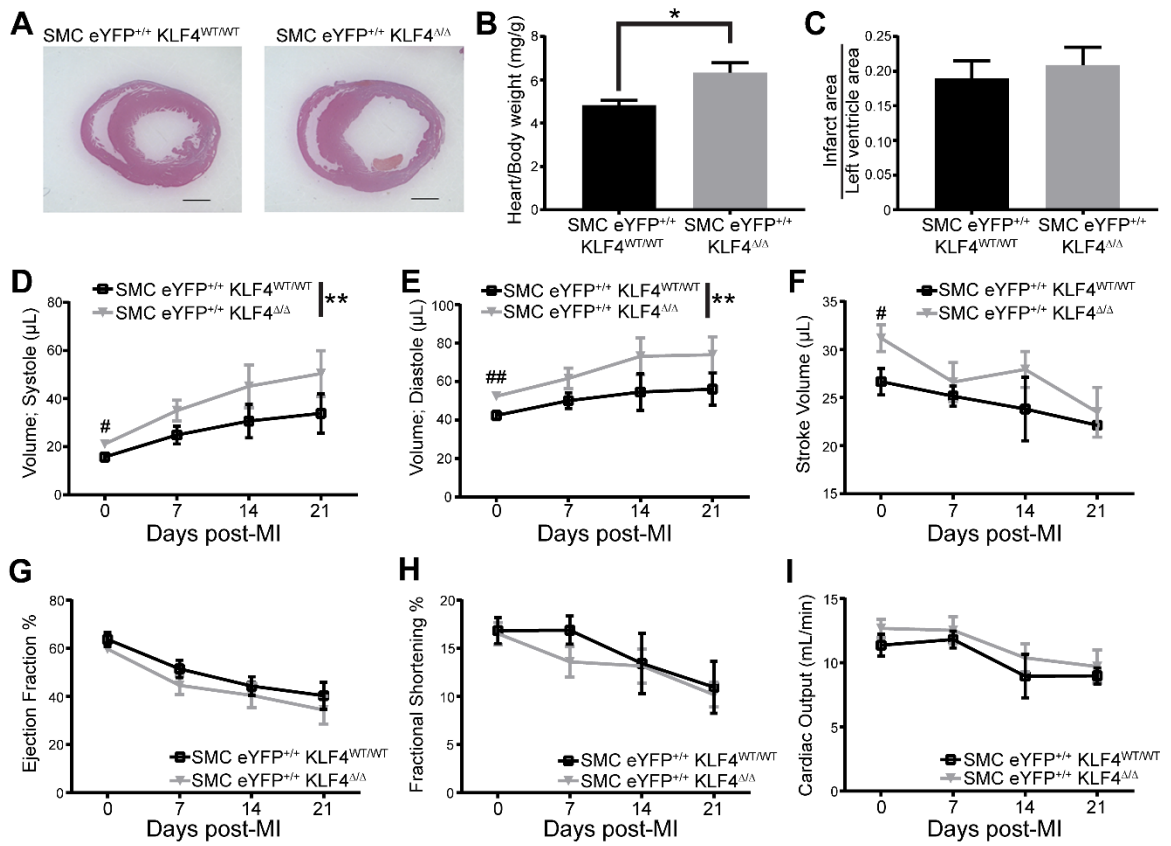


**Figure 5: SMC specific *Klf4* knockout leads to an increased cardiac dilation post MI**

**Figure 5: SMC specific *Klf4* knockout leads to an increased cardiac dilation post MI**

(A) Representative images of hematoxylin and eosin staining of SMC eYFP<sup>+/+</sup> *Klf4*<sup>WT/WT</sup> (n = 7) and SMC eYFP<sup>+/+</sup> *Klf4*<sup>Δ/Δ</sup> (n = 9) animals seven days post IRI-MI showing a cardiac dilation in the knockout animals. Scale bars represent 1 mm.

(B) Quantification of heart weight/body weight ratios for SMC eYFP<sup>+/+</sup> *Klf4*<sup>WT/WT</sup> (n = 3) and SMC eYFP<sup>+/+</sup> *Klf4*<sup>Δ/Δ</sup> (n = 4) animals twenty one days post IRI-MI. *p* value was determined by unpaired, two tailed *t*-test. (C) Quantification of infarct area as a ratio of left ventricle area for SMC eYFP<sup>+/+</sup> *Klf4*<sup>WT/WT</sup> (n = 7) and SMC eYFP<sup>+/+</sup> *Klf4*<sup>Δ/Δ</sup> (n = 9) animals seven days post IRI-MI. (D, E) Echocardiography time course of SMC eYFP<sup>+/+</sup> *Klf4*<sup>WT/WT</sup> (0 [n=12], 7 [n=6], 14 [n=3], and 21 [n=2] days post MI) and SMC eYFP<sup>+/+</sup> *Klf4*<sup>Δ/Δ</sup> (0 [n=14], 7 [n=9], 14 [n=5], and 21 [n=5] days post MI) animals. Knockout animals had increased end systolic and end diastolic volumes and an increased cardiac dilation. *p* value (\*\*) was determined by two-way ANOVA. There was also a significant increase in end systolic and end diastolic at baseline. *p* value (#, ##) was determined by unpaired, two tailed *t*-test. (F-I) Echocardiography time courses examining stroke volume, ejection fraction, fractional shortening and cardiac output show decreases as expected post IRI-MI, but no difference between knockout and wild type animals. \*\* = *p* < 0.01, # = *p* < 0.05, ## = *p* < 0.01.

animals seven days post IRI-MI (Figure 5C). The cardiac dilation in SMC eYFP<sup>+/+</sup> Klf4<sup>Δ/Δ</sup> mice was further confirmed by echocardiographic analyses of the left ventricle. Following IRI-MI, SMC specific *Klf4* knockout animals have a significantly increased end systolic and end diastolic volumes (Figure 5D & E). Functional parameters, including ejection fraction and cardiac output, were not different between knockout and wild type animals but did show a decrease over time as expected following IRI-MI (Figure 5F-I).

Closer examination of the echocardiography data showed significant increases in end systolic and end diastolic volumes at baseline, i.e. prior to IRI-MI (Figure 6A and 4B), which is only two weeks after the last tamoxifen injection and just 4 weeks since the first of our series of ten tamoxifen injections required to induce >95% Cre recombinase dependent eYFP activation and genetic knockout of *Klf4* in SMC<sup>34</sup>. The increase in end diastolic volume was larger than the increase in end systolic volume, resulting in an increase in stroke volume (Figure 6C). These data suggest that SMC eYFP<sup>+/+</sup> Klf4<sup>Δ/Δ</sup> animals had a preexisting cardiac dilation as a consequence of *Klf4* knockout in SMC. This preexisting cardiac dilation would likely negatively impact knockout animals' recovery following IRI-MI.

To investigate whether an altered myocardial capillary density, previously shown to be associated with idiopathic dilated cardiomyopathy in humans<sup>102</sup>, contributes to the cardiac dilation we see in our baseline SMC eYFP<sup>+/+</sup> Klf4<sup>Δ/Δ</sup> animals, we examined CD31+ vascular density within the left ventricle (Figure 6D). CD31+ vascular density was not altered in baseline SMC eYFP<sup>+/+</sup> Klf4<sup>Δ/Δ</sup>

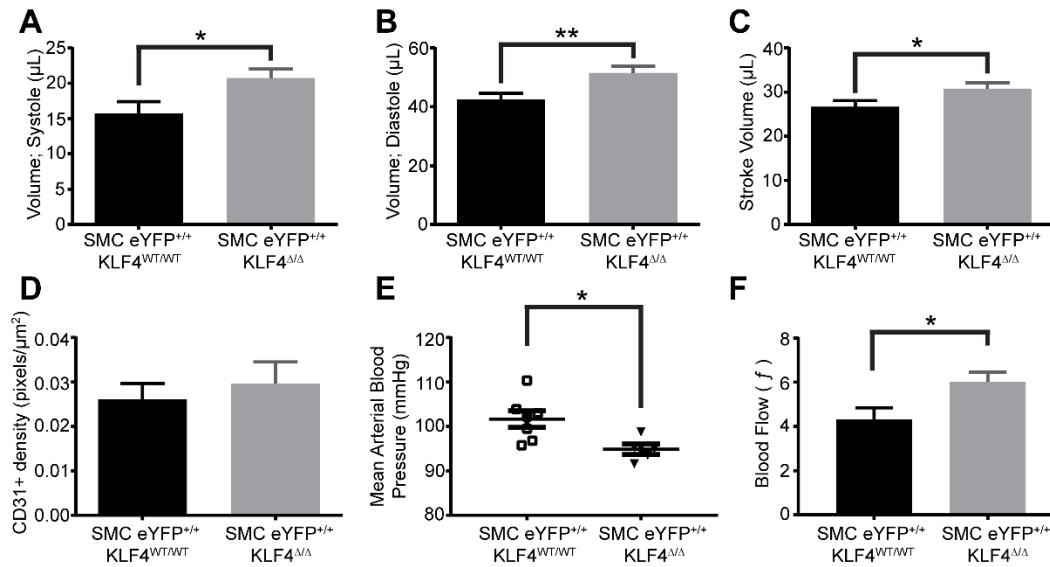


**Figure 6: SMC specific knockout of *Klf4* leads to left ventricular dilation, decreased blood pressure, and increased blood flow at baseline**

**Figure 6: SMC specific knockout of *Klf4* leads to left ventricular dilation, decreased blood pressure, and increased blood flow at baseline**

Echocardiography analysis of (A) end systolic volume, (B) end diastolic volume, (C) stroke volume at baseline in SMC eYFP<sup>+/+</sup> Klf4<sup>WT/WT</sup> (n = 12) and SMC eYFP<sup>+/+</sup> Klf4<sup>Δ/Δ</sup> (n = 14) animals. *p* value was determined by unpaired, two tailed *t*-test. (D) Quantification of CD31+ pixel density within the left ventricle of baseline SMC eYFP<sup>+/+</sup> Klf4<sup>WT/WT</sup> (n = 6) and SMC eYFP<sup>+/+</sup> Klf4<sup>Δ/Δ</sup> (n = 6) animals. (E) Blood pressure measurements were performed using a carotid blood pressure probe on SMC eYFP<sup>+/+</sup> Klf4<sup>WT/WT</sup> (n = 7) and SMC eYFP<sup>+/+</sup> Klf4<sup>Δ/Δ</sup> (n = 5) animals and showed an approximately 5 mmHg drop in blood pressure at baseline. *p* value was determined by unpaired, two tailed *t*-test. (F) Relative volumetric blood flow rate was measured by contrast ultrasound in an area of interest near the femoral artery in SMC eYFP<sup>+/+</sup> Klf4<sup>WT/WT</sup> (n = 7) and SMC eYFP<sup>+/+</sup> Klf4<sup>Δ/Δ</sup> (n = 5) animals. *p* value was determined by unpaired, two tailed *t*-test. \* = *p* < 0.05, \*\* = *p* < 0.01.

animals compared to SMC eYFP<sup>+/+</sup> *Klf4*<sup>WT/WT</sup>. Another potential cause of left ventricular dilation is a reduction in peripheral resistance. Thus, we next examined the blood pressure and blood flow rate in our mice, the two main determinants of peripheral resistance (i.e.  $Q=P/R$ ). SMC eYFP<sup>+/+</sup> *Klf4*<sup>Δ/Δ</sup> animals had an approximately 5 mmHg drop in mean arterial blood pressure at baseline when measured using a carotid blood pressure probe (Figure 6E). To calculate blood flow within the resistance arteries, we utilized contrast ultrasound combined with injectable microbubbles. We began by destroying the bubbles within the vasculature of the leg with an ultrasonic pulse and measured the subsequent bubble refill rate in a region of interest within the microvasculature of the quadriceps femoris. SMC eYFP<sup>+/+</sup> *Klf4*<sup>Δ/Δ</sup> animals had an increased relative volumetric flow rate within the region of interest (Figure 6F). Taken together, these data support the conclusion that *Klf4* has a previously unknown, protective role in SMC homeostasis and its loss results in a reduction in peripheral resistance. The main vessels responsible for peripheral resistance and blood pressure control are the resistance arteries, so we next investigated the contractile properties of the resistance arteries in our SMC *Klf4* knockout and wild type control mice.

### **SMC *Klf4* knockout resulted in increased resistance vessel passive diameter indicative of outward remodeling**

To investigate the effect of knockout of *Klf4* in SMC on resistance artery function, we performed pressure myography on first order mesenteric arteries. Under

calcium free conditions, the diameter of first order SMC eYFP<sup>+/+</sup> Klf4<sup>Δ/Δ</sup> arteries was increased at all pressures when compared to these same resistance vessels from SMC eYFP<sup>+/+</sup> Klf4<sup>WT/WT</sup> littermate control mice (Figure 7A). However, the vessel response to increasing pressure was the same between knockout and wild type mice indicating that SMC *Klf4* knockout did not alter the mechanical properties of the vessel (Figure 7B). Similarly, SMC eYFP<sup>+/+</sup> Klf4<sup>Δ/Δ</sup> resistance vessels also exhibited an increased diameter compared to those from SMC eYFP<sup>+/+</sup> Klf4<sup>WT/WT</sup> littermate controls during phenylephrine-induced contraction in calcium containing medium (Figure 7C). However, no change was seen in the ability of knockout vessels to contract in response to the phenylephrine stimulation compared to wild type vessels (Figure 7D). A possible explanation for changes in vessel diameter in our SMC eYFP<sup>+/+</sup> Klf4<sup>Δ/Δ</sup> vessels is an alternation in the vessel's response to the vasodilator NO. Thus, we examined whether there was a change in endothelial-dependent (acetylcholine treated, Figure 7E) or endothelial independent (SNP treated, Figure 7F) activation of the NO axis in isolated first order mesenteric vessels in our SMC eYFP<sup>+/+</sup> Klf4<sup>WT/WT</sup> and SMC eYFP<sup>+/+</sup> Klf4<sup>Δ/Δ</sup> animals. We observed no difference in the knockout versus wild type vessels (Figure 7E and 7F). Taken together, these results indicate that the reduced blood pressure and cardiac dilation observed in SMC-specific *Klf4* knockout mice is due at least in part to outward remodeling and/or dilation of resistance arteries. This remodeling and/or dilation is not accompanied by a change in phenylephrine dose responsiveness or the vessel's response to NO.

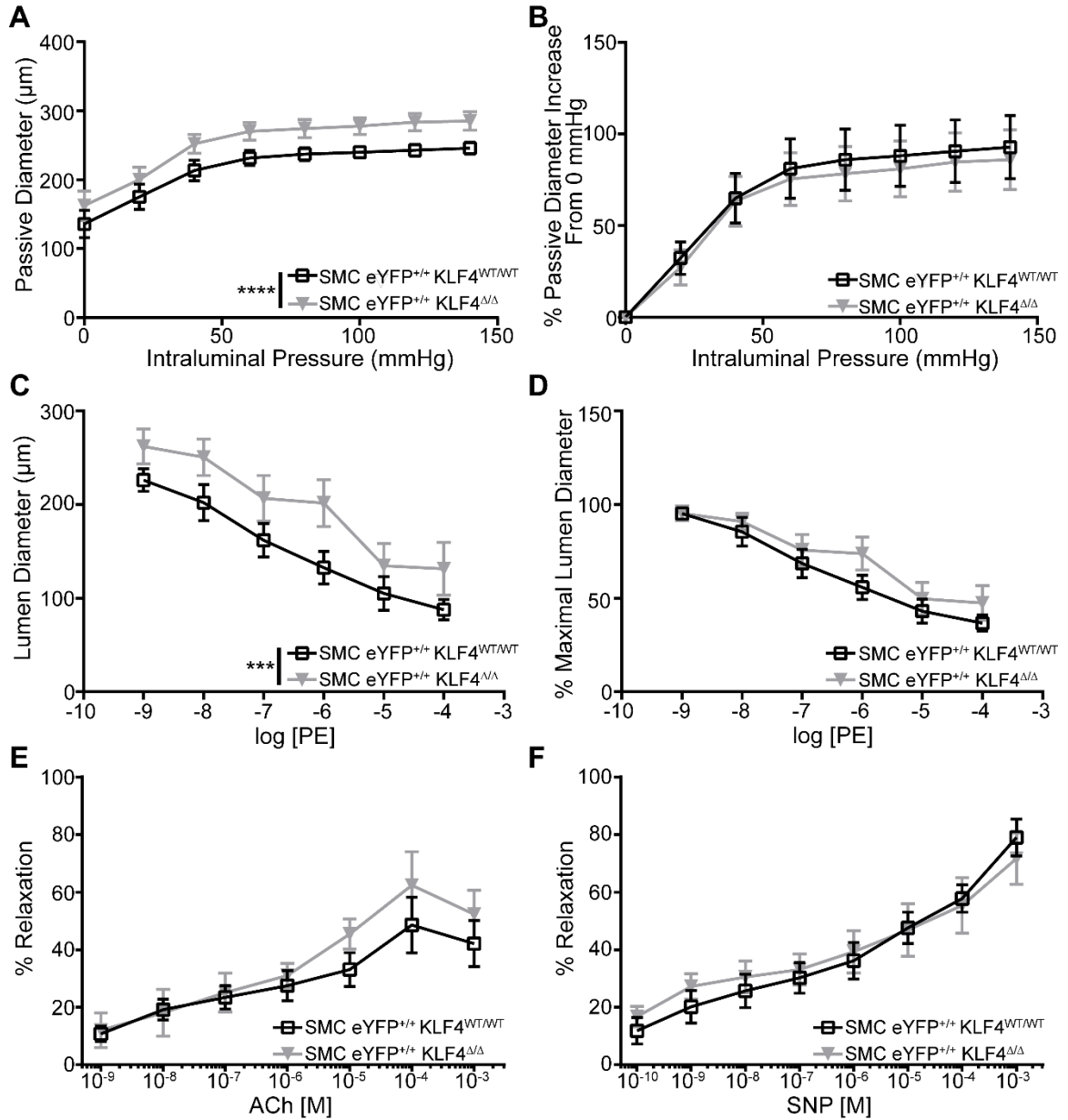


**Figure 7: SMC specific *Klf4* knockout first order mesenteric resistance arteries are dilated compared to their wild type counterparts.**

**Figure 7: SMC specific *Klf4* knockout first order mesenteric resistance arteries are dilated compared to their wild type counterparts.**

(A) Quantification of pressure myography to assess the passive properties of first order mesenteric vessels from SMC eYFP<sup>+/+</sup> *Klf4*<sup>WT/WT</sup> (n = 3) and SMC eYFP<sup>+/+</sup> *Klf4*<sup>Δ/Δ</sup> (n = 3) animals (2 vessels per animal) at baseline. SMC eYFP<sup>+/+</sup> *Klf4*<sup>Δ/Δ</sup> vessels were significantly dilated when compared to SMC eYFP<sup>+/+</sup> *Klf4*<sup>WT/WT</sup> under all pressures. *p* value was determined by two way anova. (B) Passive diameters normalized to respective diameters at 0 mmHg. (C) Quantification of pressure myography to assess the phenylephrine response of first order mesenteric vessels from SMC eYFP<sup>+/+</sup> *Klf4*<sup>WT/WT</sup> (n = 3) and SMC eYFP<sup>+/+</sup> *Klf4*<sup>Δ/Δ</sup> (n = 3) animals at baseline (2 vessels per animal). SMC eYFP<sup>+/+</sup> *Klf4*<sup>Δ/Δ</sup> vessels were significantly dilated when compared to SMC eYFP<sup>+/+</sup> *Klf4*<sup>WT/WT</sup> under all stimulations of phenylephrine. *p* value was determined by two way anova. (D) Phenylephrine stimulated lumen diameters normalized to respective maximal lumen diameters. (E) Quantification of pressure myography to assess the endothelial-dependent acetylcholine response of first order mesenteric vessels from SMC eYFP<sup>+/+</sup> *Klf4*<sup>WT/WT</sup> (n = 3, total vessels = 4) and SMC eYFP<sup>+/+</sup> *Klf4*<sup>Δ/Δ</sup> (n = 3, total vessels = 3) animals at baseline. (F) Quantification of pressure myography to assess the endothelial independent sodium nitroprussiate response of first order mesenteric vessels from SMC eYFP<sup>+/+</sup> *Klf4*<sup>WT/WT</sup> (n = 3, total vessels = 7) and SMC eYFP<sup>+/+</sup> *Klf4*<sup>Δ/Δ</sup> (n = 3, total vessels = 8) animals at baseline. \*\*\* = *p* < 0.001, \*\*\*\* = *p* < 0.0001.

That is, results indicate that *Klf4* appears to be required for maintenance of normal resistance vessel structure (i.e. size).

***In vivo* KLF4 ChIP-Seq identified PDGF signaling as a key pathway regulated by *Klf4* within the mesenteric vascular bed**

To begin to understand what genes KLF4 might regulate to cause these unexpected baseline changes in resistance vessel structure and function associated with acute SMC specific *Klf4* knockout, we performed comparative *in vivo* KLF4 ChIP-Seq analyses on the mesenteric resistance vessel arcade from our SMC eYFP<sup>+/+</sup> *Klf4*<sup>ΔΔ</sup> and SMC eYFP<sup>+/+</sup> *Klf4*<sup>WT/WT</sup> control mice to identify SMC KLF4 regulated genes and gene pathways. ChIP-Seq analysis of complex tissue samples that consist of numerous different cell types and phenotypes is usually highly problematic in that it is nearly impossible to ascertain what changes are contributed by one cell type versus another. Moreover, many differences may be lost due to inadequate sensitivity in detecting even large changes in relatively low abundance, but functionally important, cell types including SMC. In contrast, performance of these analyses in our experimental SMC *Klf4* knockout model allows us to ascertain overall changes (i.e. primary and secondary) resulting from initial conditional loss of a single gene (i.e. *Klf4*) exclusively in SMC. As such, to identify putative KLF4 target genes within SMC in resistance vessels that could mediate our observed structural and functional changes, we performed KLF4 ChIP-Seq analyses on chromatin extracted from mesenteric resistance vessel

arcades from our SMC eYFP<sup>+/+</sup> Klf4<sup>WT/WT</sup> and SMC eYFP<sup>+/+</sup> Klf4<sup>Δ/Δ</sup> animals two weeks following the last tamoxifen injection (Figure 8A).

In brief, SMC eYFP<sup>+/+</sup> Klf4<sup>WT/WT</sup> sequencing reads were normalized to SMC eYFP<sup>+/+</sup> Klf4<sup>Δ/Δ</sup> reads to identify those reads that were enriched in wild type animals. Remaining reads were then tabulated as peaks and associated with genes, resulting in a list of putative SMC-KLF4 target genes that were then subjected to pathway enrichment analysis (Figure 8A). Of major interest, results of these analyses identified the PDGF signaling pathway as the most significantly enriched pathway ( $p < 0.0001$ , Figure 8B). PDGF signaling is known to be critical for SMC investment of nascent blood vessels during vascular development and angiogenesis<sup>103–105</sup>. However, surprisingly there is no known role of PDGF signaling in the homeostasis of the normal vasculature<sup>105</sup>. Other enriched pathways included FGF signaling and angiogenesis, as well as several inflammatory pathways including Interferon-gamma signaling and Toll receptor signaling (Figure 8B). The ubiquitin proteasome pathway was also enriched in our Klf4 ChIP-Seq (Figure 8B), a pathway that is not only involved in protein degradation but also trafficking<sup>106</sup>. Intriguingly, the enriched genes within these pathways do not simply include the receptors, but also a host of kinases, phosphatases and transcription factors (Figure 8C).

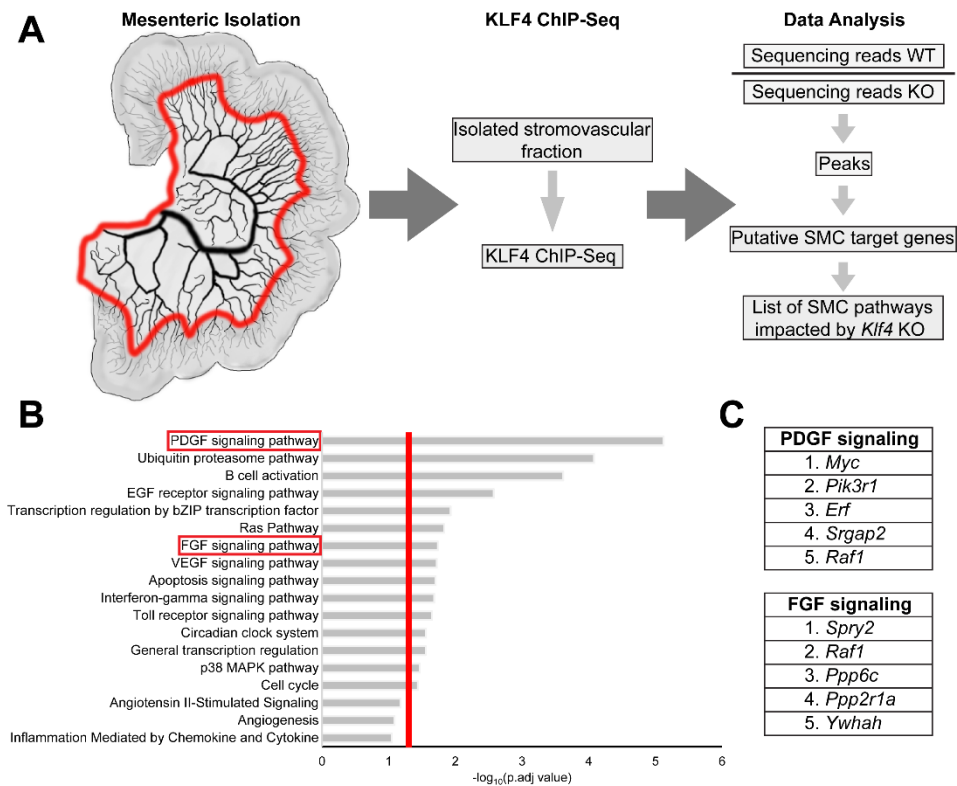


**Figure 8: KLF4 ChIP-Seq identifies PDGF signaling pathway as being differentially regulated between SMC *Klf4* knockout and wild type**

**Figure 8: KLF4 ChIP-Seq identifies PDGF signaling pathway as being differentially regulated between SMC Klf4 knockout and wild type**

(A) Cartoon representation of the area taken for the KLF4 ChIP-Seq and analysis work flow. Red line on mesentery indicates where the tissue was cut. (B) Enriched PANTHER pathways in SMC eYFP<sup>+/+</sup> Klf4<sup>WT/WT</sup> (n = 7) compared to SMC eYFP<sup>+/+</sup> Klf4<sup>Δ/Δ</sup> (n = 7) animals. Red line indicates p=0.05. *p* value calculated by DAVID software (C) Top 5 enriched genes in the PDGF and FGF signaling pathways.

## Resistance vessels from SMC *Klf4* knockout mice exhibit gaps in SMC coverage

Given our results showing that KLF4 regulates several pathways previously shown to be critical in regulating SMC growth, migration, and investment of blood vessels, we next sought to determine if SMC loss of KLF4 expression and subsequent reductions in blood pressure and peripheral resistance may be associated with morphological changes in resistance vessels. We focused our evaluations of resistance vessel morphology on the retina two weeks after the last tamoxifen injection given the ease of obtaining very high resolution, low background images of the entire vascular network using whole mount preparations. Of major interest, resistance arteries of SMC eYFP<sup>+/+</sup> *Klf4*<sup>Δ/Δ</sup> mice had an approximately four fold increase in prominent gaps in eYFP<sup>+</sup> perivascular cell coverage (eYFP<sup>-</sup> vascular area) over SMC eYFP<sup>+/+</sup> *Klf4*<sup>WT/WT</sup> animals, which only had small eYFP<sup>+</sup> coverage gaps (Figure 9A white arrows, 9B). These gaps in eYFP<sup>+</sup> coverage still had ACTA2+MYH11+ perivascular cells investing the arteriole (Figure 9A, white arrows) and were not bulging outward, suggesting these replacement perivascular cells are functional. These eYFP<sup>-</sup> gaps were also present in other vascular beds, including the spinotrapezius (Figure 9C). Notably, the eYFP<sup>-</sup> cells within the gaps are unlikely to represent SMC that failed to undergo Cre recombination given that we observed no differences in recombination frequencies within large vessels of SMC eYFP<sup>+/+</sup> *Klf4*<sup>Δ/Δ</sup> versus SMC eYFP<sup>+/+</sup> *Klf4*<sup>WT/WT</sup> mice in our previous studies in this model<sup>33,34</sup> and it is extremely unlikely the Cre recombination frequency of the eYFP

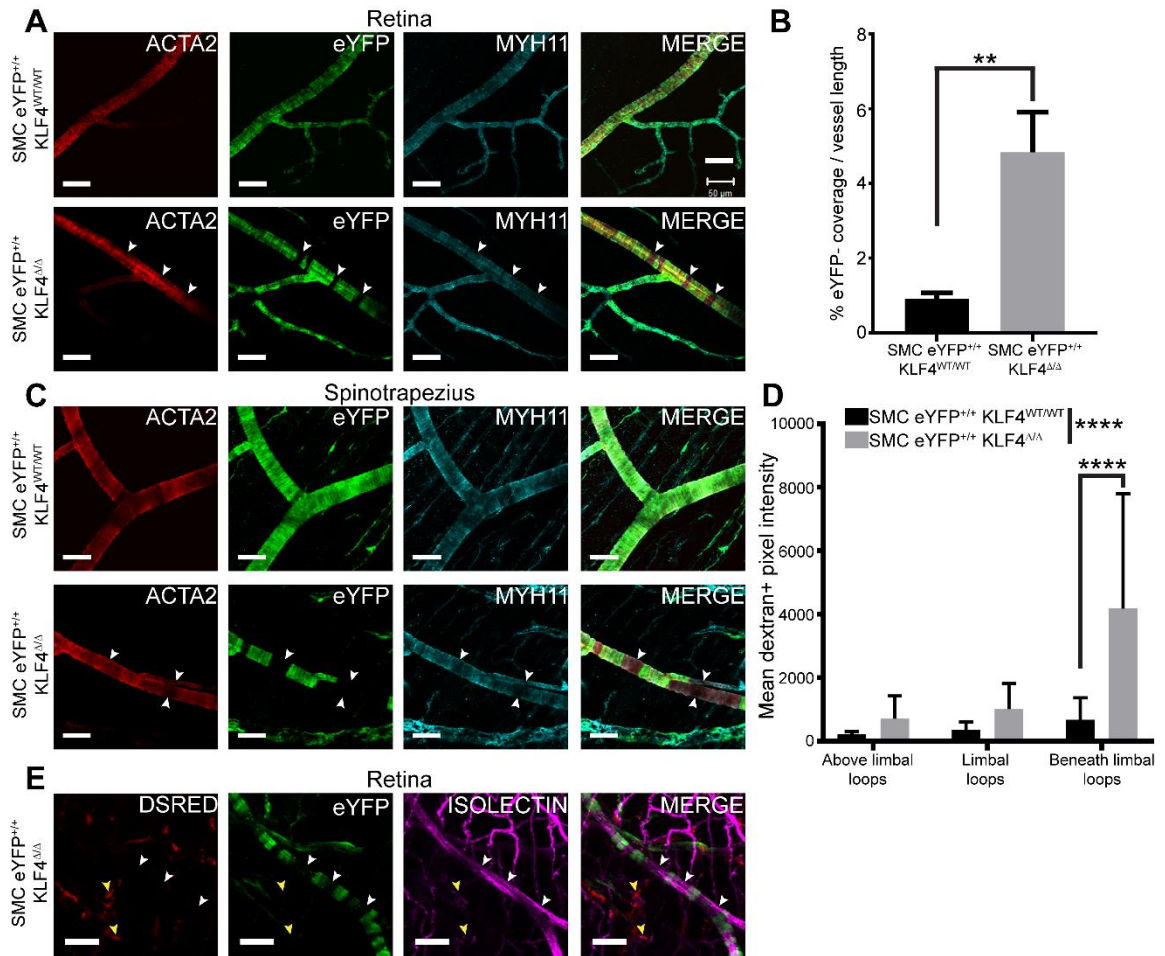


**Figure 9: SMC specific knockout of *Klf4* results in non-continuous lineage traced SMC coverage along vessels in the microvasculature.**

**Figure 9: SMC specific knockout of *Klf4* results in non-continuous lineage traced SMC coverage along vessels in the microvasculature.**

(A) Representative whole mount immunofluorescence images of SMC eYFP<sup>+/+</sup> Klf4<sup>WT/WT</sup> (n = 8) and SMC eYFP<sup>+/+</sup> Klf4<sup>Δ/Δ</sup> (n = 8) retinas. White arrows highlight gaps in eYFP<sup>+</sup> cell coverage that have been filled with cells expressing ACTA2 and MYH11 but not eYFP. Scale bars represent 50 μm. (B) Quantification of % eYFP<sup>-</sup> length compared to whole vessel length in SMC eYFP<sup>+/+</sup> Klf4<sup>WT/WT</sup> (n = 5) and SMC eYFP<sup>+/+</sup> Klf4<sup>Δ/Δ</sup> (n = 6) retinas. *p* value was determined by Mann Whitney *U* test. (C) Representative whole mount immunofluorescence images of SMC eYFP<sup>+/+</sup> Klf4<sup>WT/WT</sup> (n = 8) and SMC eYFP<sup>+/+</sup> Klf4<sup>Δ/Δ</sup> (n = 8) spinotrapezius. White arrows highlight gaps in eYFP<sup>+</sup> cell coverage that have been filled with cells expressing ACTA2 and MYH11 but not eYFP. Scale bars represent 50 μm. (D) Quantification of vascular leakage within the limbal vascular bed of the cornea based on intravital microscopic evaluation of interstitial levels of a 70 kDa dextran levels 0-1 hour post-injection. Results show the area under the curve for dextran<sup>+</sup> pixels in the interstitial space near the vasculature in SMC eYFP<sup>+/+</sup> Klf4<sup>WT/WT</sup> (n = 7) and SMC eYFP<sup>+/+</sup> Klf4<sup>Δ/Δ</sup> (n = 7). The *p* value was determined by two way anova for comparisons across the entire vascular network and Sidak's multiple comparisons between individual locations. (E) SMC eYFP<sup>+/+</sup> Klf4<sup>Δ/Δ</sup> animals were lethally irradiated and given a bone marrow transfer from whole animal constitutive DsRED<sup>+</sup> mice. No DsRED<sup>+</sup> cells (yellow arrows) were found in the eYFP<sup>+</sup> SMC gaps in the spinotrapezius (white arrows). Scale bars represent 50 μm. \*\* = *p* < 0.01, \*\*\*\* = *p* < 0.0001.

reporter gene locus would differ between SMC *Klf4* knockout and wild type mice. As such, the gaps are likely to represent loss of SMC coverage of resistance vessels and subsequent replacement by a non-SMC cell source that did not express *Myh11* at the time of tamoxifen injections.

To determine if the areas of incomplete eYFP+ cell coverage were leaky, mice were perfused with a 70 kDa dextran-Rhodamine dye and the corneas were examined for presence of the dye outside of the vasculature using real-time *in vivo* confocal microscopy. Significant leak of dye into the interstitium was seen in the areas beneath the limbal vessels in SMC eYFP<sup>+/+</sup> *Klf4*<sup>Δ/Δ</sup> mice (Figure 9D). We also saw significantly increased leak across the entire network in SMC eYFP<sup>+/+</sup> *Klf4*<sup>Δ/Δ</sup> compared to SMC eYFP<sup>+/+</sup> *Klf4*<sup>WT/WT</sup> mice. We did not observe evidence of red blood cells or fibrin deposits adjacent to the gaps suggesting there was not frank loss of endothelial integrity in these regions, although we cannot rule out the possibility that there may have been a transient loss of endothelial integrity that did not persist.

Next, we investigated whether bone marrow derived cells were the source of the replacement cells within the eYFP+ gaps. Six week old SMC eYFP<sup>+/+</sup> *Klf4*<sup>Δ/Δ</sup> mice underwent lethal irradiation and a bone marrow transfer from constitutive globally labeled DsRED+ mice. The mice were then given six weeks to recover, treated with a series of ten tamoxifen injections over two weeks, and then harvested two weeks later to simulate our original SMC *Klf4* knockout experiments. DsRED+ cells were observed in the interstitium of retina whole mounts, an indication of successful bone marrow reconstitution (Figure 9E,

yellow arrows). The microvasculature of these mice showed that the cells occupying the gaps in eYFP+ coverage (eYFP- vascular area) in SMC eYFP<sup>+/+</sup> *Klf4*<sup>Δ/Δ</sup> animals were not DsRED+ and thus not derived from a bone marrow cell source (Figure 9E, white arrows).

Taken together, these results indicate the following. *First*, pre-existing SMC normally maintain continuous SMC coverage of resistance vessels through a process that is *Klf4* dependent. *Second*, upon SMC specific conditional knockout of *Klf4*, there is loss of pre-existing differentiated SMC coverage of resistance vessels. These lost SMC are rapidly replaced from a non-bone marrow derived source of undetermined origin. *Third*, the replacement cells express classical SMC marker genes such as *Acta2* and *Myh11* but fail to maintain normal vascular integrity. *Fourth*, the overall consequence of conditional genetic loss of *Klf4* in SMC is impaired maintenance of peripheral resistance likely due in part to outward remodeling and functional dilation of resistance vessels.

## **Discussion**

*Klf4* has previously been shown to be undetectable within large conduit arteries at baseline but is rapidly upregulated upon vascular injury<sup>24,57</sup>. Herein, we show compelling evidence that *Klf4* has a previously unknown, beneficial, functional role in microvascular SMC within resistance arteries at baseline. Knockout of *Klf4* specifically in SMC resulted in far reaching cardiovascular effects, including loss of SMC perivascular coverage (Figure 9), a leaky

vasculature (Figure 9C), dilation of resistance arteries (Figure 7), an overall reduction in peripheral resistance (Figure 6E & F), and a heart dilation (Figure 6A & B). We postulate that loss of *Klf4* expression within SMC in resistance vessels resulted in transient loss of SMC perivascular coverage but ultimate replacement with ACTA2+ MYH11+ cells derived from a non-SMC and non-myeloid source yet to be determined. This replacement results in an increased permeability of the vasculature and was associated with significant dilation of resistance vessels. Although this dilation was modest, it was sufficient to result in reduced peripheral resistance as peripheral resistance changes as a function of the fourth power of changes in vessel radius. It is unclear to what extent the resistance vessel dilation is a function of outward vessel remodeling. It is also unclear whether these functional changes may be related to the loss of SMC coverage of resistance vessels in SMC *Klf4* knockout mice, and/or the lost SMC being replaced by cells from a non-SMC source. However, the net result was an increased diameter at any given intraluminal pressure which likely is the primary cause of reductions in peripheral resistance. This increased vessel diameter was not due to changes in the response to NO, but may have been the result of a change in the availability of NO which has been shown to play a key role in flow induced arteriolar remodeling <sup>107,108</sup>. The reductions in peripheral resistance (and accompanying hypotension) may contribute to the observed heart dilation as very low diastolic blood pressures have been associated with increased cardiovascular risk <sup>109-111</sup>, even in non-hypertensive individuals <sup>112,113</sup>, although the underlying mechanisms are poorly understood.

We also demonstrated *Klf4* dependent phenotypic switching of SMC to a macrophage-like state following IRI-MI. The eYFP+ SMCs made up less than 2% of macrophages within the myocardium, suggesting a limited role for this process within the healing myocardium. However, this limited number of macrophage-like SMCs may still influence the infarct zone through paracrine signaling. Our KLF4 ChIP-Seq on mesenteric arcades (Figure 8), as well as our previous KLF4 ChIP-Seq on atherosclerotic lesions <sup>34</sup>, identified >70 KLF4 regulated proinflammatory genes including numerous cytokines known to be involved in regulating recruitment and/or the function of inflammatory cells such as macrophages and T cells. These data coupled with the enrichment in the ubiquitin proteasome pathway (Figure 8B) suggest that macrophage-like SMC may indeed have a paracrine role following IRI-MI, by influencing the abundant populations of inflammatory cells that infiltrate the infarct zone post IRI-MI. The data also more broadly suggest that SMC paracrine signaling may be important in a variety of other pathological conditions such as diabetes, metabolic disease, and cancer. Indeed recent work by Murgai *et al.* demonstrated that *Klf4* dependent changes in SMC phenotype and function, including SMC deposition of fibronectin, are critical for pre-metastatic niche formation in mouse models of lung cancer <sup>114</sup>. Much like in the setting of atherosclerosis, the *Klf4* dependence of pre-metastatic niche formation in mouse models of lung cancer is likely a maladaptive function of *Klf4* in SMC.

Surprisingly, our data suggest that *Klf4* is required for maintenance of perivascular coverage at baseline. Within two weeks of the last tamoxifen

injection, SMC eYFP<sup>+/+</sup> *Klf4*<sup>Δ/Δ</sup> mice already have developed gaps in eYFP<sup>+</sup> coverage, suggesting that microvascular SMC have a higher turnover rate than previously thought and that the normal replacement cells come from preexisting SMC through a *Klf4* dependent process. Our KLF4 ChIP-Seq implicates several key SMC signaling pathways, including PDGF and FGF, not only as being KLF4 targets but also as having an important role in the maintenance of continuous SMC coverage (Figure 8B). When KLF4 is lost these pathways become dysregulated. However the direction of change is unclear as KLF4 has been shown to act as both a repressor and an activator of gene transcription<sup>27,30</sup>. One potential explanation for the loss of eYFP<sup>+</sup> SMC coverage in SMC eYFP<sup>+/+</sup> *Klf4*<sup>Δ/Δ</sup> mice is a dysregulation of potent mitogen pathways that results in the migration of SMC away from the vessel. This would appear to be unlikely, as we saw no eYFP<sup>+</sup> cells in the interstitium away from vessels in the retinas and spinotrapezius muscles of our knockout mice. Ultimately, *Klf4* loss in SMC results in activation of a compensatory process wherein a non-SMC, non-myeloid source of SMC progenitors fill the gaps in perivascular coverage and activate SMC marker genes including *Acta2* and *Myh11*. Although these replacement cells have activated the SMC gene expression profile, they may not be perfect replacements as we are able to detect functional changes in vessel diameter by pressure myography as well as an increased vessel permeability. However, we cannot ascribe the observed functional changes simply to these replacement cells. Rather, we can only conclude that the functional changes are the overall consequence of initial loss of *Klf4* exclusively in SMC plus any possible

downstream secondary effects. Given the hundreds of putative KLF4 target genes in SMC identified in our KLF4 ChIP-Seq analyses, the underlying mechanisms responsible for the observed functional changes in resistance vessels are likely to be extraordinarily complex.

The source of the MYH11+ACTA2+ replacement cells remains unknown, although we know they do not come from a bone marrow source (Figure 9E). One possible source would be an unlabeled MYH11- SMC progenitor cell. This would be difficult to investigate, as there is no known marker to label such a population. Other possible sources of replacement cells include endothelial cells undergoing endothelial to mesenchymal transitions and SCA1+ adventitial stem cells<sup>115–117</sup>. Unfortunately, these possibilities cannot be tested as lineage tracing of these populations would require a Cre recombinase-independent system since we require use of the *Myh11* ERT2-Cre lineage tracing and simultaneous *Klf4* knockout systems to generate the gaps. There is also no definitive model system for rigorous lineage tracing of SCA1+ stem cell populations since *Sca1* is also expressed by numerous other cell types.

In conclusion, results of the present studies have shown that *Klf4* has a previously unknown, crucial maintenance role within resistance vessels in that its loss is associated with dilation of resistance vessels, reduced blood pressure, and development of a cardiac dilation. Further studies will be needed to identify the complex mechanisms by which *Klf4* regulates SMC function within resistance vessels and the extent to which this process is conserved across species including in humans. Indeed, identifying unique *Klf4* targets in atherosclerosis

and cancer will be necessary for the development of any targeted treatment strategies to avoid disrupting the critical homeostatic role Klf4 plays within baseline SMC. In addition, based on recent genome association studies showing that *Klf4* polymorphisms are highly associated with coronary artery disease <sup>118</sup>, it will be important to determine how dysregulation of KLF4 expression might contribute to microvascular dysfunction associated with type 2 diabetes, metabolic disease, and obesity.

## **Chapter III: Additional Studies**

## Knockout of *Klf4* in SMC alters metabolic pathways

### Experimental background

We have previously assessed the effects of *Klf4* knockout in SMCs on the binding of KLF4 to DNA within cells of mesenteric cascades (see Figure 8). Unfortunately this ChIP Seq analysis is insufficient to give directionality to gene expression changes as KLF4 has been shown to be both an activator and repressor of gene expression<sup>27,30</sup>. To more directly assess the effects loss of KLF4 within SMCs have on gene expression in baseline animals, we performed RNA Seq on the mesentery arcades isolated from SMC eYFP<sup>+/+</sup> *Klf4*<sup>WT/WT</sup> and SMC eYFP<sup>+/+</sup> *Klf4*<sup>Δ/Δ</sup> mice.

### Results:

#### SMC specific *Klf4* knockout results in metabolic dysregulation

To perform the RNA Seq, RNA was isolated from the mesenteric arcades of SMC eYFP<sup>+/+</sup> *Klf4*<sup>WT/WT</sup> (n=9) and SMC eYFP<sup>+/+</sup> *Klf4*<sup>Δ/Δ</sup> (n=9) mice. RNA was pooled from 3 animals of the same genotype to generate a single sequencing run. Pooling in this way gave us 3 wild type and 3 knockout samples for analysis. The most dysregulated pathways are shown in Figure 10A. Intriguingly, knockout of *Klf4* within SMCs resulted in the dysregulation of oxidative phosphorylation and mitochondrial dysfunction, suggesting a role for KLF4 within SMCs in metabolism (Figure 10A). To test whether this metabolic disruption resulted in a functional change, we measured fasting blood glucose levels in our SMC eYFP<sup>+/+</sup>

Klf4<sup>WT/WT</sup> (n=7) and SMC eYFP<sup>+/+</sup> Klf4<sup>Δ/Δ</sup> (n=8) mice. At baseline, SMC eYFP<sup>+/+</sup> Klf4<sup>Δ/Δ</sup> mice did not have an altered fasting blood glucose (Figure 10C). However, when challenged with a diet induced obesity (DIO) model initiated through a 4 week high fat diet feeding SMC eYFP<sup>+/+</sup> Klf4<sup>Δ/Δ</sup> (n=12) mice had an elevated fasting blood glucose relative to their DIO SMC eYFP<sup>+/+</sup> Klf4<sup>WT/WT</sup> (n=8) controls (Figure 10C). This suggests that KLF4 within SMCs helps normalize fasting blood glucose levels when challenged in a DIO model. Overall, these data indicate that KLF4 expression within SMCs plays a role in metabolic regulation.

## Discussion

Due to the duality of KLF4's action as a transcription factor, our previous ChIP Seq results identified pathways that were affected by knockout of KLF4 in SMCs but not the direction of potential change in those pathways. To our surprise, RNA Seq results (Figure 10) implicated numerous metabolic pathways as being dysregulated. Additional studies will be required to assess whether this dysregulation is a primary effect within SMCs or through secondary mediators. The mechanism of action for this change also remains unclear, although combinatorial analysis of our KLF4 ChIP Seq and RNA Seq experiments may help identify preliminary target genes where KLF4 is bound to the gene promoter and corresponding gene expression is disrupted.

We measured the fasting blood glucose levels of our mice to test for functional consequences of disrupting the implicated metabolic pathways (Figure

10A, oxidative phosphorylation and mitochondrial dysfunction). SMC eYFP<sup>+/+</sup> Klf4<sup>Δ/Δ</sup> had similar fasting blood glucose levels to their wild type counterparts under baseline conditions, however they had a significantly increased fasting blood glucose after challenge with a high fat diet. This suggests that SMC eYFP<sup>+/+</sup> Klf4<sup>Δ/Δ</sup> mice are unable to respond to the DIO model as well as their wild type counterparts. As such, a logical next step is to perform a glucose tolerance test in all groups to examine systemic responses to acute challenge. Further discussion of future experiments to characterize this metabolic change in SMC eYFP<sup>+/+</sup> Klf4<sup>Δ/Δ</sup> can be found in the Future Directions section.

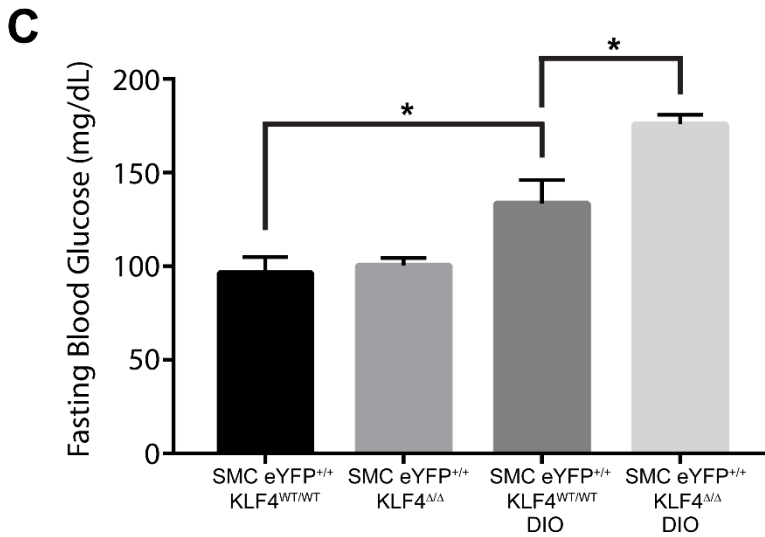
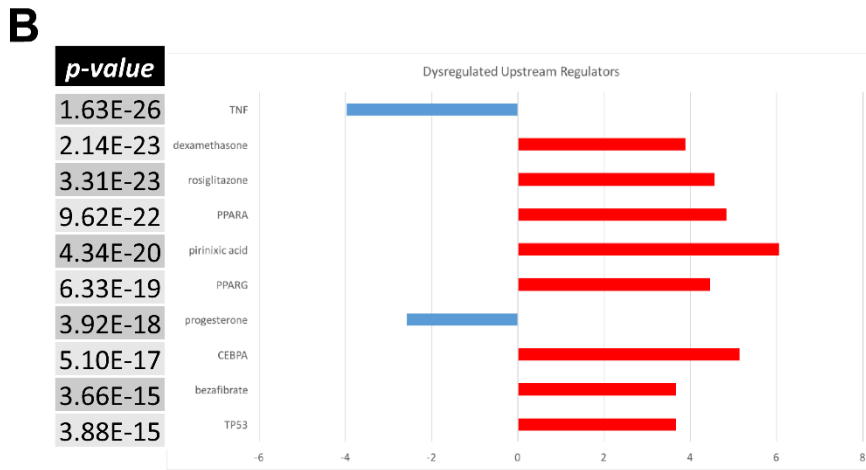
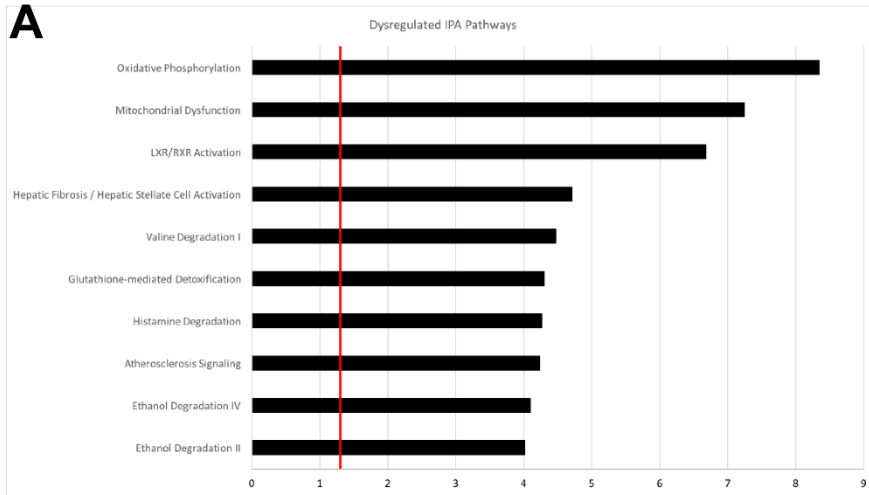


**Figure 10: SMC specific *Klf4* knockout results in disruption of metabolic pathways**

**Figure 10: SMC specific *Klf4* knockout results in disruption of metabolic pathways**

(A) Enriched IPA pathways in SMC eYFP<sup>+/+</sup> Klf4<sup>WT/WT</sup> (n=9) compared to SMC eYFP<sup>+/+</sup> Klf4<sup>Δ/Δ</sup> (n=9) animals. Red line indicates p=0.05. *p* value calculated by IPA software. (B) Most dysregulated upstream regulators as identified by IPA analysis. (C) Fasting blood glucose levels from SMC eYFP<sup>+/+</sup> Klf4<sup>WT/WT</sup> (n=7), SMC eYFP<sup>+/+</sup> Klf4<sup>Δ/Δ</sup> (n=8), SMC eYFP<sup>+/+</sup> Klf4<sup>WT/WT</sup> 4 week DIO feed fed (n=8), and SMC eYFP<sup>+/+</sup> Klf4<sup>Δ/Δ</sup> 4 week DIO feed fed (n=12) animals. *p* value was determined by unpaired, two tailed *t*-test. \* = *p* < 0.05.

## **Aging SMC eYFP<sup>+/+</sup> *Klf4*<sup>Δ/Δ</sup> and SMC eYFP<sup>+/+</sup> *Klf4*<sup>WT/WT</sup>**

### **results in gaps in eYFP<sup>+</sup> coverage within vascular beds**

#### **Experimental background**

Our previous studies had identified gaps in eYFP<sup>+</sup> SMC coverage within the microvasculature (Figure 9). These microvascular beds were also hyperpermeable and leaky (Figure 9). Hyperpermeability of microvascular beds is a hallmark of the aging vasculature (reviewed in <sup>119</sup>). As such, we hypothesized that knockout of *Klf4* in SMCs would result in a worsening of aging associated hyperpermeability. This hypothesized increase in hyperpermeability compared to an aged wild type mouse may also be associated with an increase in the abundance and/or size of the gaps in eYFP<sup>+</sup> SMC coverage.

#### **Results:**

##### **Wild type and SMC specific *Klf4* knockout mice develop gaps in eYFP<sup>+</sup> SMC coverage with age**

I began by aging a cohort of SMC eYFP<sup>+/+</sup> *Klf4*<sup>WT/WT</sup> (n = 5) and SMC eYFP<sup>+/+</sup> *Klf4*<sup>Δ/Δ</sup> (n = 4) mice to 75 weeks (~19 months) of age. The mice received tamoxifen at the normal time point of 6-8 weeks of age. Mice are considered to have reached “old age” when they are 18-24 months old, corresponding to 56-69 years of age in humans <sup>120</sup>. I isolated several microvascular beds from these mice and performed whole mount immunostaining. I observed gaps in eYFP<sup>+</sup> coverage within the spinotrapezius muscle (Figure 11A), mesentery (Figure 11B)

and retina (data not shown) in both SMC eYFP<sup>+/+</sup> Klf4<sup>WT/WT</sup> and SMC eYFP<sup>+/+</sup> Klf4<sup>Δ/Δ</sup> mice. Interestingly, these gaps did not appear to be more abundant in the aged SMC eYFP<sup>+/+</sup> Klf4<sup>Δ/Δ</sup> mice than in their younger counterparts. These gaps were in both larger (>100 μm) and smaller (<50 μm) vessels. Similar to our previously reported results in young animals, these gaps were filled with eYFP<sup>+</sup> cells that have upregulated ACTA2 and MYH11. These data demonstrate that both SMC eYFP<sup>+/+</sup> Klf4<sup>WT/WT</sup> and SMC eYFP<sup>+/+</sup> Klf4<sup>Δ/Δ</sup> mice develop gaps in eYFP<sup>+</sup> SMC coverage within their vasculature at 19 months of age.

## Discussion

Our previously results had demonstrated *Klf4* plays a role in maintenance of SMCs along microvessels, as well as the permeability of those microvessels. The results presented in Figure 11 demonstrate that at least part of this phenotype is recapitulated through aging of wild type mice. This suggests that KLF4 expression in baseline SMC plays a role in the maintenance of eYFP<sup>+</sup> SMC coverage that is lost with age. One possible mechanism that might explain this observation is that loss of KLF4 results in an increased turnover of vascular SMCs, as KLF4 has previously been shown to repress SMC proliferation<sup>24</sup>. Increased turnover might lead to exhaustion of the lineage traced population and consequent replacement of the gap cells from an alternative source. If exhaustion does occur, it would be recapitulated with age as aging would inherently result in more turnover of the vessel SMCs. Intriguingly, SMC eYFP<sup>+/+</sup>

$Klf4^{\Delta/\Delta}$  mice appeared to have a similar frequency and size of gaps as their wild type counterparts. However, further quantification is needed to determine if the percent eYFP- vessel coverage in the aged mice is greater than or equal to that seen in baseline SMC eYFP<sup>+/+</sup>  $Klf4^{\Delta/\Delta}$  mice.

Further studies are also required to determine if the aged wild type and knockout mice develop vascular leakiness, as we did not test this in this group of mice. If the wild type mice do develop vascular leakiness, it would be interesting to determine if aging alone recapitulates other aspects of the KLF4 knockout phenotype. One phenotype of particular interest would be investigating the effect of *Klf4* knockout on aging related arterial stiffness and hypertension.

Over two thirds of individuals over the age of 65 experience hypertension<sup>121</sup>. This aging associated hypertension is associated with increased arterial stiffness and an enhanced response to vasoconstrictors<sup>122</sup>. As such, I would hypothesize that knockout of *Klf4* in SMC may protect against aging related hypertension as we have demonstrated that SMC eYFP<sup>+/+</sup>  $Klf4^{\Delta/\Delta}$  mice exhibit dilation of their resistance vessels (Figure 7) and a reduction in blood pressure (Figure 6). However, SMC eYFP<sup>+/+</sup>  $Klf4^{\Delta/\Delta}$  mice also have an increased fasting blood glucose when challenged with a high fat diet. Recent work has demonstrated that metabolic syndrome, which includes hyperglycemia, promotes arterial stiffening and the development of hypertension<sup>123,124</sup>. Further studies are needed to determine whether aging SMC eYFP<sup>+/+</sup>  $Klf4^{\Delta/\Delta}$  mice would also result in an elevated fasting blood glucose when compared to wild type controls. If aged SMC eYFP<sup>+/+</sup>  $Klf4^{\Delta/\Delta}$  mice have an elevated fasting blood glucose this would

likely have a negative impact on any benefit that the reduced blood pressure seen in SMC eYFP<sup>+/+</sup> Klf4<sup>Δ/Δ</sup> mice has on aging related hypertension. Thus, the net result of KLF4 knockout in SMC may simply be no change in aging related phenotypes. Further studies will be needed to truly understand the role of *Klf4* within SMC during aging.

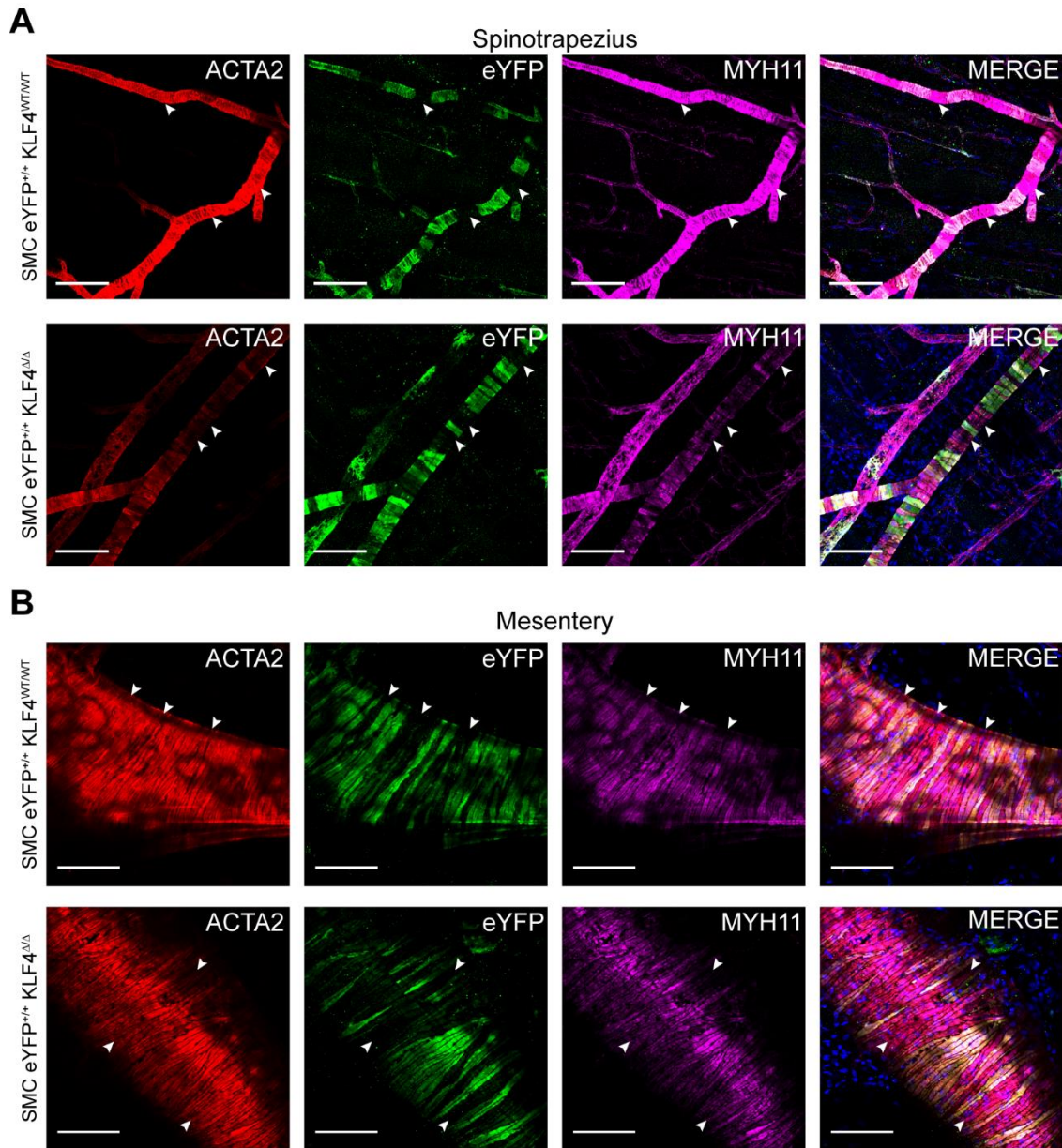


**Figure 11: Advanced age SMC eYFP<sup>+/+</sup> Klf4<sup>Δ/Δ</sup> and SMC eYFP<sup>+/+</sup> Klf4<sup>WT/WT</sup> mice have gaps in eYFP+ SMC coverage in multiple microvascular beds.**

**Figure 11: Advanced age SMC eYFP<sup>+/+</sup> Klf4<sup>Δ/Δ</sup> and SMC eYFP<sup>+/+</sup> Klf4<sup>WT/WT</sup> mice have gaps in eYFP<sup>+</sup> SMC coverage in multiple microvascular beds.**

(A) Representative whole mount immunofluorescence images of SMC eYFP<sup>+/+</sup> Klf4<sup>WT/WT</sup> (n = 5) and SMC eYFP<sup>+/+</sup> Klf4<sup>Δ/Δ</sup> (n = 4) spinotrapezius muscle. White arrows highlight gaps in eYFP<sup>+</sup> cell coverage that have been filled with cells expressing ACTA2 and MYH11 but not eYFP. Scale bars represent 100 μm.

(B) Representative whole mount immunofluorescence images of SMC eYFP<sup>+/+</sup> Klf4<sup>WT/WT</sup> (n = 5) and SMC eYFP<sup>+/+</sup> Klf4<sup>Δ/Δ</sup> (n = 4) mesenteric arcades. White arrows highlight gaps in eYFP<sup>+</sup> cell coverage that have been filled with cells expressing ACTA2 and MYH11 but not eYFP. Scale bars represent 100 μm.

## **Chapter IV: Future Directions**

The studies performed in Chapters II and III detail a novel, baseline role of the transcription factor KLF4 within vascular SMCs. Specifically, *Klf4* was shown to be critical for the maintenance of baseline vessel integrity, as well as the maintenance of continuous SMC coverage (Figure 9). SMC specific *Klf4* knockout also led to a dilation of resistance vessels and a decrease in peripheral resistance (Figures 6 and 7). Combined, the above observations suggest that *Klf4* is critical for SMC control of blood pressure. SMCs were also shown to contribute to wound healing following IRI, both through *Klf4* dependent and *Klf4* independent mechanisms (Figures 4 and 5). Similar to what has been observed in atherosclerosis, SMCs transition to a macrophage-like state through a *Klf4* dependent mechanism following IRI (Figure 4).

Although we have begun to further characterize the role of *Klf4* within SMCs, several key questions remain. *First*, what are the key KLF4 target genes that become dysregulated in knockout animals, resulting in the development of eYFP- gaps? Here we have demonstrated that gaps in eYFP+ SMC coverage occur in SMC eYFP<sup>+/+</sup> *Klf4*<sup>Δ/Δ</sup> mice in multiple microvascular beds (Figure 9). We have also shown that aged SMC eYFP<sup>+/+</sup> *Klf4*<sup>WT/WT</sup> mice develop gaps in eYFP+ SMC coverage (Figure 11). However, we have not determined the fate of the missing eYFP+ cells, nor have we identified the key dysregulated KLF4 target genes that lead to the loss of eYFP+ coverage beyond implicating several pathways through KLF4 ChIP Seq analysis (Figure 8). *Second*, what is the source of the replacement SMCs that fill in the gaps? We demonstrated that *Klf4* knockout in SMCs resulted in gaps in eYFP+ coverage throughout the

vasculature and these gaps in eYFP+ coverage were filled with replacement cells (Figure 9). These replacement cells express traditional SMC marker genes, but may not fully recapitulate normal SMC function as these microvessels exhibit increased permeability. Determining the origin of the replacement cells may provide valuable insight into how loss of KLF4 in SMCs results in gaps. *Third*, do our observed phenotypes persist, or is there eventual compensation for the loss of KLF4 in SMCs? Preliminary results demonstrated that aged SMC eYFP<sup>+/+</sup> Klf4<sup>WT/WT</sup> and SMC eYFP<sup>+/+</sup> Klf4<sup>Δ/Δ</sup> mice developed phenotypically similar gaps in size and number. This suggests that there may be eventual compensation for the loss of KLF4 within SMCs. *Fourth*, how does SMC specific *Klf4* knockout result in dysregulated metabolic pathways? RNA Seq analysis on mesenteric arcades from our wild type and knockout animals revealed dysregulation of metabolic pathways in our knockout animals (Figure 10). This dysregulation does not result in altered fasting blood glucose levels at baseline. However, knockout animals challenged with a high fat diet have significantly elevated fasting blood glucose levels when compared to high fat diet fed wild type controls. The mechanism behind this increased fasting blood glucose in a diet induced obesity model remains unclear. These questions are discussed in further detail below.

**What are the pathways downstream of KLF4 that lead to the development of gaps in eYFP+ SMC coverage within the microvasculature following SMC specific knockout of KLF4?**

One hypothesis that would explain the loss of eYFP+ cells along the microvasculature is that SMC specific *Klf4* knockout results in migration of SMCs away from the blood vessel. Our KLF4 ChIP Seq implicated several key SMC migratory pathways, including PDGF and FGF signaling, as being enriched in wild type but not knockout animals (Figure 8). PDGF and FGF signaling are known to be critical for SMC migration as well as SMC investment of nascent blood vessels during vascular development and angiogenesis<sup>103–105,125</sup>. However, there is no known role of these growth factors in the active maintenance of perivascular coverage within the normal vasculature<sup>105</sup>. Our results suggest that there may indeed be an active maintenance role for these mitogens within baseline SMCs.

There are two potential hypotheses that could explain how *Klf4* is modulating the PDGF and FGF signaling pathways. First, KLF4 within baseline SMC may be downregulating expression of the PDGF and FGF receptors. Loss of KLF4 would therefore lead to upregulation of these receptors and an increase in PDGF and FGF ligand sensitivity. These sensitive SMCs would be more prone to phenotypic modulation and migration towards PDGF and FGF ligands, resulting in gaps as they left the blood vessel and were replaced by cells from a non-SMC source. In support of this hypothesis, our KLF4 ChIP Seq analysis

revealed that KLF4 was enriched on the PDGFR $\beta$ , PDGFR $\alpha$ , and FGFR1 promoters in wild type mice compared to *Klf4* knockout mice (data not shown).

Several experiments would begin to test this hypothesis. First, immunofluorescent staining for PDGFR $\beta$ , PDGFR $\alpha$ , and FGFR1 receptors within the microcirculation would give preliminary data on which, if any, of these receptors expression profile changes with *Klf4* knockout. Performing these experiments by immunofluorescent staining enables us to utilize our lineage tracing system to specifically examine PDGFR $\beta$ , PDGFR $\alpha$ , and FGFR1 expression changes in SMCs. Utilizing this method also enables us to investigate receptor expression in eYFP- cells, potentially helping to identify a population of cells that express and/or upregulate the receptors in SMC eYFP<sup>+/+</sup> *Klf4* <sup>$\Delta/\Delta$</sup>  animals. Such a population may be the source of the replacement cells (discussed in detail in the next section). An alternative approach to quantify receptor levels would be to utilize flow cytometry. Flow cytometry would enable more discrete quantification of the expression levels of the receptors of interest. Flow cytometry also enables a larger staining panel such that an experiment could include all three receptors of interest as well as our SMC lineage tag and cell specific lineage markers for other cell populations of interest, such as endothelial cells and Sca1<sup>+</sup> cells. However, utilizing flow cytometry would result in the loss of valuable spatial information. As such, I believe it should be used as a complementary approach to immunofluorescent staining as the spatial location of the eYFP<sup>+</sup> cells expressing any of the receptors is critical. Overall, these

studies would begin to describe the capacity various cell types within the microvasculature have to respond to the PDGF and FGF ligands.

The second, related hypothesis is that KLF4 within SMC is downregulating expression of the PDGF and FGF ligands. Interestingly, KLF4 is enriched on the PDGFA, PDGFB, and PDGFC promoters in wild type animals compared to knockout animals in our KLF4 ChIP Seq (data not shown). This suggests that KLF4 is regulating both the PDGF receptors and the production of the mitogens.

To assess the levels of PDGF and FGF isoforms in SMC eYFP<sup>+/+</sup> Klf4<sup>WT/WT</sup> and SMC eYFP<sup>+/+</sup> Klf4<sup>Δ/Δ</sup> mice cytokine assays could be performed. Both ELISA and Luminex assays could be used to assay PDGF and FGF isoform levels. These studies would provide information on the levels of key mitogens within the microcirculation, and would include other key SMC signaling mitogens implicated in our ChIP Seq such as vascular endothelial growth factor (VEGF). However, ELISA and Luminex assays do not determine the source of the mitogens. To assess this, RNA FISH could be utilized in conjunction with immunofluorescent staining to visualize whether SMC eYFP<sup>+/+</sup> Klf4<sup>Δ/Δ</sup> mice exhibit changes in SMC production of the identified ligands of interest from the cytokine assays. Alternative sources of ligands could also be interrogated, such as endothelial production of PDGF or FGF. Endothelial production is of particular interest as endothelial production of PDGF and FGF could be a retention signal necessary to maintain SMCs in a perivascular location. This would appear less likely than a primary effect in SMCs as disruption of such a retention mechanism would likely result in large, systemic dropout of eYFP<sup>+</sup> SMCs. Indeed, I only

observed an approximately 5 percent drop in eYFP+ coverage in knockout animals (Figure 9). As an alternative approach, siKLF4 treatment of cultured microvascular SMCs could be used to investigate the production of PDGF and FGF ligands by SMCs. This would enable more direct integration of KLF4's interaction with these pathways. However, previous results from our lab suggest that cultured SMCs may already be de-differentiated as siKLF4 treatment results in an increase in SMC contractile genes<sup>23</sup>. Cultured SMCs also fail to recapitulate critical *in vivo* regulatory pathways, supporting the hypothesis that cultured SMCs are at least partially de-differentiated<sup>5,126</sup>. This would complicate interpretation of any cell culture experiments. Ultimately, I fear these proposed studies would simply be descriptive or that the levels of change in the FGF, PDGF, and/or other ligands of interest would be too minute to detect through these methods.

Overall, the best experiment to investigate both receptor and ligand changes for the PDGF and FGF signaling pathways as a result of *Klf4* knockout in SMCs is single cell RNA Seq. Through single cell RNA Seq, we can identify effects of SMC specific *Klf4* knockout on multiple cell populations including SMCs, endothelial cells, Sca1+ adventitial cells, interstitial fibroblasts, and tissue resident macrophages. Identification of cell populations is done by clustering cells that are expressing multiple known lineage marks of an appropriate cell type together. Through this methodology, one can identify novel subsets of a particular cell type that may have similar marker gene expression but divergent expression of other genes, such as the PDGF receptors. Recent work from the

Betsholtz lab has shown through similar single cell RNA Seq analysis that there are location specific subsets of vascular SMCs within the brain and lung <sup>127</sup>. Such subsets are presumably present in other tissues throughout the body, not just the brain and lungs. The identified SMC subsets included arterial SMC, arteriole SMC, venous SMC, and the functionally related pericyte population <sup>127</sup>.

Intriguingly, they found KLF4 expression varied within these populations with the arterial SMC having the highest expression (online data set for paper). This suggests that our observed gap phenotype may arise due to loss of KLF4 from a particular subset of SMCs. Thus, we could cluster our SMC populations based on expression of KLF4. Within the high expressing KLF4 population, we would work to identify an expression profile that is altered with KLF4 knockout. Of particular interest to this hypothesis, we would investigate expression differences in PDGF and FGF receptors and ligands as well as other known migratory gene pathways. Importantly, single cell RNA Seq allows for the examination of secondary and tertiary effects in other cell types. Thus, we could also determine whether *Klf4* knockout is altering production of PDGF and FGF in other cell types, such as endothelial cells. Overall, single cell RNA Seq would provide a wealth of data about the migratory capacity of SMCs within the microvascular tissue assayed.

Taken together, I find it unlikely that the above experiments investigating migration of SMCs away from the blood vessel will be fruitful. Indeed, while performing extensive whole mount imaging of the spinotrapezius, retinal, and mesenteric vascular beds I never found eYFP+ cells away from blood vessels in

the interstitium. As such, I do not believe migration of SMCs away from the blood vessel explains the development of the gaps in eYFP+ SMC coverage.

A second hypothesis that could explain the loss of eYFP+ cells is that SMC specific *Klf4* knockouts results in the increased apoptosis of SMCs. An increase in apoptosis in the eYFP+ SMC population would lead to gaps in eYFP+ SMC coverage, particularly if SMC specific *Klf4* knockout also effects proliferation of the surrounding SMCs (discussed in detail below). To assess this, we could perform immunofluorescent staining for cleaved caspase 3 or perform a Terminal deoxynucleotidyl transferase (TdT) dUTP Nick-End Labeling (TUNEL) assay as a marker of apoptotic cells. An increase in apoptosis would require a subsequent increase in phagocytic cell clearance at the sites of the gaps. To determine if this is occurring, we could once again do immunofluorescent staining with a macrophage marker, such as LGALS3 or F4/80, to see if there is a macrophage accumulation around the gaps. Of particular interest, immunofluorescent staining would allow us to identify if any SMCs are becoming macrophage-like, as we have demonstrated occurs during atherosclerosis and following IRI, to participate in the phagocytosis of their apoptotic neighbors. Immunofluorescent staining provides needed spatial resolution of macrophage accumulation around gaps, however it only assays macrophage accumulation at a snapshot in time. It remains uncertain when the gaps appear following tamoxifen injection. They could develop as a result of *Klf4* knockout in SMCs after the first tamoxifen injection, or develop as a result of cumulative changes due to the loss of *Klf4* up to 4 weeks after the first tamoxifen injection (2 weeks

after the last injection). Thus, examination of multiple time points is necessary to capture potential macrophage accumulation.

. A third hypothesis that could explain the loss of eYFP+ cells is that SMC specific *Klf4* knockout results in an alteration of SMC proliferation rate. An increased proliferation rate could lead to exhaustion of a progenitor pool and thus development of gaps as eYFP+ cells are no longer able to replace themselves and a secondary cell type is recruited to fill the gaps. Alternatively, SMCs in SMC eYFP<sup>+/+</sup> *Klf4*<sup>Δ/Δ</sup> mice may undergo proliferation at a reduced rate, resulting in the need for another, eYFP- cell type to contribute to the maintenance of continuous SMC coverage.

Several immunofluorescent antibody assays are available (i.e. Ki67) to investigate SMC proliferation. However, these assays only determine proliferation at a given moment in time. A better experiment would be the use of BrdU mini pumps. These pumps continuously deliver BrdU, a thymidine analog, which is incorporated into the DNA of proliferating cells. Due to the continuous nature of BrdU delivery, utilizing mini pumps enables the determination of growth fractions. Growth fractions are the integral of proliferation over the length of the experiment. Importantly, utilizing BrdU mini pumps captures any growth fraction change that occurs over the length of the experiment, whether it occurs as a result of *Klf4* knockout after the first tamoxifen injection, the last injection or at another time point.

I believe changes in proliferation are the most likely cause of the gaps in eYFP+ SMCs. Specifically, an increase in proliferation rate leading to exhaustion

of a progenitor pool. My results in aged wild type mice demonstrated that wild type animals develop phenotypically similar gaps in eYFP+ coverage as the knockout animals. As discussed previously, an increase in turnover of vascular SMCs due to loss of KLF4 could explain these results as a progenitor pool is exhausted and alternate sources are recruited to maintain SMC coverage. To investigate this hypothesis, I have generated an entire data set of SMC eYFP<sup>+/+</sup> Klf4<sup>WT/WT</sup> and SMC eYFP<sup>+/+</sup> Klf4<sup>Δ/Δ</sup> BrdU mini pump implanted animals. These animals had the BrdU mini pumps implanted at the time of their first tamoxifen injection and were sacrificed 4 weeks later. If there is an increase in proliferation due to KLF4 knockout in SMCs, it will be reflected as an increased growth fraction. Alternatively, if KLF4 knockout is having the opposite effect and reducing SMC proliferation, this will be reflected in these experiments as a decrease in growth fraction. Analysis of these animals is still ongoing.

**What is the source of the eYFP- replacement cells that fill in the eYFP+ gaps within the microvasculature?**

As discussed above, the mechanism behind the development of the gaps in eYFP+ SMC coverage remains unclear. However, it is clear that the loss of eYFP+ SMC coverage results in replacement of SMCs from an eYFP- source. It is also clear that the replacement cells are not coming from a bone marrow source (Figure 9). There are several prime candidates that may be contributing to these replacement cell populations.

First, endothelial cells may be undergoing endothelial to mesenchymal transitions to fill the gaps. Endothelial to mesenchymal transitions are a well-defined process in which endothelial cells transition to a mesenchymal phenotype, such as a SMC-like cell <sup>115,116,128</sup>. The transformation occurs during development, as well as in response to mitogens like TGF- $\beta$  <sup>115,116,129</sup>. In our system, endothelial cells may be activated as a response to loss of eYFP+ SMCs and transition to a SMC-like phenotype to maintain vascular tone in that region of the vessel. To determine whether this is occurring in our baseline model, we need a cre recombinase independent way to either lineage trace endothelial cells or a cre recombinase independent way to lineage trace SMC and knockout *Klf4* as *Klf4* knockout in SMCs is required for the formation of gaps in young animals. The Owens' lab has recently begun characterizing a system that would be capable of doing this. The dre recombinase system functions similar to a cre recombinase, but the dre recognizes a functionally distinct *rox* site <sup>130,131</sup>. Our dre system utilizes the Myh11 promoter driving dre recombinase expression, enabling similar labeling and knockout studies (using *rox* sites) as we have done previously in our Myh11 cre model. An additional advantage of the dre system is the ability to perform studies in both male and female mice as the Myh11 dre promoter construct did not insert in the Y chromosome. Using the dre system, we can breed in a lineage tracing system of our choice to determine whether that cell type contributes to the replacement gap cells. To investigate endothelial cells we could utilize a vascular endothelial cadherin lineage tracing system (driving a separate reporter such as tdTomato). Utilizing the dre/cre dual lineage tracing

system would enable us to not only see gaps in eYFP+ coverage, but also determine if lineage traced (e.g. tdTomato+) endothelial cells are undergoing endothelial to mesenchymal transitions and filling in the gaps.

Another possible cell type that may be contributing to the gap replacement cells are Sca1+ adventitial progenitor cells. These progenitor cells have been classified into two types, those that give rise to mural cells (including SMC) and those that give rise to macrophage-like cells<sup>132</sup>. These adventitial cells have been shown to contribute to SMC populations in models of atherosclerosis and *in vitro*<sup>117,133</sup>. Thus it is possible that these cells are contributing to the replacement cell population. However, determining if they do will be difficult. Unlike with endothelial cells, there is no definitive lineage tracing model for Sca1+ adventitial cells as Sca1 is expressed by a variety of cell types including activated lymphocytes<sup>134</sup>, hematopoietic stem cells<sup>135</sup>, and progenitor populations within various tissues including skeletal muscle<sup>136</sup> and the heart<sup>137,138</sup>. A more selective marker for these cells has yet to be identified.

Various interstitial cells may also be the source of the replacement cells, including interstitial fibroblasts or tissue resident macrophages. I believe this is less likely than the cell populations discussed above. Investigating these populations would also be difficult as markers for these populations vary based on tissue type and the markers tend to be nonspecific. Finally, it is possible an eYFP- SMC progenitor cell is giving rise to the replacement cells. This is currently an impossible hypothesis to test, as there is no known expression profile of such a cell so you would be unable to lineage trace them.

As an alternative to utilizing dual lineage tracing systems to investigate the populations described above, we could exploit the fact that gaps develop in wild type animals with age. Using aged mice instead of SMC specific *Klf4* knockout mice enables the use of alternative cre driven lineage reporter mice. In this way we could investigate whether the potential gap replacement cells described above, such as endothelial cells, do contribute to gap replacement. For example, we could perform whole mount immunostaining on 18 month old vascular endothelial cadherin lineage tracing mice, used to lineage trace endothelial cells, and look for lineage traced endothelial cells that are outside of their normal luminal proximity and are expressing markers of SMCs. Unfortunately, this methodology has several critical limitations. First and foremost, we have not confirmed that the gaps that develop in aged mice are occurring through the same process as the SMC specific knockout of *Klf4* gaps. This is an important first step. As discussed previously, we hypothesize that the aged mice would develop similar hyperpermeability defects as the *Klf4* knockouts, however this is still untested. We have also demonstrated extensive systemic vascular changes in the *Klf4* knockout mice that would affect the environmental cues SMCs in the microvasculature sense. We have not determined if any of these parameters are altered in the aged mice. Second, not utilizing a SMC lineage tracing system prohibits confirmation that gaps develop in lineage traced SMC coverage. For example, you would not be able to determine if an endothelial cell has undergone an endothelial to mesenchymal transition and moved to replace a missing SMC, or if it has undergone this transition for another purpose. Third, no alternative

hypotheses can be tested through these experiments. That is, if the experiments reveal the lineage traced cell type does not contribute to the replacement cell population, the only future direction is to try another lineage tracing system. Finally, these studies would be extremely expensive to perform as they would require complex mouse lines and extensive time in a vivarium.

Ultimately, efforts to determine what the source/sources of the replacement cells are would be extremely costly and time consuming while contributing mostly descriptive information. It is not entirely surprising that there is a replacement mechanism for lost SMCs, as there would be strong evolutionary selection pressure on such a mechanism to maintain vascular tone. Importantly, we have no direct evidence that it is the development of gaps, and subsequent replacement from non eYFP+ sources, that leads to our observed phenotypes. We do know that what we have observed is the summation of changes as a result of knockout of *Klf4* specifically in SMCs.

### **Is there a compensatory mechanism for loss of KLF4 in SMC?**

As discussed at length throughout this dissertation, a functioning vasculature is critical for the survival of an individual. Thus, having a compensatory mechanism to enable the vasculature's proper function (i.e. normalized vessel diameter and blood pressure) would be highly selected for during evolution. Therefore, I hypothesize that there is eventual compensation for loss of *Klf4* in SMCs. Preliminary results from our aged mice demonstrated that both SMC eYFP<sup>+/+</sup> *Klf4*<sup>WT/WT</sup> and SMC eYFP<sup>+/+</sup> *Klf4*<sup>Δ/Δ</sup> mice develop gaps (Figure

11). Interestingly, it does not appear that knockout mice had significantly more or larger gaps than their wild type littermates. One explanation for this is that the initial loss of *Klf4* results in the increased turnover of SMCs (hypothesis discussed in detail above), but there is eventual compensation for its loss.

Additional studies are required to determine if the other vascular phenotypes we observed in SMC eYFP<sup>+/+</sup> *Klf4*<sup>Δ/Δ</sup> mice normalize with time. Normalization of our observed phenotypes would be suggestive of compensation for the loss of *Klf4*. Specifically, examination of functional cardiovascular parameters is needed. To begin, I would perform an echocardiography time course to examine functional changes in heart performance over time. As echocardiography is a noninvasive procedure, we could do this once every 3 months until we reach a final aged time point of 18-24 months. To assay peripheral vasculature parameters, I would utilize carotid artery telemetry. Telemetry systems allow for the monitoring of blood pressure and blood flow for up to a month in a freely moving animal. Performing telemetry at an intermediate time point of 6 months of age, as well as an aged time point of 18 months would begin to describe the effects of *Klf4* knockout on the peripheral vasculature over time. Examination of vascular permeability would also be necessary at an intermediate and late age. Vascular permeability would be determined by dextran perfusion assays as detailed in Chapter II. Combined, these techniques would determine if there is functional recovery of cardiovascular performance over time in the SMC eYFP<sup>+/+</sup> *Klf4*<sup>Δ/Δ</sup> mice, or if performance remains impaired.

Two likely genes that might compensate for the loss of *Klf4* are *Klf2* and *Klf5*. As discussed in the introduction, *Klf5* performs similar functions to *Klf4* within SMCs. *Klf5* has also been shown to share several common regulatory pathways with *Klf4*<sup>61,69</sup>. Thus, the loss of *Klf4* may result in the upregulation of *Klf5* within SMCs. We could examine this directly by performing KLF5 immunohistochemistry in our SMC eYFP<sup>+/+</sup> *Klf4*<sup>WT/WT</sup> and SMC eYFP<sup>+/+</sup> *Klf4*<sup>Δ/Δ</sup> mice. We could also perform a western blot to determine if *Klf4* knockout in SMC leads to an increase in total *Klf5* levels in various vascular beds. Initial flow sorting of eYFP<sup>+</sup> cells from vascular beds could be used for cell type specificity for such a western blot experiment. Less is known about the role of *Klf2* within vascular SMCs. KLF2-deficient mice have relatively normal vasculogenesis and angiogenesis during development, but do not survive beyond E12.5-E14.5 due to severe hemorrhage<sup>1,139</sup>. More recent studies have demonstrated that KLF2 is necessary for SMC migration and investment of endothelial tubes during development<sup>140</sup>. If KLF2 within vascular SMCs plays a similar role in the adult, it may be upregulated upon loss of *Klf4* in an attempt to resolve the vascular leak that occurs with loss of KLF4. Similar studies to those described above can be performed to examine the regulation of *Klf2*. Importantly, even if compensation does occur, our conclusion that *Klf4* is important in baseline SMC maintenance remains true.

If the preceding studies do identify compensation for loss of *Klf4* by *Klf2* and/or *Klf5*, the logical follow up experiment is combinatorial knockout of *Klf2*, *Klf4* and *Klf5*. Such an approach would allow us to determine if compensation for

loss of *Klf4* is happening through these genes. Therefore, we would assess whether the functional cardiovascular parameters including blood pressure reduction, hyperpermeability, and cardiac dilation decline further, potentially leading to the death of the animals. Generation of a triple knockout system would involve the breeding of our *Klf4* knockout mouse with mice containing floxed *Klf2* and *Klf5* genes, as conventional knockout of *Klf2*<sup>1,139</sup> and *Klf5*<sup>68</sup> are embryonic lethal. We would also want to investigate mice that only had 2 of the 3 floxed genes (*Klf4* and *Klf2* floxed, *Klf4* and *Klf5* floxed) to determine whether any combination of two *Klf* genes is sufficient for any observed phenotypes. Each of these individual mice would need to be extensively validated and characterized. In particular, we would need to assess knockout efficiency in these mice. With our *Klf4* knockout mouse there is an assumption (backed by data) that cells that are eYFP+ are highly likely to have also excised the *Klf4* flox sites. This assumption would need to be rigorously tested in a proposed double or triple knockout system to ensure that eYFP labeling is a good indicator of knockout efficiency for both (in the double *Klf* floxed systems) or all three genes (triple *Klf* flox). Overall, these experiments would be extremely costly and time consuming. As such, they should only be pursued if there is a strong indication that compensation is occurring.

## How does SMC specific *Klf4* knockout result in dysregulated metabolic pathways?

RNA Seq analysis on our SMC specific *Klf4* knockout and wild type mice revealed that there is significant dysregulation of metabolic pathways in the knockout mice (Figure 10). Examining fasting blood glucose levels in the knockout mice, we observed no differences (Figure 10C). However, upon stimulation with a DIO model of high fat diet feeding, SMC eYFP<sup>+/+</sup> *Klf4*<sup>Δ/Δ</sup> had significantly elevated fasting blood glucose levels when compared to their DIO fed wild type litter mates (Figure 10C). The mechanism that leads to elevated blood glucose levels after DIO remains unclear, although it appears that SMC eYFP<sup>+/+</sup> *Klf4*<sup>Δ/Δ</sup> mice are primed for metabolic dysfunction that manifests itself upon challenge.

Our RNA Seq was done on the mesentery of our mice. The mesentery is a pathological fat pad that has been implicated in the pathogenesis of various metabolic diseases including obesity and diabetes. During the progression of these diseases, pathological fat pads become highly inflamed (reviewed in <sup>141</sup>). This inflammation is associated with an influx of macrophages and other immune cells into the tissue. Macrophages are generally characterized into two subtypes, M1 and M2 macrophages. M1 macrophages are proinflammatory, while M2 macrophages are anti-inflammatory <sup>142,143</sup>. As we have previously demonstrated both here (Figure 4) and elsewhere <sup>30,34</sup>, SMCs contribute to macrophage populations during the setting of injury repair and disease pathogenesis. Therefore, SMCs may be contributing to these macrophage cell populations

following high fat diet feeding. Knockout of KLF4 would presumably disrupt these transitions, similar to what we have seen in previous models. Interestingly M2 macrophages preferentially perform oxidative phosphorylation (reviewed in <sup>144</sup>). Our RNA Seq results on baseline mice identified dysregulation of oxidative phosphorylation in our knockout mice. This may be due, at least in part, to a reduction in a baseline conversion of SMC to M2 macrophage-like cells. A loss of SMC derived M2 macrophages would likely worsen any pathologic changes that result from DIO feeding as this may result in there being fewer anti-inflammatory M2 macrophages within the tissue and thus more unresolved inflammation. As such, I hypothesize SMCs undergo phenotypic transitions to a M2 macrophage-like state under baseline conditions.

Preliminary flow cytometry studies in baseline mice have identified SMC derived macrophage-like cells in both the mesentery and epididymal fat (Dr. Anh Nguyen and R. Haskins, unpublished observations). Interestingly, we have also identified these macrophage-like SMCs in a variety of nonfat tissues at baseline including the diaphragm and heart, although they are very low in number (Dr. Anh Nguyen and R. Haskins, unpublished observations). Following DIO high fat diet feeding (2, 4 or 8 weeks of diet), Dr. Gamze Bulut and Dr. Anh Nguyen in the Owens' lab have also identified SMC derived macrophage-like cells in both the mesentery and epididymal fat. Further studies are needed to determine what the relative abundance of these macrophage-like SMCs is within these tissues, both at baseline and after DIO feeding. The *Klf4* dependence of this transition also needs to be determined, although I hypothesize it would be *Klf4* dependent. It

also remains unclear whether these macrophage-like SMCs are M1 or M2 macrophage-like cells. Taken together, we believe the above data may represent a novel source of tissue resident macrophages. If this hypothesis proves to be correct, it would be extremely significant to numerous fields of study. As such, this has become the main project of Dr. Bulut in the lab.

Further potential support for a baseline SMC to macrophage-like conversion can be found in recent reports in the literature that have shown that CD206+ macrophages control permeability within microvascular tissues, including the mesentery <sup>145</sup>. Interestingly, these macrophages were predominately M2 <sup>145</sup>. I would hypothesize that SMCs contribute to this population of macrophages under baseline conditions and that KLF4 knockout in SMC would prevent SMC transitions to this macrophage-like state. This hypothesis would fit with our data that demonstrated SMC eYFP<sup>+/+</sup> Klf4<sup>Δ/Δ</sup> mice had increased microvascular permeability (Figure 9). Further studies are needed to determine if our macrophage-like SMCs express CD206 and are found in perivascular locations, like those described by the Iruela-Arispe group.

Overall, I believe that the metabolic changes we observed as a result of knockout of *Klf4* in SMC can be attributed in part to a loss of these hypothesized SMC derived M2 macrophage-like cells throughout the body. As discussed above, I believe that SMCs may contribute to the subset of M2 macrophages that control permeability within the microvasculature. Disruptions in vessel permeability, like those we observe in our SMC eYFP<sup>+/+</sup> Klf4<sup>Δ/Δ</sup> mice, would result in disruption of the normal diffusion gradients of nutrients into the surrounding

tissue thus changing substrate availability and potentially the cells metabolic state. Macrophages are also known to produce a host of cytokines<sup>146</sup>. A reduction in SMC derived macrophage-like cells would likely alter the paracrine signals a variety of cell types within the microvasculature sense. Additional studies are required to determine what these cytokines might be, and the cell types they are affecting. Initial screens could be done utilizing cytokine arrays. In particular, investigation of changes in proinflammatory cytokines as well as angiogenic factors and known SMC cytokines would be of interest.

## Summary

I believe two of the future studies discussed here should be given priority over the others. First, is there eventual compensation, by *Klf2/Klf5* or otherwise, for loss of *Klf4*? It is critical to know whether the phenotypes we have demonstrated occur in SMC eYFP<sup>+/+</sup> *Klf4*<sup>Δ/Δ</sup> mice persist beyond our experimental time point of 10 weeks of age (2 weeks after the last tamoxifen injection). If they do persist, this is important to take into account when interpreting all future studies with these mice. This may be of particular relevance to the other priority study, which is the investigation of whether SMCs are a novel source of tissue resident macrophages. These studies are a priority as they would be the first demonstrated circumstance of SMC phenotypic transitions to a macrophage-like state in a non-pathological condition. As such, this may be one of the *Klf4* dependent SMC functions that is beneficial and thus has been selected for during evolution. Identifying a novel source of tissue resident

macrophages would also have wide ranging implications on the study of macrophages in various pathological conditions including cardiovascular disease, obesity, and cancer.

## **Chapter V: References**

1. Kuo CT, Veselits ML, Barton KP, Lu MM, Clendenin C, Leiden JM. The LKLF transcription factor is required for normal tunica media formation and blood vessel stabilization during murine embryogenesis. *Genes Dev.* 1997;11:2996–3006.
2. Oh SP, Seki T, Goss KA, Imamura T, Yi Y, Donahoe PK, Li L, Miyazono K, ten Dijke P, Kim S, Li E. Activin receptor-like kinase 1 modulates transforming growth factor-beta 1 signaling in the regulation of angiogenesis. *Proc Natl Acad Sci U S A.* 2000;97:2626–31.
3. Oshima M, Oshima H, Taketo MM. TGF-beta receptor type II deficiency results in defects of yolk sac hematopoiesis and vasculogenesis. *Dev Biol.* 1996;179:297–302.
4. Alexander MR, Owens GK. Epigenetic Control of Smooth Muscle Cell Differentiation and Phenotypic Switching in Vascular Development and Disease. *Annu Rev Physiol.* 2012;74:13–40.
5. Owens GK, Kumar MS, Wamhoff BR. Molecular Regulation of Vascular Smooth Muscle Cell Differentiation in Development and Disease PLAYS A KEY ROLE IN A NUMBER OF. 2004;:767–801.
6. Owens GK. Regulation of differentiation of vascular smooth muscle cells. *Physiol Rev.* 1995;75:487–517.
7. Mulvany MJ, Aalkjaer C. Physiological Reviews of Small Arteries. *Physiol Rev.* 1990;70:921–961.
8. Segal SS, Duling BR. Communication between feed arteries and microvessels in hamster striated muscle: segmental vascular responses are functionally coordinated. *Circ Res.* 1986;59:283–290.
9. Stekiel WJ, Contney SJ, Lombard JH. Small vessel membrane potential, sympathetic input, and electrogenic pump rate in SHR. *Am J Physiol.* 1986;250:C547-56.
10. Moncada S, Palmer RM, Higgs EA. Nitric oxide: physiology, pathophysiology, and pharmacology. *Pharmacol Rev.* 1991;43:109–42.
11. Lundberg JO, Weitzberg E, Gladwin MT. The nitrate-nitrite-nitric oxide pathway in physiology and therapeutics. *Nat Rev Drug Discov.* 2008;7:156–67.
12. Knowles RG, Moncada S. Nitric oxide synthases in mammals. *Biochem J.* 1994;298:249–58.

13. Lincoln TM, Cornwell TL. Towards an understanding of the mechanism of action of cyclic AMP and cyclic GMP in smooth muscle relaxation. *Blood Vessels*. 1991;28:129–37.
14. Lincoln TM, Cornwell TL. Intracellular cyclic GMP receptor proteins. *FASEB J*. 1993;7:328–38.
15. Bolotina VM, Najibi S, Palacino JJ, Pagano PJ, Cohen R a. Nitric oxide directly activates calcium-dependent potassium channels in vascular smooth muscle. *Nature*. 1994;368:850–853.
16. Ignarro L, Lipton H, Edwards J, Baricos W, Hyman A, Kadowitz P, Gruetter C. Mechanism of vascular smooth muscle relaxation by organic nitrates, nitrites, nitroprusside and nitric oxide: evidence for the involvement of S-nitrosothiols as active intermediates. *J Pharmacol Exp Ther*. 1981;218:739–749.
17. Dora KA, Doyle MP, Duling BR, Berne RM. Elevation of intracellular calcium in smooth muscle causes endothelial cell generation of NO in arterioles. *Physiology*. 1997;94:6529–6534.
18. Straub AC, Billaud M, Johnstone SR, Best AK, Yemen S, Dwyer ST, Looft-Wilson R, Lysiak JJ, Gaston B, Palmer L, Isakson BE. Compartmentalized connexin 43 S-nitrosylation/denitrosylation regulates heterocellular communication in the vessel wall. *Arterioscler Thromb Vasc Biol*. 2011;31:399–407.
19. Jackson WF, Boerman EM, Lange EJ, Lundback SS, Cohen KD. Smooth muscle  $\alpha 1D$ -adrenoceptors mediate phenylephrine-induced vasoconstriction and increases in endothelial cell Ca<sup>2+</sup> in hamster cremaster arterioles. *Br J Pharmacol*. 2008;155:514–524.
20. Brozovich F V, Nicholson CJ, Degen C V, Gao YZ, Aggarwal M, Morgan KG. Mechanisms of Vascular Smooth Muscle Contraction and the Basis for Pharmacologic Treatment of Smooth Muscle Disorders. *Pharmacol Rev*. 2016;68:476–532.
21. Potente M, Gerhardt H, Carmeliet P. Basic and therapeutic aspects of angiogenesis. *Cell*. 2011;146:873–887.
22. Carmeliet P, Jain RK. Molecular mechanisms and clinical applications of angiogenesis. *Nature*. 2011;473:298–307.
23. Deaton R a, Gan Q, Owens GK. Sp1-dependent activation of KLF4 is required for PDGF-BB-induced phenotypic modulation of smooth muscle. *Am J Physiol Heart Circ Physiol*. 2009;296:H1027–H1037.

24. Yoshida T, Kaestner KH, Owens GK. Conditional deletion of Krüppel-like factor 4 delays downregulation of smooth muscle cell differentiation markers but accelerates neointimal formation following vascular injury. *Circ Res*. 2008;102:1548–1557.
25. Kanisicak O, Khalil H, Ivey MJ, Karch J, Maliken BD, Correll RN, Brody MJ, J Lin S-C, Aronow BJ, Tallquist MD, Molkentin JD. Genetic lineage tracing defines myofibroblast origin and function in the injured heart. *Nat Commun*. 2016;7:12260.
26. Liao Y, Regan CP, Manabe I, Owens GK, Day KH, Damon DN, Duling BR. Smooth muscle-targeted knockout of connexin43 enhances neointimal formation in response to vascular injury. *Arterioscler Thromb Vasc Biol*. 2007;27:1037–1042.
27. Salmon M, Gomez D, Greene E, Shankman L, Owens GK. Cooperative binding of KLF4, pELK-1, and HDAC2 to a G/C repressor element in the SM22 $\alpha$  promoter mediates transcriptional silencing during SMC phenotypic switching in vivo. *Circ Res*. 2012;111:685–696.
28. Ailawadi G, Moehle CW, Pei H, Walton SP, Yang Z, Kron IL, Lau CL, Owens GK. Smooth muscle phenotypic modulation is an early event in aortic aneurysms. *J Thorac Cardiovasc Surg*. 2009;138:1392–1399.
29. Starke RM, Chalouhi N, Ding D, Raper DMS, Mckisic MS, Owens GK, Hasan DM, Medel R, Dumont AS. Vascular smooth muscle cells in cerebral aneurysm pathogenesis. *Transl Stroke Res*. 2014;5:338–46.
30. Cherepanova OA, Gomez D, Shankman LS, Swiatlowska P, Williams J, Sarmiento OF, Alencar GF, Hess DL, Bevard MH, Greene ES, Murgai M, Turner SD, Geng YJ, Bekiranov S, Connelly JJ, Tomilin A, Owens GK. Activation of the pluripotency factor OCT4 in smooth muscle cells is atheroprotective. *Nat Med*. 2016;22:657–665.
31. Feil S, Fehrenbacher B, Lukowski R, Essmann F, Schulze-Osthoff K, Schaller M, Feil R. Transdifferentiation of vascular smooth muscle cells to macrophage-like cells during atherogenesis. *Circ Res*. 2014;115:662–667.
32. Durgin BG, Cherepanova OA, Gomez D, Karaoli T, Alencar GF, Butcher JT, Zhou Y-Q, Bendeck MP, Owens GK, Connelly JJ, affiliations A. Smooth muscle cell-specific deletion of Col15a1 unexpectedly leads to impaired 1 development of advanced atherosclerotic lesions 2 3. 2017;4403. doi:10.1152/ajpheart.00029.2017.
33. Gomez D, Shankman L, Nguyen A, Owens G. Detection of histone modifications at specific gene loci in single cells in histological sections.

*Nat Methods*. 2013;10:171–177.

34. Shankman LS, Gomez D, Cherepanova O a, Salmon M, Alencar GF, Haskins RM, Swiatlowska P, Newman A a C, Greene ES, Straub AC, Isakson B, Randolph GJ, Owens GK. KLF4-dependent phenotypic modulation of smooth muscle cells has a key role in atherosclerotic plaque pathogenesis. *Nat Med*. 2015;21:628–37.
35. Miano JM. Serum response factor: Toggling between disparate programs of gene expression. *J Mol Cell Cardiol*. 2003;35:577–593.
36. Hautmann MB, Madsen CS, Mack CP, Owens GK. Substitution of the degenerate smooth muscle (SM)  $\alpha$ -actin CC(AT-rich)6GG elements with c-fos serum response elements results in increased basal expression but relaxed SM cell specificity and reduced angiotensin II inducibility. *J Biol Chem*. 1998;273:8398–8406.
37. Chang PS, Li L, McAnally J, Olson EN. Muscle Specificity Encoded by Specific Serum Response Factor-binding Sites. *J Biol Chem*. 2001;276:17206–17212.
38. Hendrix JA, Wamhoff BR, McDonald OG, Sinha S, Yoshida T, Owens GK. 5' CARG degeneracy in smooth muscle  $\alpha$ -actin is required for injury-induced gene suppression in vivo. *J Clin Invest*. 2005;115:418–427.
39. Wang DZ, Chang PS, Wang Z, Sutherland L, Richardson JA, Small E, Krieg PA, Olson EN. Activation of cardiac gene expression by myocardin, a transcriptional cofactor for serum response factor. *Cell*. 2001;105:851–862.
40. Chen J, Kitchen CM, Streb JW, Miano JM. Myocardin: A component of a molecular switch for smooth muscle differentiation. *J Mol Cell Cardiol*. 2002;34:1345–1356.
41. Mack CP, Thompson MM, Lawrenz-Smith S, Owens GK. Smooth muscle alpha-actin CARG elements coordinate formation of a smooth muscle cell-selective, serum response factor-containing activation complex. *Circ Res*. 2000;86:221–232.
42. Wang Z, Wang D-Z, Pipes GCT, Olson EN. Myocardin is a master regulator of smooth muscle gene expression. *Proc Natl Acad Sci U S A*. 2003;100:7129–34.
43. Parmacek MS. Myocardin - Not quite MyoD. *Arterioscler Thromb Vasc Biol*. 2004;24:1535–1537.
44. Kornberg RD. Chromatin structure: a repeating unit of histones and DNA.

- Science*. 1974;184:868–71.
45. Jenuwein T, Allis CD. Translating the histone code. *Science*. 2001;293:1074–80.
  46. Tse C, Sera T, Wolffe a P, Hansen JC. Disruption of higher-order folding by core histone acetylation dramatically enhances transcription of nucleosomal arrays by RNA polymerase III. *Mol Cell Biol*. 1998;18:4629–4638.
  47. Narlikar GJ, Fan HY, Kingston RE. Cooperation between complexes that regulate chromatin structure and transcription. *Cell*. 2002;108:475–487.
  48. McDonald OG, Wamhoff BR, Hoofnagle MH, Owens GK. Control of SRF binding to CARG box chromatin regulates smooth muscle gene expression in vivo. *J Clin Invest*. 2006;116:36–48.
  49. Pray-Grant MG, Daniel JA, Schieltz D, Yates JR, Grant PA. Chd1 chromodomain links histone H3 methylation with SAGA- and SLIK-dependent acetylation. *Nature*. 2005;433:434–438.
  50. Gomez D, Swiatlowska P, Owens GK. Epigenetic Control of Smooth Muscle Cell Identity and Lineage Memory. *Arterioscler Thromb Vasc Biol*. 2015;35:2508–2516.
  51. Holycross BJ, Blank RS, Thompson MM, Peach MJ, Owens GK. Platelet-derived growth factor-BB-induced suppression of smooth muscle cell differentiation. *Circ Res*. 1992;71:1525–1532.
  52. Pidkovka NA, Cherepanova OA, Yoshida T, Alexander MR, Deaton RA, Thomas JA, Leitinger N, Owens GK. Oxidized phospholipids induce phenotypic switching of vascular smooth muscle cells in vivo and in vitro. *Circ Res*. 2007;101:792–801.
  53. Cherepanova OA, Pidkovka NA, Sarmiento OF, Yoshida T, Gan Q, Adiguzel E, Bendeck MP, Berliner J, Leitinger N, Owens GK. Oxidized phospholipids induce type VIII collagen expression and vascular smooth muscle cell migration. *Circ Res*. 2009;104:609–618.
  54. Shields JM, Christy RJ, Yang VW. Identification and Characterization of a Gene Encoding a Gut-enriched Krüppel-like Factor Expressed during Growth Arrest. *J Biol Chem*. 1996;271:20009–20017.
  55. Dang DT, Pevsner J, Yang VW. The biology of the mammalian Krüppel-like family of transcription factors. *Int J Biochem Cell Biol*. 2000;32:1103–1121.

56. Adam PJ, Regan CP, Hautmann MB, Owens GK. Positive- and negative-acting Kruppel-like transcription factors bind a transforming growth factor  $\beta$  control element required for expression of the smooth muscle cell differentiation marker SM22 $\alpha$  in vivo. *J Biol Chem*. 2000;275:37798–37806.
57. Liu Y, Sinha S, McDonald OG, Shang Y, Hoofnagle MH, Owens GK. Kruppel-like factor 4 abrogates myocardin-induced activation of smooth muscle gene expression. *J Biol Chem*. 2005;280:9719–9727.
58. Yoshida T, Gan Q, Owens GK. Kruppel-like factor 4, Elk-1, and histone deacetylases cooperatively suppress smooth muscle cell differentiation markers in response to oxidized phospholipids. *Am J Physiol Cell Physiol*. 2008;295:C1175-82.
59. Wang Z, Wang D, Hockemeyer D, Mcanally J, Nordheim A, Olson EN. Myocardin and ternary complex factors compete for SRF to control smooth muscle gene expression. *Nature*. 2004;428:185–189.
60. Yoshida T, Gan Q, Shang Y, Owens GK. Platelet-derived growth factor-BB represses smooth muscle cell marker genes via changes in binding of MKL factors and histone deacetylases to their promoters. *Am J Physiol Cell Physiol*. 2007;292:C886-95.
61. Turner EC, Huang CL, Govindarajan K, Caplice NM. Identification of a Klf4-dependent upstream repressor region mediating transcriptional regulation of the myocardin gene in human smooth muscle cells. *Biochim Biophys Acta - Gene Regul Mech*. 2013;1829:1191–1201.
62. Calin GA, Croce CM. MicroRNA signatures in human cancers. *Nat Rev Cancer*. 2006;6:857–866.
63. Zhao Y, Srivastava D. A developmental view of microRNA function. *Trends Biochem Sci*. 2007;32:189–197.
64. Kloosterman WP, Plasterk RHA. The Diverse Functions of MicroRNAs in Animal Development and Disease. *Dev Cell*. 2006;11:441–450.
65. Cordes KR, Sheehy NT, White MP, Berry EC, Morton SU, Muth AN, Lee T-H, Miano JM, Ivey KN, Srivastava D. miR-145 and miR-143 regulate smooth muscle cell fate and plasticity. *Nature*. 2009;460:705–710.
66. Davis-Dusenbery BN, Chan MC, Reno KE, Weisman AS, Layne MD, Lagna G, Hata A. Down-regulation of Krüppel-like Factor-4 (KLF4) by microRNA-143/145 is critical for modulation of vascular smooth muscle cell phenotype by transforming growth factor- $\beta$  and bone morphogenetic protein 4. *J Biol Chem*. 2011;286:28097–28110.

67. Xu N, Papagiannakopoulos T, Pan G, Thomson JA, Kosik KS. MicroRNA-145 Regulates OCT4, SOX2, and KLF4 and Represses Pluripotency in Human Embryonic Stem Cells. *Cell*. 2009;137:647–658.
68. Shindo T, Manabe I, Fukushima Y, Tobe K, Aizawa K, Miyamoto S, Kawai-Kowase K, Moriyama N, Imai Y, Kawakami H, Nishimatsu H, Ishikawa T, Suzuki T, Morita H, Maemura K, Sata M, Hirata Y, Komukai M, Kagechika H, Kadowaki T, Kurabayashi M, Nagai R. Krüppel-like zinc-finger transcription factor KLF5/BTEB2 is a target for angiotensin II signaling and an essential regulator of cardiovascular remodeling. *Nat Med*. 2002;8:856–63.
69. Cheng Y, Liu X, Yang J, Lin Y, Xu DZ, Lu Q, Deitch EA, Huo Y, Delphin ES, Zhang C. MicroRNA-145, a novel smooth muscle cell phenotypic marker and modulator, controls vascular neointimal lesion formation. *Circ Res*. 2009;105:158–166.
70. Jiang J, Chan YS, Loh YH, Cai J, Tong GQ, Lim CA, Robson P, Zhong S, Ng HH. A core Klf circuitry regulates self-renewal of embryonic stem cells. *Nat Cell Biol*. 2008;10:353–360.
71. Nguyen AT, Gomez D, Bell RD, Campbell JH, Clowes AW, Gabbiani G, Giachelli CM, Parmacek MS, Raines EW, Rusch NJ, Speer MY, Sturek M, Thyberg J, Towler DA, Weiser-Evans MC, Yan C, Miano JM, Owens GK. Smooth muscle cell plasticity: fact or fiction? *Circ Res*. 2013;112:17–22.
72. Sheikh AQ, Misra A, Rosas IO, Adams RH, Greif DM. Smooth muscle cell progenitors are primed to muscularize in pulmonary hypertension. *Sci Transl Med*. 2015;7:308ra159.
73. Wirth A, Benyó Z, Lukasova M, Leutgeb B, Wettschureck N, Gorbey S, Orsy P, Horváth B, Maser-Gluth C, Greiner E, Lemmer B, Schütz G, Gutkind S, Offermanns S. G12-G13-LARG-mediated signaling in vascular smooth muscle is required for salt-induced hypertension. *Nat Med*. 2008;14:64–68.
74. Libby, P.; Ridker, P. M.; Hansson GK. Progress and challenges in translating the biology of atherosclerosis. *Nature*. 2011;473:317–325.
75. Lusis AJ. Atherosclerosis. *Nature*. 2000;407:233–241.
76. Benjamin EJ, Virani SS, Callaway CW, Chang AR, Cheng S, Chiuve SE, Cushman M, Delling FN, Deo R, de Ferranti SD, Ferguson JF, Fornage M, Gillespie C, Isasi CR, Jiménez MC, Jordan LC, Judd SE, Lackland D, Lichtman JH, Lisabeth L, Liu S, Longenecker CT, Lutsey PL, Matchar DB, Matsushita K, Mussolino ME, Nasir K, O'Flaherty M, Palaniappan LP,

- Pandey DK, Reeves MJ, Ritchey MD, Rodriguez CJ, Roth GA, Rosamond WD, Sampson UKA, Satou GM, Shah SH, Spartano NL, Tirschwell DL, Tsao CW, Voeks JH, Willey JZ, Wilkins JT, Wu JH, Alger HM, Wong SS, Muntner P. Heart Disease and Stroke Statistics—2018 Update: A Report From the American Heart Association. ; 2018: 1-CIR.0000000000000558. doi:10.1161/CIR.0000000000000558.
77. Christopher Glass AK, Witztum JL. Atherosclerosis: The Road Ahead Review approach to evaluating potential roles of specific pro. *Cell*. 2001;104:503–516.
  78. Caplice NM, Bunch TJ, Stalboerger PG, Wang S, Simper D, Miller D V, Russell SJ, Litzow MR, Edwards WD. Smooth muscle cells in human coronary atherosclerosis can originate from cells administered at marrow transplantation. *Proc Natl Acad Sci U S A*. 2003;100:4754–9.
  79. Crisan M, Yap S, Casteilla L, Chen CW, Corselli M, Park TS, Andriolo G, Sun B, Zheng B, Zhang L, Norotte C, Teng PN, Traas J, Schugar R, Deasy BM, Badylak S, Buhring HJ, Giacobino JP, Lazzari L, Huard J, Péault B. A Perivascular Origin for Mesenchymal Stem Cells in Multiple Human Organs. *Cell Stem Cell*. 2008;3:301–313.
  80. Crisan M, Corselli M, Chen WCW, Péault B. Perivascular cells for regenerative medicine. *J Cell Mol Med*. 2012;16:2851–2860.
  81. Armulik A, Genové G, Betsholtz C. Pericytes: Developmental, Physiological, and Pathological Perspectives, Problems, and Promises. *Dev Cell*. 2011;21:193–215.
  82. Vannella KM, Wynn TA. Mechanisms of Organ Injury and Repair by Macrophages. *Annu Rev Physiol*. 2017;79:593–617.
  83. Dobaczewski M, Gonzalez-Quesada C, Frangogiannis NG. The extracellular matrix as a modulator of the inflammatory and reparative response following myocardial infarction. *J Mol Cell Cardiol*. 2010;48:504–511.
  84. González A, Ravassa S, Beaumont J, López B, Díez J. New targets to treat the structural remodeling of the myocardium. *J Am Coll Cardiol*. 2011;58:1833–1843.
  85. van den Borne SWM, Díez J, Blankesteyn WM, Verjans J, Hofstra L, Narula J. Myocardial remodeling after infarction: the role of myofibroblasts. *Nat Rev Cardiol*. 2010;7:30–37.
  86. Sun Y, Weber KT. Infarct scar: a dynamic tissue. *Cardiovasc Res*.

2000;46:250–6.

87. Heidt T, Courties G, Dutta P, Sager HB, Sebas M, Iwamoto Y, Sun Y, Da Silva N, Panizzi P, Van Der Lahn AM, Swirski FK, Weissleder R, Nahrendorf M. Differential contribution of monocytes to heart macrophages in steady-state and after myocardial infarction. *Circ Res.* 2014;115:284–295.
88. Epelman S, Lavine KJ, Beaudin AE, Sojka DK, Carrero JA, Calderon B, Brija T, Gautier EL, Ivanov S, Satpathy AT, Schilling JD, Schwendener R, Sergin I, Razani B, Forsberg EC, Yokoyama WM, Unanue ER, Colonna M, Randolph GJ, Mann DL. Embryonic and adult-derived resident cardiac macrophages are maintained through distinct mechanisms at steady state and during inflammation. *Immunity.* 2014;40:91–104.
89. Long JZ, Svensson KJ, Tsai L, Zeng X, Roh HC, Kong X, Rao RR, Lou J, Lokurkar I, Baur W, Castellot JJ, Rosen ED, Spiegelman BM. A smooth muscle-like origin for beige adipocytes. *Cell Metab.* 2014;19:810–820.
90. Nahrendorf M, Swirski FK, Aikawa E, Stangenberg L, Wurdinger T, Figueiredo J-L, Libby P, Weissleder R, Pittet MJ. The healing myocardium sequentially mobilizes two monocyte subsets with divergent and complementary functions. *J Exp Med.* 2007;204:3037–3047.
91. Klibanov AL, Rychak JJ, Yang WC, Alikhani S, Li B, Acton S, Lindner JR, Ley K, Kaul S. Targeted ultrasound contrast agent for molecular imaging of inflammation in high-shear flow. *Contrast Media Mol Imaging.* 2006;1:259–66.
92. Wei K, Jayaweera R, Firoozan S, Linka A, Skyba DM, Kaul S. Quantification of myocardial blood flow with ultrasound-induced destruction of microbubbles administered as a constant venous infusion. *Circulation.* 1998;97:473–483.
93. Billaud M, Lohman AW, Straub AC, Parpaite T, Johnstone SR, Isakson BE. Characterization of the Thoracodorsal Artery: Morphology and Reactivity. *Microcirculation.* 2012;19:360–372.
94. Langmead B, Trapnell C, Pop M, Salzberg SL. Ultrafast and memory-efficient alignment of short DNA sequences to the human genome. *Genome Biol.* 2009;10:R25.
95. Li H, Handsaker B, Wysoker A, Fennell T, Ruan J, Homer N, Marth G, Abecasis G, Durbin R. The Sequence Alignment/Map format and SAMtools. *Bioinformatics.* 2009;25:2078–2079.

96. Zhang Y, Liu T, Meyer CA, Eeckhoute J, Johnson DS, Bernstein BE, Nussbaum C, Myers RM, Brown M, Li W, Liu XS. Model-based Analysis of ChIP-Seq (MACS). *Genome Biol.* 2008;9:R137.
97. Quinlan AR, Hall IM. BEDTools: A flexible suite of utilities for comparing genomic features. *Bioinformatics.* 2010;26:841–842.
98. Huang DW, Sherman BT, Lempicki RA. Systematic and integrative analysis of large gene lists using DAVID bioinformatics resources. *Nat Protoc.* 2008;4:44–57.
99. Mi H, Muruganujan A, Casagrande JT, Thomas PD. Large-scale gene function analysis with the PANTHER classification system. *Nat Protoc.* 2013;8:1551–1566.
100. Kelly-Goss MR, Ning B, Bruce AC, Tavakol DN, Yi D, Hu S, Yates PA, Peirce SM. Dynamic, heterogeneous endothelial Tie2 expression and capillary blood flow during microvascular remodelling. *Sci Rep.* 2017;7:1–12.
101. Iwata H, Manabe I, Fujiu K, Yamamoto T, Takeda N, Eguchi K, Furuya A, Kuro-O M, Sata M, Nagai R. Bone marrow-derived cells contribute to vascular inflammation but do not differentiate into smooth muscle cell lineages. *Circulation.* 2010;122:2048–2057.
102. Tsagalou EP, Anastasiou-Nana M, Agapitos E, Gika A, Drakos SG, Terrovitis J V., Ntalianis A, Nanas JN. Depressed Coronary Flow Reserve Is Associated With Decreased Myocardial Capillary Density in Patients With Heart Failure Due to Idiopathic Dilated Cardiomyopathy. *J Am Coll Cardiol.* 2008;52:1391–1398.
103. Smith CL, Baek ST, Sung CY, Tallquist MD. Epicardial-derived cell epithelial-to-mesenchymal transition and fate specification require PDGF receptor signaling. *Circ Res.* 2011;108:e15-26.
104. French WJ, Creemers EE, Tallquist MD. Platelet-Derived Growth Factor Receptors Direct Vascular Development Independent of Vascular Smooth Muscle Cell Function. *Mol Cell Biol.* 2008;28:5646–5657.
105. Andrae J, Gallini R, Betsholtz C. Role of platelet-derived growth factors in physiology and medicine. *Genes Dev.* 2008;22:1276–312.
106. Hicke L, Dunn R. Regulation of Membrane Protein Transport by Ubiquitin and Ubiquitin-Binding Proteins. *Annu Rev Cell Dev Biol.* 2003;19:141–172.
107. Rudic RD, Shesely EG, Maeda N, Smithies O, Segal SS, Sessa WC.

- Direct evidence for the importance of endothelium-derived nitric oxide in vascular remodeling. *J Clin Invest*. 1998;101:731–736.
108. Guzman RJ, Abe K, Zarins CK. Flow-induced arterial enlargement is inhibited by suppression of nitric oxide synthase activity in vivo. *Surgery*. 1997;122:273–280.
  109. Franklin SS, Gokhale SS, Chow VH, Larson MG, Levy D, Vasani RS, Mitchell GF, Wong ND. Does low diastolic blood pressure contribute to the risk of recurrent hypertensive cardiovascular disease events?: The framingham heart study. *Hypertension*. 2015;65:299–305.
  110. Franklin SS, Lopez VA, Wong ND, Mitchell GF, Larson MG, Vasani RS, Levy D. Single versus combined blood pressure components and risk for cardiovascular disease the framingham heart study. *Circulation*. 2009;119:243–250.
  111. Kannel WB, Wilson PWF, Nam BH, D'Agostino RB, Li J. A likely explanation for the J-curve of blood pressure cardiovascular risk. *Am J Cardiol*. 2004;94:380–384.
  112. Protogerou AD, Safar ME, Iaria P, Safar H, Le Dudal K, Filipovsky J, Henry O, Ducimetière P, Blacher J. Diastolic blood pressure and mortality in the elderly with cardiovascular disease. *Hypertension*. 2007;50:172–180.
  113. Lubsen J, Wagener G, Kirwan B-A, de Brouwer S, Poole-Wilson P a. Effect of long-acting nifedipine on mortality and cardiovascular morbidity in patients with symptomatic stable angina and hypertension: the ACTION trial. *J Hypertens*. 2005;23:641–648.
  114. Murgai M, Ju W, Eason M, Kline J, Beury DW, Kaczanowska S, Miettinen MM, Kruhlak M, Lei H, Shern JF, Cherepanova OA, Owens GK, Kaplan RN. KLF4-dependent perivascular cell plasticity mediates pre-metastatic niche formation and metastasis. *Nat Med*. 2017;23:1176–1190.
  115. Chen PY, Qin L, Barnes C, Charisse K, Yi T, Zhang X, Ali R, Medina PP, Yu J, Slack FJ, Anderson DG, Kotlianski V, Wang F, Tellides G, Simons M. FGF Regulates TGF- $\beta$  Signaling and Endothelial-to-Mesenchymal Transition via Control of let-7 miRNA Expression. *Cell Rep*. 2012;2:1684–1696.
  116. Chen PY, Qin L, Baeyens N, Li G, Afolabi T, Budatha M, Tellides G, Schwartz MA, Simons M. Endothelial-to-mesenchymal transition drives atherosclerosis progression. *J Clin Invest*. 2015;125:4514–4528.
  117. Passman JN, Dong XR, Wu S-P, Maguire CT, Hogan KA, Bautch VL,

- Majesky MW. A sonic hedgehog signaling domain in the arterial adventitia supports resident Sca1+ smooth muscle progenitor cells. *Proc Natl Acad Sci U S A*. 2008;105:9349–9354.
118. van der Harst P, Verweij N. Identification of 64 Novel Genetic Loci Provides an Expanded View on the Genetic Architecture of Coronary Artery Disease. *Circ Res*. 2018;122:433–443.
  119. Oakley R, Tharakan B. Vascular Hyperpermeability and Aging. *Aging Dis*. 2014;5:114–125.
  120. Fox J, Barthold S, Davisson M, Newcomer C, Quimby F, Smith A, eds. The Mouse in Biomedical Research, Volume 1, Second. Academic Press; 2007: 1-352.
  121. Chobanian A V., Bakris GL, Black HR, Cushman WC, Green LA, Izzo JL, Jones DW, Materson BJ, Oparil S, Wright JT, Roccella EJ. Seventh report of the Joint National Committee on Prevention, Detection, Evaluation, and Treatment of High Blood Pressure. *Hypertension*. 2003;42:1206–1252.
  122. Sun Z. Aging, arterial stiffness, and hypertension. *Hypertension*. 2015;65:252–256.
  123. Safar ME, Thomas F, Blacher J, Nzietchueng R, Bureau JM, Pannier B, Benetos A. Metabolic syndrome and age-related progression of aortic stiffness. *J Am Coll Cardiol*. 2006;47:72–75.
  124. Ferreira I, Van De Laar RJ, Prins MH, Twisk JW, Stehouwer CD. Carotid stiffness in young adults: A life-course analysis of its early determinants: The Amsterdam growth and health longitudinal study. *Hypertension*. 2012;59:54–61.
  125. Jackson CL, Reidy MA. Basic fibroblast growth factor: its role in the control of smooth muscle cell migration. *Am J Pathol*. 1993;143:1024–31.
  126. Owens GK, Vernon SM, Madsen CS. Molecular regulation of smooth muscle cell differentiation. *J Hypertens Suppl*. 1996;14:S55-64.
  127. Vanlandewijck M, He L, Mäe MA, Andrae J, Ando K, Del Gaudio F, Nahar K, Lebouvier T, Laviña B, Gouveia L, Sun Y, Raschperger E, Räsänen M, Zarb Y, Mochizuki N, Keller A, Lendahl U, Betsholtz C. A molecular atlas of cell types and zonation in the brain vasculature. *Nature*. 2018;554:475–480.
  128. Zeisberg EM, Tarnavski O, Zeisberg M, Dorfman AL, McMullen JR, Gustafsson E, Chandraker A, Yuan X, Pu WT, Roberts AB, Neilson EG,

- Sayegh MH, Izumo S, Kalluri R. Endothelial-to-mesenchymal transition contributes to cardiac fibrosis. *Nat Med*. 2007;13:952–961.
129. Chen Q, Zhang H, Liu Y, Adams S, Eilken H, Stehling M, Corada M, Dejana E, Zhou B, Adams RH. Endothelial cells are progenitors of cardiac pericytes and vascular smooth muscle cells. *Nat Commun*. 2016;7:12422.
130. Plummer NW, Evsyukova IY, Robertson SD, de Marchena J, Tucker CJ, Jensen P. Expanding the power of recombinase-based labeling to uncover cellular diversity. *Development*. 2015;142:4385–4393.
131. He L, Li Y, Li Y, Pu W, Huang X, Tian X, Wang Y, Zhang H, Liu Q, Zhang L, Zhao H, Tang J, Ji H, Cai D, Han Z, Han Z, Nie Y, Hu S, Wang QD, Sun R, Fei J, Wang F, Chen T, Yan Y, Huang H, Pu WT, Zhou B. Enhancing the precision of genetic lineage tracing using dual recombinases. *Nat Med*. 2017;23:1488–1498.
132. Majesky MW. Adventitia and perivascular cells. *Arterioscler Thromb Vasc Biol*. 2015;35:e31–e35.
133. Hu Y, Zhang Z, Torsney E, Afzal AR, Davison F, Metzler B, Xu Q. Abundant progenitor cells in the adventitia contribute to atherosclerosis of vein grafts in ApoE-deficient mice. *J Clin Invest*. 2004;113:1258–65.
134. van de Rijn M, Heimfeld S, Spangrude GJ, Weissman IL. Mouse hematopoietic stem-cell antigen Sca-1 is a member of the Ly-6 antigen family. *Proc Natl Acad Sci U S A*. 1989;86:4634–4638.
135. Okada S, Nakauchi H, Nagayoshi K, Nishikawa S, Miura Y, Suda T. In vivo and in vitro stem cell function of c-kit- and Sca-1-positive murine hematopoietic cells. *Blood*. 1992;80:3044–3050.
136. Lee JY, Qu-Petersen Z, Cao B, Kimura S, Jankowski R, Cummins J, Usas A, Gates C, Robbins P, Wernig A, Huard J. Clonal isolation of muscle-derived cells capable of enhancing muscle regeneration and bone healing. *J Cell Biol*. 2000;150:1085–1099.
137. Oh H, Bradfute SB, Gallardo TD, Nakamura T, Gaussin V, Mishina Y, Pocius J, Michael LH, Behringer RR, Garry DJ, Entman ML, Schneider MD. Cardiac progenitor cells from adult myocardium: Homing, differentiation, and fusion after infarction. *Proc Natl Acad Sci*. 2003;100:12313–12318.
138. Matsuura K, Nagai T, Nishigaki N, Oyama T, Nishi J, Wada H, Sano M, Toko H, Akazawa H, Sato T, Nakaya H, Kasanuki H, Komuro I. Adult Cardiac Sca-1-positive Cells Differentiate into Beating Cardiomyocytes. *J*

- Biol Chem.* 2004;279:11384–11391.
139. Wani MA, Means RT, Lingrel JB. Loss of LKLF function results in embryonic lethality in mice. *Transgenic Res.* 1998;7:229–238.
  140. Wu J, Bohanan CS, Neumann JC, Lingrel JB. KLF2 transcription factor modulates blood vessel maturation through smooth muscle cell migration. *J Biol Chem.* 2008;283:3942–3950.
  141. Reilly SM, Saltiel AR. Adapting to obesity with adipose tissue inflammation. *Nat Rev Endocrinol.* 2017;13:633–643.
  142. Stein M, Keshav S, Harris N, Gordon S. Interleukin 4 potently enhances murine macrophage mannose receptor activity: a marker of alternative immunologic macrophage activation. *J Exp Med.* 1992;176:287–92.
  143. Porcheray F, Viaud S, Rimaniol AC, Léone C, Samah B, Dereuddre-Bosquet N, Dormont D, Gras G. Macrophage activation switching: An asset for the resolution of inflammation. *Clin Exp Immunol.* 2005;142:481–489.
  144. Gaber T, Strehl C, Buttgereit F. Metabolic regulation of inflammation. *Nat Rev Rheumatol.* 2017;13:267–279.
  145. He H, Mack JJ, Güç E, Warren CM, Squadrito ML, Kilarski WW, Baer C, Freshman RD, McDonald AI, Ziyad S, Swartz MA, De Palma M, Iruela-Arispe ML. Perivascular Macrophages Limit Permeability. *Arterioscler Thromb Vasc Biol.* 2016;36:2203–2212.
  146. Lavin Y, Mortha A, Rahman A, Merad M. Regulation of macrophage development and function in peripheral tissues. *Nat Rev Immunol.* 2015;15:731–744.